2009

Downhole water loop (DWL) well completion for water coning control --- theoretical analysis

Lu Jin
Louisiana State University and Agricultural and Mechanical College, ljin1@tigers.lsu.edu

DOWNHOLE WATER LOOP (DWL) WELL COMPLETION FOR WATER CONING CONTROL --- THEORETICAL ANALYSIS

A Thesis

Submitted to the Graduate Faculty of the
Louisiana State University and
Agricultural and Mechanical College
in partial fulfillment of the
Requirements for the degree of
Master of Science in Petroleum Engineering

in

The Department of Petroleum Engineering

by
Lu Jin
B.S., Daqing Petroleum Institute, Daqing, 2005
December, 2009

DEDICATION

To my parents, Weiqin Jin and Huiying Qi.

ACKNOWLEDGEMENTS

I would like to express my appreciation to my major professor, Dr. Andrew K. Wojtanowicz, for his guidance, supervision, and help provided to this study.

I would also like to thank Dr. Christopher D. White and Dr. Richard G. Hughes for being my examining committee members. I appreciate their effective instruction and discussion during this study.

I wish to express my gratitude to the LSU Downhole Water Sink Technology Initiative (DWSTI) for supporting this research.

I also wish to thank my friends: Wenjing Li, for her support and tolerance; Gbolahan Afonja, Venu Nagineni and many others, for their help in this research.

TABLE OF CONTENTS

DEDICATION ii

ACKNOWLEDGEMENTS iii

ABSTRACT vi

CHAPTER 1. INTRODUCTION 1

CHAPTER 2. LITERATURE REVIEW 4
- 2.1. Experimental Studies of Water Coning 5
- 2.2. Numerical Simulation Studies of Water Coning 8
- 2.3. Water Coning Control Methods 14
  - 2.3.1. Downhole Water Sink (DWS) Technology 17
- 2.4. Partial Penetration Skin Factor 21
- 2.5. Water Injection Methods 23
- 2.6. Nodal Analysis of DWS and Smart Wells 28

CHAPTER 3. WATER CONING CRITICAL RATE WITH PARTIAL PENETRATION, ANISOTROPY AND CAPILLARY PRESSURE 33
- 3.1. Mechanisms of Water Coning 33
- 3.2. Critical Cone Height and Critical Oil Rate 35
  - 3.2.1. Critical Cone Height 35
  - 3.2.2. Critical Oil Rate 44
- 3.3. Partial Penetration Skin 46
- 3.4. Anisotropic/Isotropic System Transformation 47
- 3.5. Modified Critical Oil Rate Correlation 56
- 3.6. Effect of Capillary Pressure on Critical Oil Rate 63
- 3.7. Discussion 66

CHAPTER 4. DOWNHOLE WATER LOOP (DWL) TECHNOLOGY FOR WATER CONING CONTROL 67
- 4.1. DWL Well Completion Method and Mechanisms 67
- 4.2. DWS and DWL as Smart Completions 69
  - 4.2.1. Comparison of DWS and DWL Wells 69
  - 4.2.2. DWS and DWL as “Smart” Wells 70

CHAPTER 5. CRITICAL RATE MODELS FOR DWL 77
- 5.1. Analytical Model of DWL with Segregated Inflow of Oil and Water 77
- 5.2. Verification of the Analytical Model with Field Data 84
- 5.3. Comparison of the DWL Analytical and Numerical Models 87
- 5.4. Use of DWL Model for Determining the Critical D/I Spacing 95
- 5.5. Discussion 98

CHAPTER 6. PERFORMANCE ANALYSIS OF DWL IN RESERVOIR WITH BOTTOM WATER 99
6.1. DWL Well Performance before Water Breakthrough 99
6.2. DWL Well Performance after Fluid Breakthrough 101
6.2.1. Prevent Oil Breakthrough into the Bottom Completions 101
6.2.2. Water Cut Development after Water Breakthrough 102
6.3. DWL Well Performance (Nodal) Analysis 109
6.4. Discussion 114

CHAPTER 7. CONCLUSIONS AND RECOMMENDATIONS 116
7.1. Conclusions 116
7.2. Recommendations 117

NOMENCLATURE 119

REFERENCES 123

VITA 139

ABSTRACT

The Thesis is an analytical and numerical analysis of a new method for completing and producing oil wells affected by water coning. The method enables producing oil with no or minimal water cut while keeping the water subsurface with downhole water loop (DWL) installation. Typically, a DWL well is triple-completed in the oil and water zones with the three completions separated by parkers. The top completion produces oil to the surface while the middle and bottom completions drain from and inject into the bottom water zone, respectively.

Segregated-inflow operation of DWL well requires keeping the production and drainage-injection rates below their critical values. Therefore, the theory of water coning is re-visited and examined using analytical modeling of critical height and dynamic stability of water cone. The analytical model employs transformation from anisotropic to equivalent isotropic radial flow system. Also, considered are the effects of partial penetration and capillary-pressure transition zone.

The analytical model is used to determine operational domain of DWL for different well-reservoir systems. The results are then compared with data from commercial simulator and real field showing good match. Also investigated is the effect of the distance between water drainage and injection completions (D/I spacing), which is the most important design parameter for DWL wells. The results show that DWL wells could successfully work in reservoirs with relatively small aquifer as the DWL operational domain is only sensitive to small values of D/I spacing.

A commercial simulator is employed to build a numerical model of DWL operations outside the segregated-inflow domain where the top completion produces oil

with water. The steady demonstrates the flexibility of DWL in controlling water cut. Then, the model is used to study DWL performance with controlled water production using a modified nodal analysis approach that includes the D/I spacing constraint. The results show that DWL could improve critical oil rate and reduce water cut before and after water breakthrough, respectively. Nodal analysis is used to seek the possible production operations of DWL which would help to design the D/I spacing and decide if one or two downhole pumps were needed for the system.

CHAPTER 1. INTRODUCTION

Excessive water production has been a continuing problem for operators since the beginning of petroleum industry (Ambrose, 1921). In 1998, 40 counties in Colorado produced about 220.6 million barrels of additional water with only about 22.46 million barrels of oil over the same period and the produced water oil ratio (WOR) was 9.8. In 2001, 360 million barrels of water were produced against 25.5 million barrels of crude oil in the same state and the WOR was up to 14. Now, the largest volume of waste associated with oil and gas production operations in Louisiana, as well as nationally, is produced water (Inikori, 2002). Oilfield produced water has become one of the biggest environmental problems facing some major oil production countries such as Oman today. The volume of produced water is currently estimated at more than 6.5 times greater than that of oil production. According to a report by Schlumberger Water Solutions, 75 % of the total production from petroleum reservoirs is only water, equivalent to 220 million barrels of water per day worldwide which costs about 11 million dollars per day to address it (Arslan, 2005). Seright et al. (2003) categorized various water problems in oilfield from least to most difficult to solve, and stated that water coning and underruning are the most difficult ones with no easy, low-cost solutions.

The water coning problem has been studied since Muskat and Wyckoff (1935) discussed the coning mechanisms. Until now, countless efforts have been done to understand and control this phenomenon using varies methods: perforating far above the original OWC; keeping production rate below the critical value, creating a permeability barrier between the oil and water zones by injecting resins, polymers or gels, using horizontal well to delay the coning speed, controlling the fluids mobility in the reservoir, injecting the produced fluid back to the reservoir, producing oil and water separately by Downhole water sink (DWS) wells and so on.

However, most of these methods just delay the water coning development and could not totally solve the water coning problem. The critical oil rate is usually too low to be economical for most conventional wells and short penetration could not solve this problem in nature. Permeability barrier just delays the coning development speed and it might depress the water drive; water could bypass barrier and breakthrough to the oil perforation when the oil rate is high. Water cresting is hard to solve in horizontal well as water coning in vertical well. Produced fluid injection back is effective at the beginning of oil production, more and more oil should be injected back to the reservoir with the development of oilfield which makes it impossible to carry out in real practice.

DWS well is a relatively new method compared to the others. It can control water coning from its source and even completely eliminate it. It is more effective than other methods when the water drive is strong. However, it has its own drawbacks: a lot of energy is needed to lift a large amount of water to the surface, especially when the well is deep and water coning is strong; a lot of money is needed to treat so much water on the surface, especially in offshore fields where facilities are limited by available space; it may cause environmental problems when a large quantity of produced water is disposed; the reservoir may be depleted fast when both oil and water are drained out of the formations, as a result, there may not be enough energy to drive the oil left in the reservoir to the well and it may reduce the final recovery.

In order to keep the advantages of DWS well and conquer its drawbacks, a new technology is studied in this thesis --- Downhole Water Loop (DWL) technology, which is triply completed in the oil and water zones: oil is produced from the top completion and water is drained and injected via the middle and bottom completion in the aquifer, respectively. Because DWL injects the water back into the same aquifer instead of pumping it to the surface, the produced water in the surface would be dramatically reduced and the water drive in the reservoir could be maintained. This is important in bottom water drive reservoirs, especially when the aquifer is weak.

The objectives of this study can be summarized as follows:

1. Understanding the mechanisms of water coning in reservoirs with bottom water;
2. How to consider partial penetration by skin factor;
3. How to transform the anisotropic reservoir to an equivalent isotropic one;
4. Understanding the mechanisms of DWL for water coning control;
5. Modeling DWL analytically and numerically to predict its behavior and investigate its application in real field;
6. Evaluating the coning control effects of DWL and its performance in reservoirs with bottom water.

CHAPTER 2. LITERATURE REVIEW

Water coning became a thorny problem in front of reservoir engineers shortly after the beginning of petroleum industry. It seriously impacts the well productivity and influences the overall recovery of the oil reservoirs. Unnecessary water production also adds the cost of water handling and disposal, causes corrosive problems in production facilities and makes the early shut down of the infected wells. Although many methods have been used to control it, water coning, is still a nightmare in many oil fields all over the world. Literature survey shows that tons of work has been done in order to understand and control this problem.

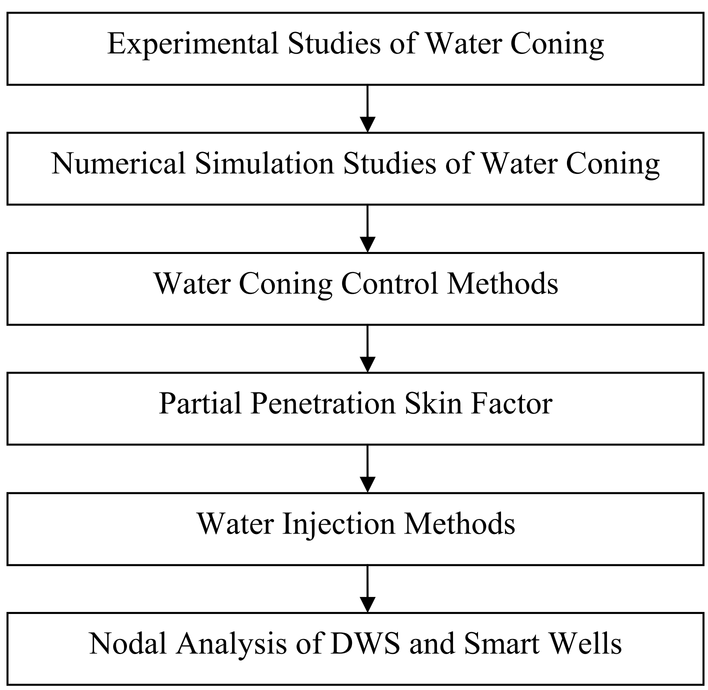

Figure 2.1 Flow chart of literature review

Studies of water coning can be roughly grouped into three time stages: physical modeling and experimental study stage (before 1970), theoretical modeling and simulation stage (after 1970) and control technology development stage (after 1980). Several correlations have been developed to calculate the critical oil production rate to avoid water breakthrough, predict water breakthrough time and post breakthrough behaviors such as water cut development etc. An overview of research work related to water coning control will be presented in this chapter as shown in Figure 2.1.

2.1. Experimental Studies of Water Coning

Before 1970, most of the work on water coning problem focused on coning mechanisms and experimental studies. Many basic questions about water coning were solved in this stage. Muskat and Wyckoff (1935) published the first paper to analyze water coning in oil production theoretically. They presented the fundamental physical principles underlying the behavior of the water oil contact (OWC) when oil was produced from a partial penetrated well in the oil zone before water breakthrough to the well. They suggested that, water coning was induced by the pressure differential existing in the well and the reservoir, and the advance of the OWC was directly proportional to this pressure differential.

They also pointed out that, it was impossible to eliminate bottom water when producing from a thin oil zone unless the production rate of the well was reduced to uneconomically low values. Their calculation results showed that, water-free oil production rate could be maintained for a short-penetrated well, and this rate decreased with the increasing of well penetration. They defined the critical oil production rate (q_{oc}) as the maximum allowable oil flow rate that can be imposed on the well to avoid a cone breakthrough. The critical rate would correspond to the development of a stable cone to an elevation just below the bottom of the perforated interval in an oil-water reservoir. By analytically solving the Laplace equation for single phase flow, they developed a correlation to calculate the critical rate for partial completed wells as:

$$q_{oc} = \frac{4\pi k_h \Delta P_o \sum a_n b_n}{\mu_o \left\{ \phi_e - \frac{4}{h_o} \sum a_n b_n \log \frac{4h_o}{r_e} \right\}} \qquad (2.1)$$

In 1946, Muskat presented the way to determine the shape of water cones for various pressure drops in homogeneous reservoirs; he concluded that the critical pressure drop at the beginning of water coning was a function of well penetration and oil-zone thickness, and the critical oil production rate was controlled by the pressure gradient caused by the oil production.

Meyer and Garder (1954) derived a correlation for the critical oil rate required to achieve a stable water cone. They found that the critical rate for a well was determined by: the length of well penetration, density difference of oil and water and the oil zone thickness. Their correlation for critical oil rate expressed as:

$$q_{oc} = 0.246 \times 10^{-4} \frac{\Delta\rho}{\ln \frac{r_e}{r_w}} \frac{k_o}{\mu_o B_o} \left(h_o^2 - h_{op}^2\right) \qquad (2.2)$$

where, all the parameters are in field units.

Chaney et al. (1956) developed a set of working curves to determine the critical oil rate. Their curves were generated by using a potentiometric analyzer study and applying the water coning mathematical theory as developed by Muskat and Wyckoff (1935).

Chierici et al. (1964) used a potentiometric model to study the coning behavior in vertical oil wells. They developed dimensionless graphs to address the water and gas coning problems and considered the vertical and horizontal permeability in their dimensionless graphs. With given reservoir and fluid properties, position and length of the perforated interval, the graphs could be used to determine the maximum oil production rate without gas/water coning. The graphs could also be used to determine the optimum position of the perforated interval with only reservoir and fluid properties. They also developed a correlation to calculate critical oil rate in oil/water reservoir:

$$q_{oc} = 0.492 \times 10^{-4} \frac{h_o^2 \Delta\rho}{\mu_o B_o} k_{ro} k_h \psi_w \left(r_{De}, \xi, \delta_w \right) \quad (2.3)$$

$$r_{De} = \frac{r_e}{h_o} \sqrt{\frac{K_h}{K_v}} \quad (2.4)$$

$$\xi = \frac{h_{op}}{h_o} \quad (2.5)$$

$$\delta_w = \frac{D_b}{h_o} \quad (2.6)$$

where, all the parameters are in field units.

Sobocinski and Cornelius (1965) presented a correlation to calculate the breakthrough time, which is the time needed for a water cone to enter the perforation after the beginning of oil production. Based on the experimental and modeling data, they developed a correlation to estimate the breakthrough time by using dimensionless cone height and dimensionless breakthrough time.

Bournazel and Jeanson (1971) simplified Sobocinski and Cornelius's correlation of breakthrough time by only using dimensionless breakthrough time. They also provided a fast water coning evaluation relation for the critical oil rate in isotropic reservoir as:

$$q_{oc} = 5.14 \times 10^{-5} \frac{k_h h_o^2 \Delta\rho g \left(1 - \frac{h_{op}}{h_o} \right)}{\mu_o} \quad (2.7)$$

And for anisotropic reservoir, they used the following correlation to calculate the critical oil rate:

$$q_{oc} = 5.14\times 10^{-5} \frac{k_h^2 h_o^2 \Delta\rho g\left(1-\dfrac{h_{op}}{h_o}\right)}{\mu_o k_v} \qquad (2.8)$$

where, all the parameters are in field units.

Khan (1970) used a three-dimensional scaled laboratory model to observe the coning behavior in a reservoir with natural water drive. Their results indicated that the degree of water coning and the value of the water cut increase with production rate, the mobility ratio and the ratio of aquifer to oil-sand thickness. They found that the mobility ration had great influence on the value of water cut and the degree of water coning at a given total production value: the higher the mobility ratio, the faster water coning develops.

2.2. Numerical Simulation Studies of Water Coning

With the increase of computing power and improvement of simulation technology, several computer simulators were available after 1970. This makes it possible to simulate more complex coning problems in computer, while it saves much time comparing to physical experiments. Although several people used numerical simulation to study water coning problem before 1970, the major coning simulation publications turned up after 1970. People began to investigate complicated coning behavior after water breakthrough in this stage, however, critical oil rate was still an important topic.

The first numerical simulation research on coning problem was carried out by Welge and Weber in 1964. They applied two-phase, two-dimensional model using the alternating direction implicit procedure (ADIP) in the gas and water coning simulation. They found that special computational techniques must be used after cone breakthrough to achieve reliable results and keep calculation costs within reasonable limits. Their simulation results matched the producing histories of a laboratory sandpacked model and of several producing wells experiencing water or free gas production by coning. They suggested that the average horizontal and vertical permeability and the k_h / k_v ratio are critical parameters in the coning study.

Pirson and Metha (1967) developed a computer program to simulate water coning based on the Welge and Weber's mathematical model. They studied the effects of various factors such as vertical to horizontal permeability ratio, mobility ratio between oil and water, specific gravity differential between the two phases and flow rate on the advance of a water cone. The cone shapes and positions were drawn for each case, and the results were found to agree with known phenomena. Comparing their results to Muskat's approximate method, they found that Muskat's method gave higher critical rate because of ignoring the water-oil transition zone.

MacDonald and Coats (1970) described and evaluated three methods for the simulation of well coning behavior. They improved upon the small time step restriction of coning problems by making the production and transmissibility terms implicit, and it could increase the simulation speed much more than the traditional IMPES (Implicit Pressure Explicit Saturation) method.

Letkeman and Ridings (1970) presented a numerical coning model based on implicit transmissibilities and linear interpolation which could use much larger time steps than those in IMPES simulators. The model exhibited stable saturation and production behavior during cone formation and after breakthrough. Their work made coning simulation became practical and economical using modified equations.

Byrne and Morse (1973) presented a systematic numerical coning simulation study which included the effects of reservoir and well parameters. Their results showed that the critical oil rate decreased with the increase of well penetration depth, water breakthrough time decreased and WOR (water oil ratio) increased significantly when the production rate increased, however, the ultimate recovery was independent of production rate. The wellbore radius was not so important on water breakthrough time and WOR.

Schols (1972) developed an empirical formula for critical oil rate based on results obtained from numerical simulator and laboratory experiments as:

$$q_{oc} = 0.0783 \times 10^{-4} \left[\frac{\Delta \rho k_o \left(h_o^2 - h_{op}^2 \right)}{\mu_o B_o} \right] \left[0.432 + \frac{\pi}{\ln \frac{r_e}{r_w}} \right] \left(\frac{h_o}{r_e} \right)^{0.14} \quad \text{..........................(2.9)}$$

where, all the parameters are in field units.

Miller and Rogers (1973) presented detailed coning simulation which was suitable to evaluate water coning problem for a single well in a reservoir with bottom water. They simulated a single well using radial coordinates and a grid system which could be used to determine the most important parameters in water coning on both short term and long term production. Their results for critical oil rate matched well with Schols' critical rate correlation.

Mungan (1975) presented experimental and numerical studies on water coning in an oil producing well under two phase, immiscible and incompressible flow conditions. His results indicated that the numerical model simulated the experiments adequately. Increasing the production rate or the wellbore penetration led to earlier water breakthrough, however, oil recovery was independent of production rate. The oil recovery at any given WOR became greater when the ratio of gravity to viscous forces increased. High vertical permeability decreased the oil recovery, while the opposite was true for horizontal permeability.

Chappelear and Hirasaki (1976) developed a correlation to evaluate the critical oil production rate for a partially perforated well in a reservoir with bottom water. Their coning model was derived by assuming vertical equilibrium and segregated flow in two-phase, two-dimensional reservoir. Their critical oil rate correlation expressed as:

$$q_{oc} = \frac{2\pi h_t k_h k_{ro} \Delta\rho g \left(h_o - h_{cb}\right)}{887.2 \mu_o B_o \overline{\ln r'}} \qquad (2.10)$$

$$r' = 4h_o \sqrt{k_h / k_v} \left(\left\| \frac{h_o - h_{cb}}{h_o - h_{ct}} \right\| \right) \qquad (2.11)$$

$$\overline{\ln r'} = \frac{\ln\left[r_e / \left(r_w + r'\right)\right]}{\left[1 - \left(r_w + r'\right)^2 / r_e^2\right]} - \frac{1}{2} \qquad (2.12)$$

where, all parameters are in field units.

Kuo and DesBrisay (1983) used a numerical simulation to determine the sensitivity of water coning behavior to various reservoir parameters. Based on the simulation results, they developed a simplified correlation to predict the water cut in bottom water drive reservoirs.

Chaperon (1986) proposed a simple correlation to estimate the critical rate of a vertical well in an anisotropic formation. The correlation accounted for the distance between the production well and boundary. Comparing to other works, his correlation was more sensitive to anisotropy: critical rate slightly increased when vertical permeability decreased, but critical cone elevation did not change significantly. The proposed correlation has the following form:

$$q_{oc} = 0.0783 \times 10^{-4} \left[\frac{\Delta\rho k_h \left(h_o^2 - h_{op}^2 \right)}{\mu_o B_o} \right] \left[0.7311 + \frac{1.943}{\frac{r_e}{h_o} \sqrt{\frac{k_v}{k_h}}} \right] \quad \text{.............................(2.13)}$$

where, all parameters are in field units.

Hoyland et al. (1989) presented two methods to predict critical oil rate for a partially penetrated well in an anisotropic bottom water drive reservoirs. The first method was an analytical solution, and the second was a numerical solution to the coning problem. Based on Muskat and Wyckoff's theory, they used the method of images and superimpose to address boundary conditions, and they developed a correlation to predict the critical rate in steady state condition as:

$$q_{oc} = 0.246 \times 10^{-4} \left[\frac{\Delta\rho k_h h_o^2}{\mu_o B_o} \right] q_{CD} \quad \text{..(2.14)}$$

where, q_{CD} , is the dimensionless production rate which can be checked from their dimensionless plot.

Based on a large number of simulation runs with more than 50 critical rate values, the authors used a regression analysis routine to develop the critical oil rate correlations for isotropic and anisotropic reservoirs. For isotropic reservoirs, the correlation expressed as:

$$q_{oc} = \frac{k_o(\rho_w - \rho_o)}{173.35 B_o \mu_o}\left[1 - \left(\frac{h_{op}}{h_o}\right)^2\right]^{1.325} \left[\ln(r_e)\right]^{-1.990} h_o^{2.238} \quad \text{.....................................(2.15)}$$

where, all the parameters are in field units.

For anisotropic reservoirs, the authors correlated the dimensionless critical rate with the dimensionless radius and five different fractional well penetrations. The correlation was presented in a graphical form.

Guo and Lee (1993) demonstrated that the existence of the unstable water cone which depended on the vertical pressure gradient beneath the wellbore. They found that when the vertical pressure gradient was higher than the hydrostatic pressure gradient of the water, an unstable water cone happened. Based on the simulation data, they developed a correlation to calculate the critical oil rate and determine the optimized well penetration length as:

$$q_{oc} = \frac{\Delta\rho k_v}{\mu_o}\left[r_e - \sqrt{r_e^2 - r_e(h_o - h_{op})}\right]^2 \left[\frac{k_v}{\sqrt{k_h^2 + k_v^2}} + \frac{h_{op}\left[\frac{1}{r_w} - \frac{1}{r_e}\right]}{\ln\frac{r_e}{r_w}}\right] \quad \text{...................(2.16)}$$

where, all the parameters are in field units.

Menouar and Hakim (1995) studied the effects of various reservoir parameters such as anisotropy ratio and mobility ratio on water coning behavior. They estimated the critical oil rate based on the large number of simulation data and their results were similar with the other published work.

2.3. Water Coning Control Methods

People began to seek ways to control water coning problem shortly after knowing the coning phenomenon. However, literature survey shows that most coning control work was published after 1980. Several practical solutions have been developed to delay the water breakthrough time and minimize the severity of water coning in vertical wells. The basic methods included increasing the distance between the bottom perforation and the original OWC, separating oil and water in the OWC using horizontal impermeable barriers, controlling the fluids mobility in the reservoir, producing oil and water separately by Downhole water sink (DWS) wells and so on. Some of the methods are briefly described as followings:

Karp et al. (1962) considered several factors involved in creating, designing and locating horizontal barriers for controlling water coning. They studied different designs of the horizontal barriers, such barrier radius, thickness, permeability and position. They established an experimental apparatus to test the effects of different cement barriers and choose the right materials for different reservoirs. They found that reservoirs with high-density or high viscosity crude oils, low permeability or thin oil-zone thickness were not suitable to use this technology. On the other hand, this technology might impede the water drive from the field point of view. Pirson and Mehta (1967) found that the horizontal barrier just delayed the water breakthrough time while it did not provide absolute remedy to the water-coning problem. Water would overpass the barrier and breakthrough to the production interval when the cone radius became greater than the barrier. It is useful only where the horizontal fracture is available to form such an impermeable barrier.

Smith and Pirson (1963) investigated the effect of fluid injection to control water coning in oil and gas wells. They considered position and length of the completion interval, point of fluid injection, the viscosity of the injected fluid and thicknesses of the oil and water sections. They found that the WOR was reduced by injecting oil at a point below the producing interval and the reduction was improved if the injected fluid was more viscous than the reservoir oil. From the experimental results, they concluded that: the optimum point of fluid injection was the point closest to the bottom of the producing interval that did not interfere with the oil production when the production rate is normal; the injection point moved down with the increase of production rate for maximizing the coning control efficiency. However, more and more fluid should be injected back to the reservoir with the increase of time.

Mobility control means injecting chemical additives such as surfactants and polymers or other gelling agents into the water phase to control its mobility. Paul and Strom (1988) proposed to inject water-soluble polymeric gels to control the bottom water mobility. They designed different polymeric gels for various water properties and carried out a serial of experiments in the lab.

Kisman et al (1991, 1992) proposed two methods to reduce the water cut in the well by injecting a composite slug comprising water wetting agent into the reservoir to modify the reservoir matrix to increase its water-wetted character, and non-condensable gas for further laterally extending the matrix surface modification. The slug of a water-wetting agent ensured the main path of the following gas slag through the water zone where it would increase gas saturation area. Thus relative permeability to water would be reduced. The methods could delay the water breakthrough time and reduce water cut in the produced fluids.

Comparing to the vertical wells, horizontal wells can be drilled along the top of the formation, and the distance between the producing interval and oil-water contact can be optimized. Thus, they can achieve a higher flow rate with the same pressure drawdown and have greater areal sweep efficiency (Joshi, 1991; Chen, 1993; Permadi et al. 1997). Gilman et al. (1995) gave a good field example of the application of horizontal wells in the Yates Field Unit in West Texas where the horizontal wells successfully reduced the gas and water coning in thin oil columns. Wu et al. (1995) described Texaco's efforts to evaluate, justify and drill a horizontal well in Amber Field to suppress gas and water coning problems. The target reservoir contained a very thin pancake oil zone sandwiched between a large gas cap and a strong bottom water aquifer. They numerically evaluated the possibility of using horizontal wells to reduce water coning and improve oil recovery in the Amber Field. The simulation results and field histories indicated that horizontal wells completed in the gas cap could significantly reduce water coning and improve the ultimate oil recovery in a thin oil reservoir with a moderate sized gas cap. However, water cresting problem in horizontal wells is also a big challenge to engineers which is very hard to control as well as water coning in vertical wells.

In recent years, downhole oil-water separation (DOWS) technology as a technique of separating water downhole to reduce surface water production has been developed. This technique allows water to be separated in the wellbore and injected into a suitable injection zone downhole while oil is produced to the surface. Shortly after the introduction of the DOWS technology to the oil industry in the 1990's, considerable research work has been done and several trial applications have been undertaken to test the technology. Matthews et al. (1996) reported the successful installation of DOWS in Alliance Field, Canada. They concluded that the system held considerable promise to be both technically and economically feasible for mature fields producing at high water oil ratio. However, this technology does not solve the oil-bypass problem caused by the water development.

Ehlig-Economides et al. (1996) studied the effects of well's total penetration well on water coning control. The perforation interval of the well is extended to cover the entire oil zone and into the bottom water zone. In this way, the radial flow of fluid can be maintained to avoid the water cone development and the oil-bypass problem can be solved. This completion method can get higher oil production rate and ultimate recovery comparing with the partial penetration method. However, it produces much more water to the surface than other methods, so the cost of water handling is increased and large amount of water disposal may cause environmental problems.

2.3.1. Downhole Water Sink (DWS) Technology

In 1955, Widmyer introduced and patented a novel coning control idea to the petroleum industry ---downhole water sink (DWS) technology. In his patent, he used two separated completions in one well to control water coning: one produced oil from the oil zone and the other drained water in the aquifer. Thus, the water coning could be controlled by the two opposite pressure drawdown. Pirson and Mehta (1967) numerically tested this technology and concluded that, DWS might reduce the growth of water cone. Driscoll (1972) refined the idea by having multiple completions with the lowermost completion below the oil/water contact. However, little attention was paid to this technology at that time, the reasons might be that, industry had low confidence to install it and water coning problem was not as serious as nowadays at that time.

The interest of the oil industry returned to the DWS technology after Wojtanowicz et al. improved it even further into a more workable and successful method when they simulated a dual completion using a "tailpipe water sink" in 1991 as shown in Figure 2.2 (Shirman, 1998). First, an oil well is drilled through the oil-bearing zone to the underlying aquifer. Then, the well is dually completed both in the oil and water zones. A packer separates the oil and water perforations. During production, oil flows into the upper completion being produced up the annulus between the tubing and the casing, while water is drained through the lowermost completion through perforations in the casing and then lifted up through the open tubing below the initial OWC. As a result, the produced oil is water free and the drained water is oil free.

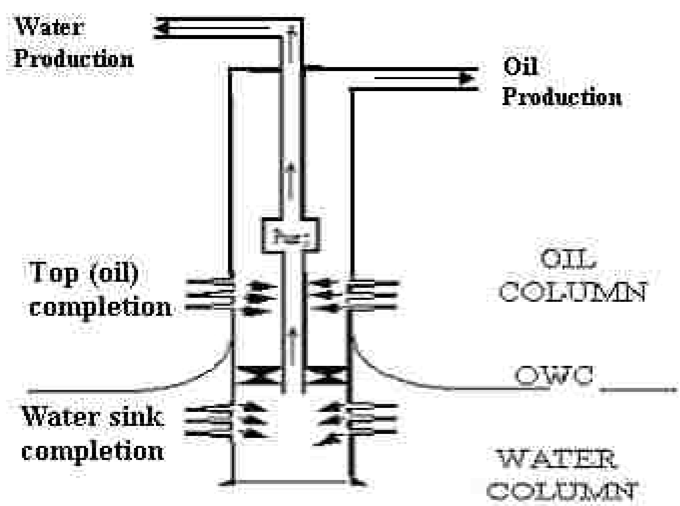

Figure 2.2 Downhole water sink (DWS) well completion

Swisher and Wojtanowicz (1995a, 1995b) described the first field application of DWS well in the Nebo-Hemphill Field, LaSalle Parish, Louisiana. The DWS well could not only prevent water coning, but also reverse the water cone after breakthrough. The well greatly increased oil production rate compared with conventional wells. Bowlin et al. (1997) reported another field application of the technology by Texaco Inc. with the name of in-situ gravity segregation in Kern County, California. The well was installed in a location with 10 years of prior water coning problems. The results showed that this installation successfully controlled the water coning problem, and the oil production rate was doubled.

After that, considerable efforts have been put on the research of DWS worldwide (Shirman and Wojtanowicz, 1997; Gunning et al, 1999; Ould-amer et al, 2004; Siemek and Stopa, 2002, Utama, 2008 and so on). Until now, DWS completion has been field tested in numerous reservoirs all over the world with good results. Results also indicate that water coning develops fast while the oil reversing is a slow process. The drawback of this technology is that, it brings large amount of water to the surface which requires more water processing facility and adds the production costs.

In order to conquer this disadvantage of DWS system, Wojtanowicz and Xu (1992) proposed a concept of Downhole Water Loop (DWL) technique to cut back the volume of formation water produced by an oil well from a hydrocarbon reservoir underlain by a water zone. The method employed dual completion of the well inside the water zone, below the OWC to install the water loop equipment (separated by a packer) in addition to the conventional completion in the oil zone (above the OWC). The water loop installation included a submersible pump, the upper (water sink) perforations and the lower (water source) perforations. A submersible pump would drain the formation water around the well from the water sink, and then would reinject the same water back to the water zone through the water source perforations. A simulation study was conducted to investigate hydrodynamic performance of the method to restrain water movement towards oil-producing perforations. The downhole water loop was mathematically modeled by computing flow potential distribution generated by two constant-rate sinks (oil and water) and one constant-rate source (water) located between the three linear boundaries and the constant-pressure outer radial boundary. The study revealed that the shape of the dynamic OWC in the well's vicinity could be effectively controlled by the method so that the oil production rates could be 2-4 times higher than the critical rates obtained when using conventional completion. Also, the method had the advantage to become a solution to the environmental compliance problem associated with disposal of produced water. From the standpoint of the reservoir engineering theory presented in their study, formation water could be kept away from oil-production perforations so that the oil recovery per well could also be improved.

In another DWL study, Wojtanowicz and Shirman (1996) determined the effect of hydraulic communication (cement leak) between the water drainage and injection zones. The leak would reduce the size of the water drainage zone under the oil-producing perforations and make the system inefficient. In that study, the downhole drainage injection was mathematically modeled as a system of three sinks operating under steady-state flow conditions in a multilayered porous medium. The results of simulation runs revealed principal relationships between the reservoir engineering factors (fluid mobilities, configuration of geological strata, and the degree of zonal isolation) and the production design factors (the position of well completions, and the oil production and water injection rates). Also, the study showed that for a determined geological conditions and well completion geometry, there was a unique relationship between the water injection and oil production rates, which ensured stability of OWC resulting in the continuous production of oil with minimum amount of water.

2.4. Partial Penetration Skin Factor

In 1949, Van Everdingen and Hurst introduced the concept of skin factor to the petroleum industry. They noticed that, the measured bottom hole flowing pressure was less than the calculated value for a given flow rate. It indicated that there was an additional pressure drop in the reservoir-well system, and this additional pressure drop was independent of time. In order to address this problem, they attributed this pressure drop to a small zone around thee wellbore, where the permeability was supposed to be changed. Drilling and completion operation might be the reason of permeability change in this small zone. Van Everdingen and Hurst called this pressure drop as "skin factor effect". They found the skin factor in wells could vary from +1 to +10, and even higher.

Hawkins (1956) improved the concept of skin factor. He proposed that the positive skin meant the reduction of permeability around the wellbore, while negative skin indicated the permeability was increased. Because of this modification, people found negative skin factor could present fractured or stimulated wells. In these cases, the bottom-hole pressure was higher than the computed value, and higher production rate could be obtained.

Joshi (1991) studied the skin factor of stimulated wells. He found that, the skin factor value of stimulated wells could reach as high as -6. He also proposed that, horizontal wells could be represented as vertical wells with large negative skin factors, which indicated that horizontal wells could be treated as highly stimulated vertical wells.

Brons and Marting (1960) first considered the partial penetration problem as skin factor. They concluded that different partial penetration wells were used in various reservoir conditions: top-penetrated well was often used in bottom water drive reservoir to avoid water coning problem; central penetration was applied when there were both gas cap and bottom water in the reservoir; well with several intervals open to production was used in normal reservoirs. They proposed a correlation to calculate skin factor for all three penetrations which was suitable to use in isotropic reservoirs.

Gringarten and Ramey (1975) systematically studied the transient flow to partially penetrating wells and provided detailed review of previous studies on this problem. They proposed a new skin factor correlation to approximate partial penetration well by numerical technique.

Streltsova-Adams (1979) used a uniform-flux well and calculated an average pressure drop at the wellbore by integrating along the interval open to flow. She also derived explicit formulas for pseudoskin caused by restricted flow entry in the form of infinite series.

Reynolds et al (1984) examined the pseudoskin factor caused by partial penetration in a two-layer reservoir when only one layer was open to flow. They found that the pseudoskin factor could be correlated as a unique function of three combined parameters which depended primarily on individual layer horizontal and vertical permeabilities. They provided mathematical model and numerical procedure to calculate the skin factor. The results showed the model was applicable to multiphase flow situations.

Papatzacos (1987) provided a comprehensive review of previous work on partial penetration pseudoskin for infinite conductivity wells. He used the method of images to obtain the steady-state pressure drop at the wellbore of a partial-penetrated well, and presented a simple formula for the pseudoskin factor of a well with restricted flow entry where infinite conductivity was taken into account analytically. His results matched well with other complex correlations.

2.5. Water Injection Methods

The number of injection well increased fast in the past 50 years with the development of industries, especially petroleum industry (Liu and Ortoleva, 1996; Caudle, 2002). The disposal of fluid waste by deep well injection becomes an environmental issue of great concern. According to the USEPA (U.S. Environmental Protection Agency) regulations, five classes of injection wells have been established, which were based on similarity in the fluids injected, activities, construction, injection depth, design, and operating techniques. This categorization ensures that wells with common design and operating techniques are required to meet appropriate performance criteria for protecting underground sources of drinking water (USDWs) (USEPA, 2009):

Class I: Inject hazardous wastes, industrial non-hazardous liquids, or municipal wastewater beneath the lowermost USDW, currently there are 549 this kind of wells in the U.S.

Class II: Inject brines and other fluids associated with oil and gas production, and hydrocarbons for storage. They inject beneath the lowermost USDW, currently there are 143,951 wells this kind of wells in the U.S.

Class III: Inject fluids associated with solution mining of minerals beneath the lowermost USDW, currently there are 18,505 this kind of wells in the U.S.

Class IV: Inject hazardous or radioactive wastes into or above USDWs. These wells are banned unless authorized under a federal or state ground water remediation project, currently there are 32 this kind of wells in the U.S.

Class V: All injection wells which are not included in Classes I-IV. In general, Class V wells inject non-hazardous fluids into or above USDWs and are typically shallow, on-site disposal systems. However, there are some deep Class V wells that inject below USDW. Currently, there are 400,000 to 650,000 this kind of wells in the U.S.

Hazebroek et al. (1958) were the early authors who began to model water injection wells. They noticed that if there was a considerable skin effect in the early life of an injection well, remedial measures could be started before carrying out full-scale pattern water flooding. Determination of the static pressure in the water injection well might show that the water entered the thief zone rather than the desired reservoir. Based on the one dimensional radial flow model, they found the following approximation for a water injection well:

$$\lim_{r\to 0} r\frac{\partial p}{\partial r} = -\frac{q_i \mu_w}{2\pi k_h h_{wi}} \quad \text{.........(2.17)}$$

The bottom hole injection pressure could be expressed as:

$$p_{oi} = p_e + \frac{q_i \mu_w}{2\pi k_h h_{wi}}\left[S_{wi} + \ln\frac{r_e}{r_w}\right] \quad \text{.........(2.18)}$$

Woodward and Thambynayagam (1983) presented an analytical solution for the pressure response of the fully penetrated water injection well in undersaturated oil reservoir. The validity of their method was demonstrated by comparison with results of numerical simulation studies and field examples. Their method could be used to determine the reservoir characteristics, such as mobility ratio and skin factor, from short term water injection tests. The theoretical basis of their method was one dimensional radial flow model. By applying this model to the infinite homogeneous well-reservoir system, two governing equations could be obtained:

Invaded zone:

$$\frac{1}{r}\frac{\partial}{\partial r}\left(r\frac{\partial p}{\partial r}\right)=\left(\frac{\phi\mu_w c_1}{k_w}\right)\frac{\partial p}{\partial t} \qquad (2.19)$$

Uninvaded zone:

$$\frac{1}{r}\frac{\partial}{\partial r}\left(r\frac{\partial p}{\partial r}\right)=\left(\frac{\phi\mu_o c_2}{k_o}\right)\frac{\partial p}{\partial t} \qquad (2.20)$$

Thambynayagam (1984) extended the above method to the partial penetrated water injection well cases with more outer boundary conditions: infinite, bounded and constant pressure. The physical model considered in his analysis consisted of a well located in an anisotropic medium of uniform thickness. The formation and fluid properties were independent of pressure, the fluids of small compressibility and gravity effects were negligible. Water was injected through a small portion of the formation thickness. The governing equations could be expressed by two dimensional cylinder flow model:

Invaded zone:

$$\frac{1}{r}\frac{\partial}{\partial r}\left(r\frac{k_{wr}}{\mu_w}\frac{\partial p}{\partial r}\right)+\frac{\partial}{\partial z}\left(\frac{k_{wz}}{\mu_w}\frac{\partial p}{\partial z}\right)=\phi c_1\frac{\partial p}{\partial t} \qquad (2.21)$$

Uninvaded zone:

$$\frac{1}{r}\frac{\partial}{\partial r}\left(r\frac{k_{or}}{\mu_o}\frac{\partial p}{\partial r}\right)+\frac{\partial}{\partial z}\left(\frac{k_{oz}}{\mu_o}\frac{\partial p}{\partial z}\right)=\phi c_2\frac{\partial p}{\partial t} \quad \text{...(2.22)}$$

Barkve (1985) proposed a model to describe isothermal water injection into an oil reservoir with no free gas phase via fully penetrating vertical wells. He considered a piston-like displacement problem with a line source well, and the effects of capillary pressure, relative permeability variations and gravity were all neglected. His analytical model was the same as that of Woodward and Thambynayagam (1983), however, he applied a quasi-stationary method to construct solutions for the equations.

Koning (1985) proposed an analytical model for the fracturing of a water injection well during water flooding. In his model, the water injection well fully penetrated the oil reservoir and fracturing occurred out of the injection well. The injection well was modeled in three dimensional Cartesian coordinates as:

$$\frac{\partial^2 p}{\partial x^2}+\frac{\partial^2 p}{\partial y^2}+\frac{\partial^2 p}{\partial z^2}=-\frac{1+\upsilon}{1-\upsilon}\alpha_p\frac{\partial p}{\partial t} \quad \text{...(2.23)}$$

where, υ, is the Poisson's ratio; α_p, is the linear poro-elastic expansion coefficient.

Abbaszadeh and Kamal (1989), Bratvold and Horne (1990) derived analytical injection and falloff solutions using the radial flow Buckley-Leverett model. Both papers were restricted to radial flow from a fully penetration vertical well. Their model can be expressed in dimensionless form as:

$$\frac{1}{r_D}\frac{\partial}{\partial r_D}\left(r_D\frac{\partial p_{1D}}{\partial r_D}\right)=\frac{\partial p_{1D}}{\partial t_D},\quad 0<r_D\le a_D \quad \text{...(2.24)}$$

$$\frac{1}{r_D}\frac{\partial}{\partial r_D}\left(r_D\frac{\partial p_{2D}}{\partial r_D}\right)=F_\eta\frac{\partial p_{2D}}{\partial t_D},\quad a_D\le r_D\le\infty \quad \text{...(2.25)}$$

$$p_{1D}=p_{2D},\quad r_D=a_D \quad \text{..(2.26)}$$

where, a_D, is the dimensionless injection constant; F_η, is the diffusivity ratio of water and oil; subscripts 1 and 2 stand for water and oil, respectively.

Abbaszadeh and Kamal's injection solution was obtained by using a multi-composite solution based on the total mobility profile at a given injection time. The injection solution of Bratvold and Horne was based on the validity of the Boltzmann transform. Both papers assumed that a mechanical skin factor can be simply added to the zero skin solution.

Patzek and Silin (2001) modeled water injection through a growing vertical hydrofracture penetrating a low-permeability reservoir which was useful in oilfield waterflood applications and in liquid waste disposal through reinjection. Using Duhamel's principle, they extend the Gordeyev and Entov's (1997) self-similar 2D solution of pressure diffusion from a growing fracture to the case of variable injection pressure. By neglecting the capillary pressure, their injection well model satisfies the well-known pressure diffusion equation:

$$\frac{\partial p(t,x,y)}{\partial t} = \alpha_w \nabla^2 p(t,x,y) \qquad (2.27)$$

where, $p(t,x,y)$, is the pressure at point *(x, y)* of the reservoir at time t; α_w, is the overall hydraulic diffusivity coefficient which combines both the formation and fluid properties; ∇^2, is the Laplace operator.

Boughrara et al. (2007) extended Thambynayagam's (1984) model to construct an analytical injection pressure solution for a restricted-entry vertical well and for a horizontal well with unequal offsets in an anisotropic reservoir. The main innovation needed to construct such solutions was the development of models and methods to construct the distribution of water saturation in the reservoir. In their paper, they used the coordinate transformation method to analyze the anisotropy effects and reduced the 2D cylinder flow model to 1D radial flow model, which was much easier to get the analytical solutions.

More people use numerical software to study water injection well recently, however, the analytical models still work well comparing to the simulation results. For example, Moreno et al (2006) got similar results to the results calculated by Hazebroek et al.'s (1958) model, Jøranson et al.'s (2007) simulation results matched well with those of Koning's (1985) model.

2.6. Nodal Analysis of DWS and Smart Wells

All production wells are drilled and completed to move the oil and gas from reservoir to the stock tanks or sales lines. The fluids travel through the reservoir and piping system until arriving to the separators. Movement and transportation of these fluids need energy to overcome friction losses in the system and lift the fluids to the surface. The pressure drop in the total system at any time will be the initial fluid pressure minus the final fluid pressure. This pressure drop is the sum of the pressure drops occurring in all of the components in the system. Every single component can influence the whole system's behavior because of the interaction among the components. The production of a well can be restricted by the performance of only component. In order to get the maximum profits from a well, all components in the system should be optimized in the most economical way. Nodal analysis provides a way to analyze a well which can determine the producing capacity for any combination of components.

Gilbert (1954) proposed the first outlines of system analysis principles for oil production wells. He presented that one of the main objectives of system analysis is to determine the liquid flow rate of a given production system. An oil well could be considered as a series-connected hydraulic system made up of its components bracketed by appropriately placed nodes. The flow rate of the oil well could be found with proper consideration of the specific features of the system. He compared different lifting methods in oil production and found that production by natural flow rightly topped the list of these methods, since it produced more oil than all other methods combined and proceeded with minimum cost in relative absence of operating difficulties. In his paper, Gilbert described the two-phase vertical-lift function, explained the hydraulics of natural flow, summarized methods for estimating individual well capabilities and included approximations for solution of natural-flow and gas-lift problems for different tubing sizes.

Brown and Beggs (1977) and Mach et al. (1979) systematically studied Gilbert's idea and further improved the system analysis method. They clearly defined the concept of nodal analysis: it is a method presented for applying systems analysis to the complete well system from the outer boundary of the reservoir to the sand face, across the perforations and completion section to the tubing intake, up the tubing string including any restrictions and down hole safety valves, the surface choke, the flow line and separator. By analyzing the complex production system, they schematically simplified it to three phases:

1. Flow through porous medium;
2. Flow through vertical or directional conduit;

3. Flow through horizontal pipe.

They also provided different examples to show the details of nodal analysis process.

Golan and Whitson (1986) and Beggs (1991) published two books about well performance and production optimization using nodal analysis, respectively. With the wide selection of available calculation models and advent of computers, they not only applied nodal analysis method to many producing oil and gas well problems, but also to the analysis of injection well performance by appropriate modification of the inflow and outflow expressions. The following is a list of possible applications of nodal analysis:

1. Selecting tubing size;
2. Selecting flowline size;
3. Gravel pack design;
4. Surface choke sizing;
5. Subsurface safety valve sizing;
6. Analyzing an existing system for abnormal flow restrictions;
7. Artificial lift design;
8. Well stimulation evaluation;
9. Determining the effect of compression on gas well performance;
10. Analyzing effects of perforating density;
11. Predicting the effect of depletion on producing capacity;
12. Allocating injection gas among gas lift wells;
13. Analyzing a multiwall producing system;
14. Relating field performance to time.

Golan and Whitson (1986) and Beggs (1991) pointed out that, the essentials of nodal analysis could be expressed in two formulas for the flow into the node and for the flow out the node:

Inflow:

$$p_{inlet} - \Delta p(upstream\ components) = p_{node} \quad (2.28)$$

Outflow:

$$p_{outlet} + \Delta p(downstream\ components) = p_{node} \quad (2.29)$$

And two criteria must be met:

1. Flow into the node equals flow out of the node;
2. Only one pressure can exist at the node for a given flow rate.

Takacs and Turzo (1994) proposed the object-oriented programming (OOP) techniques in the development of a computer program for nodal system analysis. Development of computer programs for nodal systems analysis is a complex and time-consuming task, mainly because of the complexity of the system. In order to make the task easier, Takacs and Turzo used this "black box" method which did not consider all details of the subject matter when solving a specific problem. Their method not only made the nodal analysis programming easier to carry out, but also made a giant step toward a new age of computerized problem solving.

Arslan (2005) extended nodal analysis to DWS well. He found that conventional nodal analysis could not provide a solution for DWS wells because the critical rates for water coning change with water drainage rate. He used a reservoir simulator to model two-phase flow to the dual completions, then suites of simulations were run and managed to generate inflow performance relationships (IPR) and tubing performance relationships

(TPR) by some algorithms. In his new successive nodal analysis approach, operational range of top and bottom rates could be identified. Together with the stepwise optimization methods, the new approach could evaluate the best performance for a given moment and time increment.

Nodal analysis is a main factor in assessing the size of the valve and the tubing in smart well design (Konopczynski and Ajayi, 2004). Reservoir properties such as productivity index and expected rate govern the design size. If the smart well design contains more than one formation, all the formations properties should be used to design the best combinations of valves to provide best production or injection results.

CHAPTER 3. WATER CONING CRITICAL RATE WITH PARTIAL PENETRATION, ANISOTROPY AND CAPILLARY PRESSURE

Water coning is a serious problem in many oil fields. It costly adds the water handling, seriously reduces the well's productivity and badly influences the depletion degree and overall recovery efficiency of the oil reservoirs. Reducing the production of water is one of the most important factors to maximize the field's ultimate oil recovery. Since water coning has important influence on operations, recovery, and economics, it is the objective of this chapter to provide a detailed theoretical analysis of coning problem in reservoir with bottom water.

3.1. Mechanisms of Water Coning

Oil reservoirs with bottom water drive have high oil recovery due to supplemental energy from the aquifer. As shown in Figure 3.1, wells are often penetrated in the top section of the oil formation to minimize or delay water coning when there is no gas cap in the reservoir. The main reason of water coning is that, water moves to the direction of least resistance in the reservoir while balanced by its gravity to keep equilibrium. It is clear in Figure 3.1 that, oil production in the well creates a pressure drawdown which elevates the oil water contact (OWC) in the immediate vicinity of the well. Water has the tendency to remain below the oil because of its higher density, which counterbalances the pressure drawdown caused by the oil production. These counterbalancing forces deform the OWC into a cone shape as we see in Figure 3.1. Because the production rate of a well is directly proportional to both the pressure drawdown and the reservoir permeability, one has to impose a larger pressure drawdown in a low permeability reservoir to achieve a given production rate than in a high permeability reservoir. As a result, water coning is easier to happen in a reservoir with low permeability.

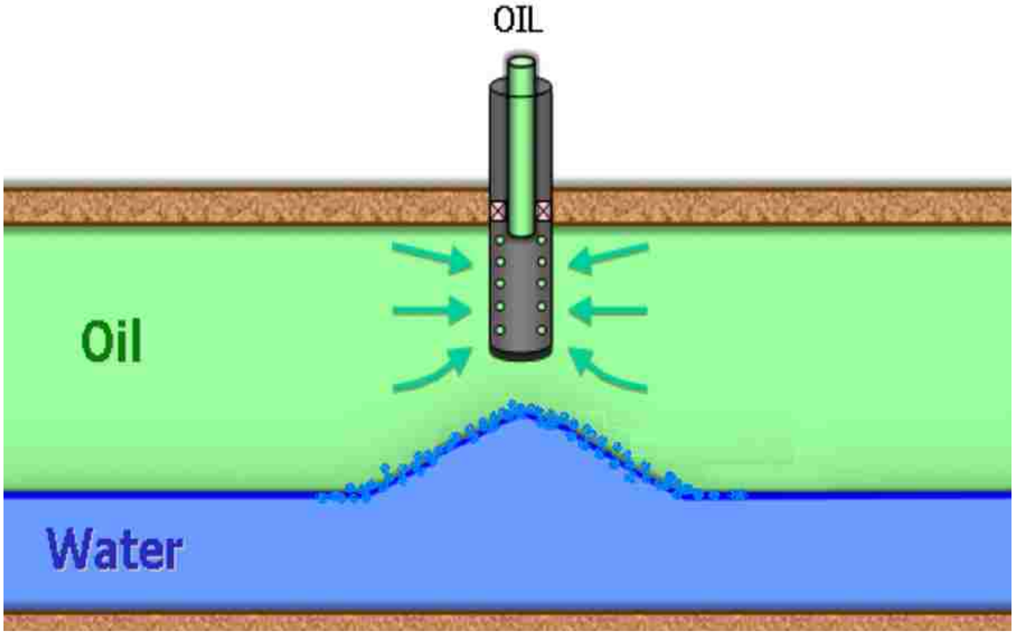

Figure 3.1 Schematic of water coning in reservoir with bottom water (Hernandez, 2007)

Generally, there are three forces that affect the fluid flow distribution around the wellbore: capillary force, gravity force and viscous force. Capillary force is quite small in almost most cases and is always ignored in water coning studies. Gravity force is downward in the vertical direction and arises from fluid density differences. Viscous force is the pressure drawdown causing fluids flowing in the reservoir as described by Darcy's Law. At a given time, there is a balance of these forces at any points in the reservoir. When the oil production rate is constant in a well and the viscous force acting in the vertical direction is less than the gravity force at the wellbore, then the water cone is stable and will not break into the well. If the oil production rate is increased and makes the vertical-acting viscous force exceed the gravity force at the wellbore, the cone will rise and eventually break into the oil well, and is called water breakthrough. The minimum oil production rate at which breakthrough occurs is called the critical production rate.

From the above discussion, it is clear to see that water coning can be minimized by reducing the pressure drawdown in the vicinity of the well. However, it is difficult to do in practice. Because the pressure drawdown is direct proportional to the oil production rate, reduction of pressure drawdown means the reduction of oil production rate at the same time. It is almost impossible to practice in the real fields. Engineers always reduce the well penetration or stimulate the horizontal permeability to reduce water coning. However, significantly additional pressure drawdown will be caused by short penetration skin which will accelerate the water coning. It is hard to lessen the vertical permeability, although the ratio of horizontal to vertical permeability can be increased by acidizing or hydraulically fracturing the formation.

3.2. Critical Cone Height and Critical Oil Rate

3.2.1. Critical Cone Height

Experiments (Henley et al., 1961; Khan, 1970) show that when the well penetration is short and located at the top of the oil zone, the water cone (dynamic OWC) is stable under a certain height with a relatively small production rate. Increasing the oil rate slowly, the stable cone height will rise up too, when the oil rate reaches a certain value (q_{oC}), the cone height rises up to a maximum location (h_{oC}) to keep stable. If the oil rate exceeds a little bit than q_{oC}, the water cone will lose stability and water will breakthrough to the oil well immediately. The q_{oC} and h_{oC} are called critical oil rate and critical cone height, respectively.

Chaperon (1986) observed the similar phenomenon in oil wells with gas coning problems and she derived the correlations to calculate the critical cone height and critical oil rate in gas-oil system. Based on her methodology, the critical cone height and critical oil rate in water-oil system could be obtained as shown in the following derivations.

Suppose a vertical well is penetrated in the top of the oil zone. The penetration length is short enough to be treated as a point source as shown in Figure 3.2, the apex of the water cone is located at point " S " where is " Z_S " away from the point source.

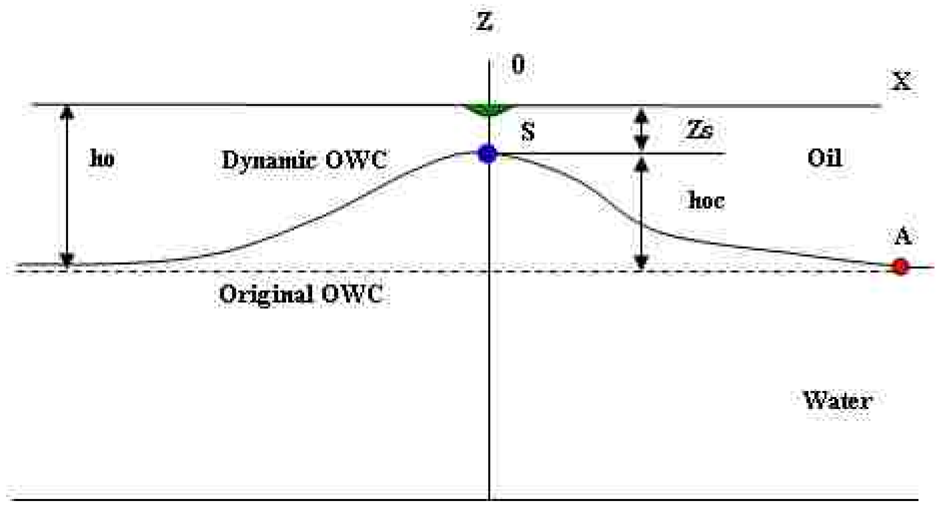

Figure 3.2 Water coning caused by short-penetrated vertical well

First, let's consider the isotropic formation and then the results could be extended to anisotropic system. According to Chaperon (1986), the flow potential corresponding to hemispherical flow induced by a point source located at the origin of a semi-infinite porous medium, limited by a no flow plane at $Z = 0$ is:

$$\Psi_M = \frac{q_o \mu_o}{2\pi k}\left(-\frac{1}{r}\right) \qquad (3.1)$$

Where " r " is the distance between the well point to any other point in the oil zone.

Because of the limitation of oil zone thickness, the no-flow boundary ($Z = h_o$) may be addressed by the method of images. The image well locations are $Z_n = \pm 2nh_o, X_n = 0$ as shown in Figure 3.3.

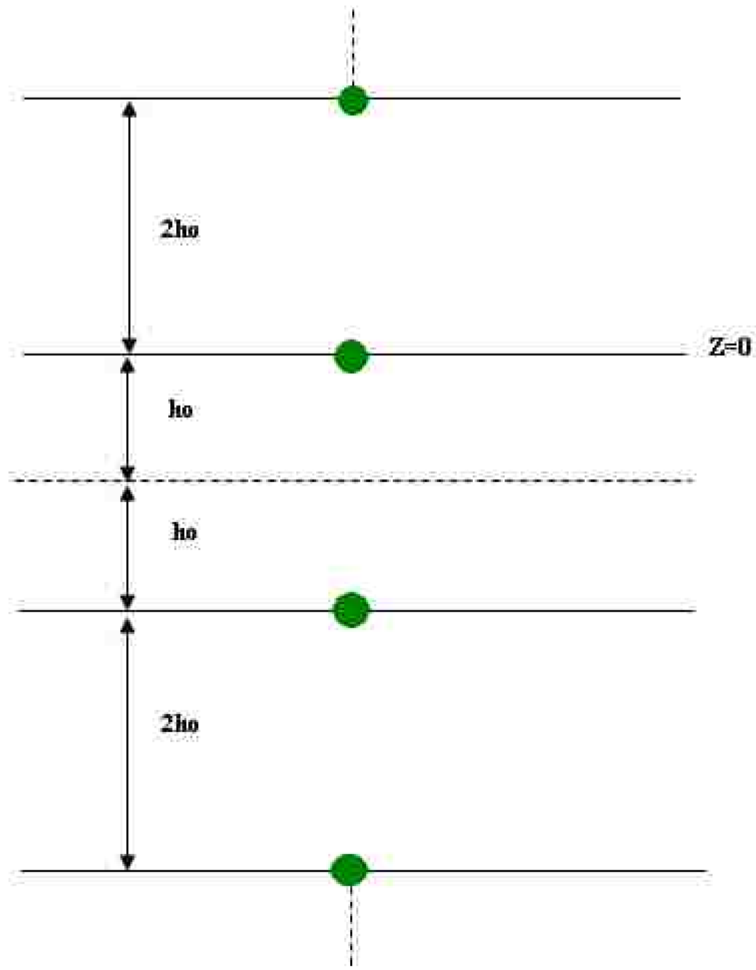

Figure 3.3 Image wells generated by no-flow boundary at $Z = h_o$

The viscous flow potential caused by each image well could be calculated by Equation 3.1. If we consider a point A, which is located at the OWC far away from the production well with coordinates (r_A, h_o), and "S" is the apex of the water cone in equilibrium with coordinates ($0, Z_s$) below the well with oil rate "q_o"as shown in Figure 3.2. The potential difference between points "S" and "A" may be expressed as follows:

$$\Phi_A - \Phi_S = \frac{q_o \mu_o}{2\pi k} \sum_{n=-\infty}^{n=\infty} \left[\frac{1}{|Z_s + 2nh_o|} - \frac{1}{\left(r_A^2 + (Z_s + 2nh_o)^2\right)^{1/2}} \right] \text{.................................(3.2)}$$

The above potential difference should be equal to the potential of gravity forces under static equilibrium condition, which is:

$$\Phi_A - \Phi_S = \Delta\rho g (h_o - Z_s) \text{...(3.3)}$$

Solve Equation 3.3, we can get the oil rate to keep the system in equilibrium as:

$$q_o = \frac{1}{h_o \sum_{n=-\infty}^{n=\infty} \left[\frac{1}{|Z_s + 2nh_o|} - \frac{1}{\left(r_A^2 + (Z_s + 2nh_o)^2\right)^{1/2}} \right]} \frac{kh_o}{\mu_o} (\Delta\rho g h_o) 2\pi \left(1 - \frac{Z_s}{h_o}\right) \text{..........(3.4)}$$

A dimensionless oil rate " q_o^* " and cone height " z_{SC}^* " can be defined from Equation 3.4 as follows:

$$q_o^* = \frac{1}{h_o \sum_{n=-\infty}^{n=\infty} \left[\frac{1}{|Z_s + 2nh_o|} - \frac{1}{\left(r_A^2 + (Z_s + 2nh_o)^2\right)^{1/2}} \right]} 2\pi \left(1 - \frac{Z_s}{h_o}\right) \text{............................(3.5)}$$

$$z_{SC}^* = \frac{Z_s}{h_o} \text{...(3.6)}$$

In addition to static equilibrium, dynamic equilibrium (stability condition) should be achieved too, which means that, if a perturbation of the interface occurs, water should not breakthrough to the oil well. Mathematically, this condition could be satisfied if the change of gravity potential is greater than the change of viscous potential:

$$\Delta\rho g \geq \frac{d}{dZ_s} (\Phi_A - \Phi_S) \text{...(3.7)}$$

The critical water cone height could be obtained when the left hand item is equal to the right hand item in Equation 3.7.

Notice that, the above derivation only considered the isotropic formation where the vertical permeability is equal to the horizontal permeability. However, these two permeabilities are not the same in most cases, in other words, most formations are anisotropic ($k_h \neq k_v$). In order to analyze the coning problem in anisotropic reservoirs, it is necessary to transform the anisotropy to isotropy first. Transformation factors are used for this purpose (detailed derivation of these factors will be shown in section 3.4) as follows:

$$\bar{k} = k' = \sqrt[3]{k_h^2 k_v} \qquad (3.8)$$

$$\begin{cases} r_A' = \sqrt{\dfrac{\bar{k}}{k_h}} r_A \\ h_o' = \sqrt{\dfrac{\bar{k}}{k_v}} h_o \\ \Delta\rho' = \sqrt{\dfrac{k_v}{\bar{k}}} \Delta\rho \end{cases} \qquad (3.9)$$

Substitute Equations 3.8 and 3.9 to Equation 3.5, another dimensionless number could be defined as the permeability ratio:

$$\alpha = \frac{r_A}{h_o}\sqrt{\frac{k_v}{k_h}} \qquad (3.10)$$

The critical cone height can be observed by plotting the dimensionless oil rate versus the dimensionless cone height as shown in Figure 3.4. It can be seen from the figure that, the dimensionless cone height varies between 0.3 and 0.5 within a wide permeability ratio range. Chaperon's (1986) presented that the relative error of this method is smaller than 25% when $1.7 \le \alpha \le 44.7$, which indicates that the dimensionless cone height may vary between 0.2 and 0.6 within the same permeability ratio range.

However, people usually penetrate wells about half of the oil zone (Bournazel and Jeanson, 1971), which means water may breakthrough to the wells before reach the critical height. This maybe one of the reasons why people assume the critical height is equal to the distance from well bottom to the original OWC when calculating the critical oil rate.

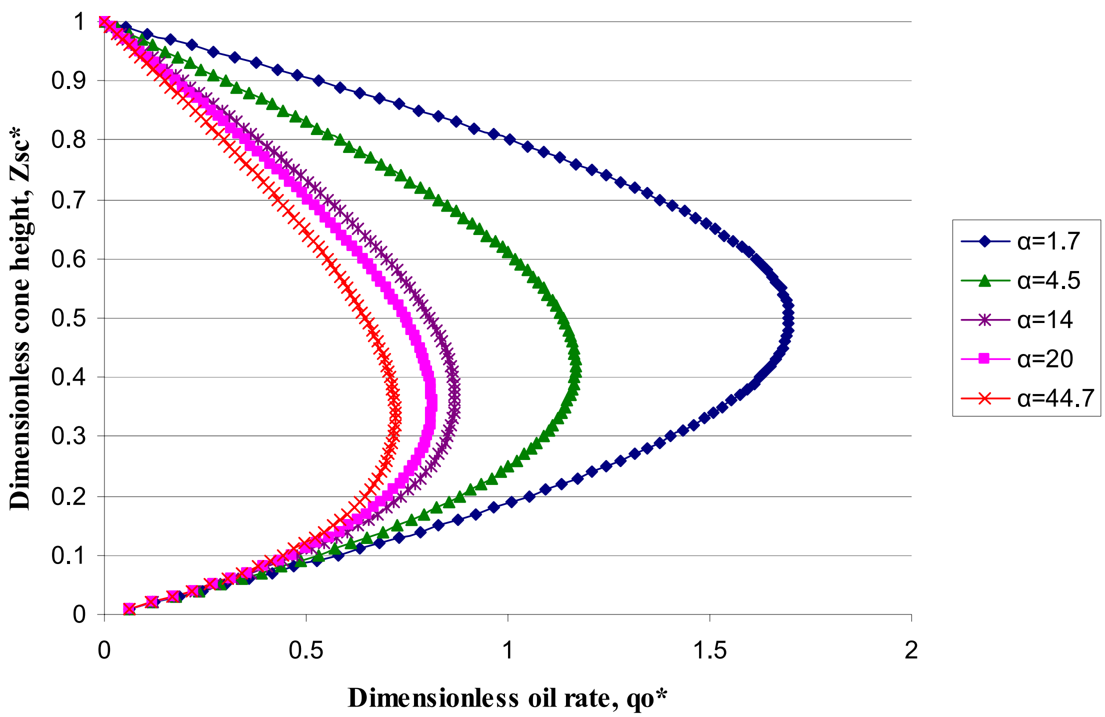

Figure 3.4 Dimensionless cone height vs. dimensionless oil rate

Although the existence of critical water cone height was proved both analytically and experimentally (Chaperon, 1986; Henley et al., 1961; Khan, 1970), it was not always observed (Abass and Bass, 1988). And in order to simplify the calculation in water coning problems, people usually assume that the critical cone height is equal to the distance from the well bottom to the original OWC (Meyer and Gardner, 1954; Guo and Lee, 1993; Armenta, 2003; Ahmed, 2006; Tabatabaei et al, 2008), although this assumption is not really true for all situations, it is reasonable in calculation, which was explained by Guo and Lee in 1993 as follows:

In the development of water coning, the upward dynamic force resulting from the pressure drawdown causes the bottom water to rise to a height where the dynamic force is balanced by the weight of water beneath this point. The balance makes the OWC shape as a stable cone. Oil flows above the OWC, while water remains stationary below it. As the production rate increases, the height of the cone above the original OWC also increases until, at a certain production rate, the cone becomes unstable and water is produced into the well.

The water cone becomes unstable at a certain point because the dynamic pressure gradient above this point (beneath the well bottom) is greater than the hydrostatic pressure gradient of water. Therefore, the water in the cone above this critical point cannot remain stationary and flows upward to search for another balance until water breakthrough to the well. This phenomenon usually occurs when rock conductivity is low, which can be called as low conductivity case. In this case, the oil pressure gradient curve can intersect the water pressure gradient line at two points. The height of the lower intersection point is the height of the stable water cone. With the increase of oil production rate, the pressure drawdown increases in the oil zone, which makes the lower intersection point shift upward and the upper intersection point shift downward until they meet at one point. The height of this point is the maximum height of the stable water cone. Because the oil pressure gradient everywhere above this point is greater than hydrostatic water pressure gradient, the water cone above this point is unstable. The oil production rate at this maximum cone height is called as critical rate. Figure 3.5

illustrates water coning in the low conductivity case. Line A-B represents the pressure distribution in the oil zone when the oil production rate is zero, and line B-C represents the pressure distribution in the water cone. With the increase of oil rate, the oil pressure distribution curve shifts to the left until it is tangential to line B-C at point D, which is the critical cone height. In this case, the unstable cone exists and it could be observed above point D.

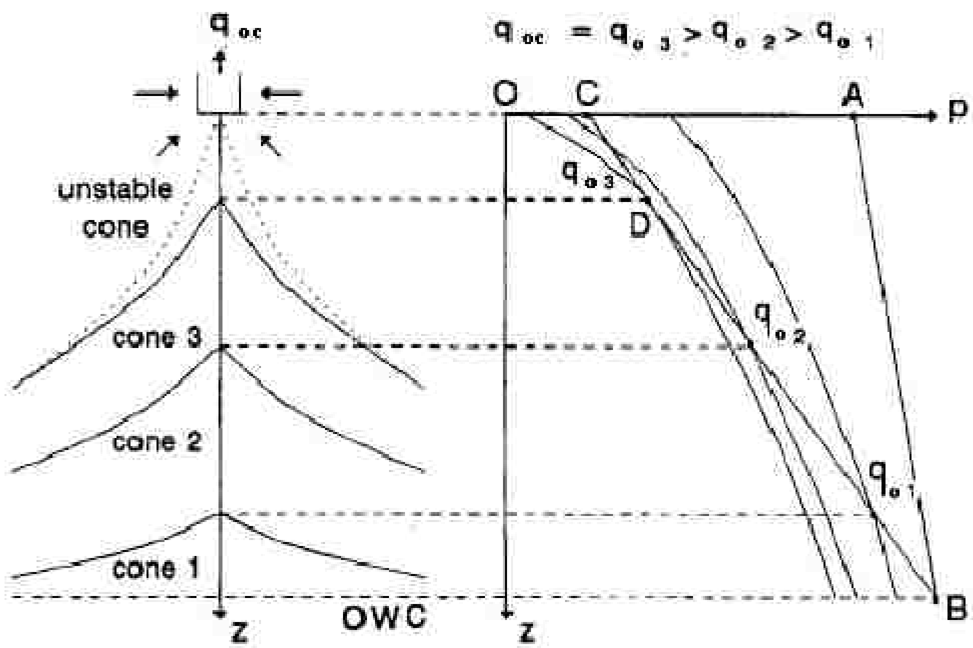

Figure 3.5 Low conductivity case, unstable cone exists (Guo and Lee, 1993)

However, when the conductivity of reservoir is high, the unstable cone might not happen before the water cone reaches to the bottom of the well. In other words, with the increase of oil production rate, the stable water cone can grow to the bottom of the wellbore without losing stability along the way. In this situation, the unstable cone and the associated critical rate could not be observed because the stable cone touches the well bottom before the appearance of the unstable water cone. In this case, the oil pressure gradient curve intersects the water pressure gradient line at only one point. The height of the intersection point is the height of the stable water cone for a given oil production rate. Figure 3.6 illustrates this case: the water cone reaches to the bottom of the well before the oil pressure distribution curve can be tangential to line B-C. Therefore, in high conductivity case, the critical cone height is equal to the distance from the well bottom to the original OWC, and the critical rate can be determined when the water cone touches the bottom of the well.

Because water coning happens in a region near the wellbore and people usually stimulate this region to make the fluids easier to flow, which indicates the conductivity is always high in the near wellbore area. Therefore, the high conductivity case is used in this study as well as many other researchers (Meyer and Gardner, 1954; Abass and Bass, 1988; Guo and Lee, 1993; Armenta, 2003; Tabatabaei et al, 2008), the distance from well bottom to original OWC is used to approximate the critical cone height.

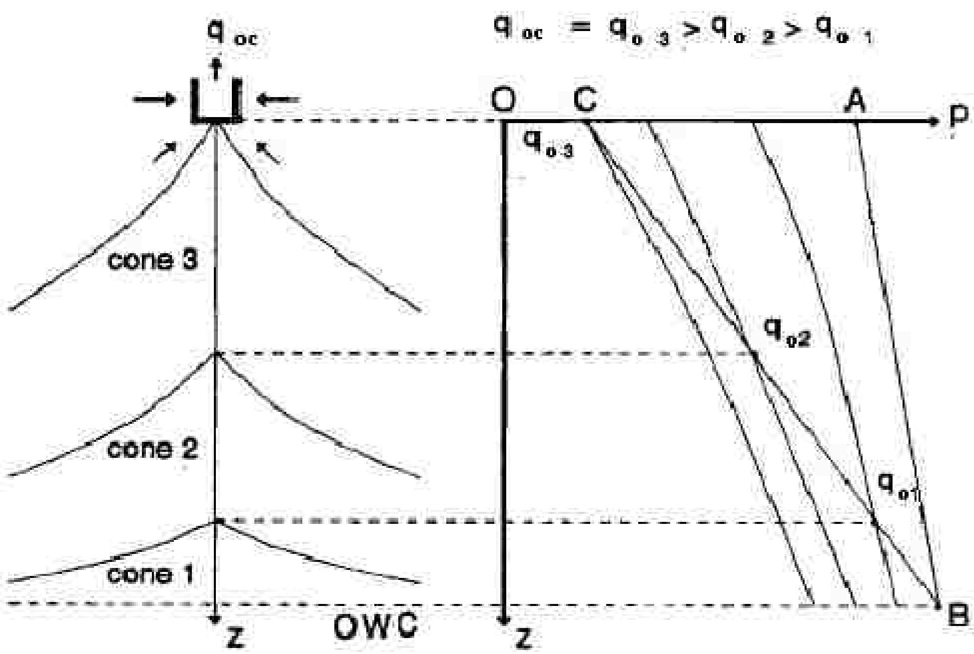

Figure 3.6 High conductivity case, no unstable cone exists (Guo and Lee, 1993)

3.2.2. Critical Oil Rate

Equation 3.4 could be used to calculate the critical oil rate. However, the inconveniences of this equation are that, many iteration steps are needed to get a single critical oil rate, no explicit solution exists for critical height and the effects of well radius and partial penetration cannot be considered. The relative error of Equation 3.4 is influenced by α as shown in Figure 3.7, which can be as high as 25%.

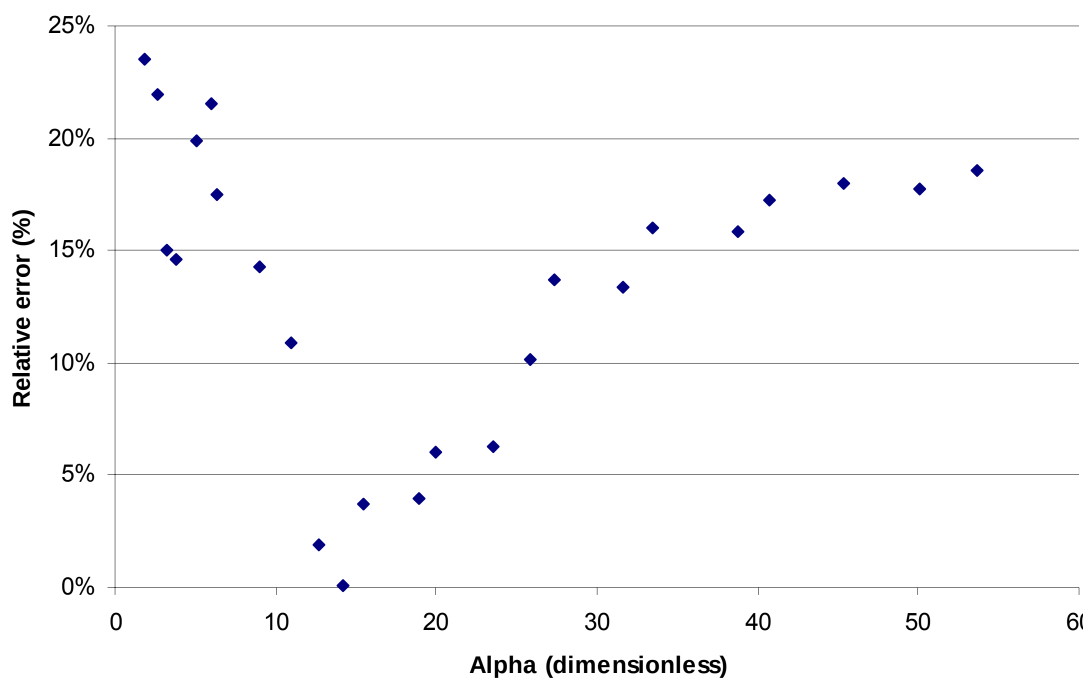

Figure 3.7 Relative error of Chaperon's method

Chaperon (1986) noticed the relative error of this formula, but she did not explain why there existed such an error. Based on the above discussion of critical cone height, the reasons of the error of Chaperon's method could be explained as follows:

In spherical flow model, the pressure gradient in the oil zone is inversely proportional to the squared radius of the cone, which is approximated by the squared radius of the drainage area in Chaperon's formula, the greater the drainage radius, the smaller the pressure gradient. The critical cone height is directly proportional to the pressure gradient. As a result, the critical cone height will be smaller and the calculated critical oil rate will be lower with the increase of the drainage radius, which means water will be easier to breakthrough to the oil well when the drainage radius is greater. However, the cone radius is much smaller than the drainage radius in real field. Chaperon included the drainage radius in the dimensionless number α as shown in Equation 3.10. As shown in Figure 3.7, the relative error decreases when the drainage radius approaches to the cone radius and it increases when the drainage radius keeps increasing and deviating from the cone radius.

Since we know that, the distance from well bottom to original OWC could be used to approximate the critical cone height, the following method could be used to calculate the critical oil rate instead of Equation 3.4.

In an isotropic reservoir ($k_h = k_v$), the pressure drawdown caused by oil production can be expressed in steady-state homogeneous radial equation (Darcy's Law) as:

$$\Delta p_{op} = \frac{141.2 q_o \mu_o B_o}{k_o h_o} \ln \frac{r_e}{r_w} \quad \text{.......(3.11)}$$

Because wells are often partially penetrated, the partial penetration will cause an additional pressure drawdown expressed as:

$$\Delta p_S = \frac{141.2 q_o \mu_o B_o}{k_o h_o} S_{pp} \quad \text{.......(3.12)}$$

Thus, the total pressure drawdown is the sum of them:

$$\Delta p_o = \frac{141.2 q_o \mu_o B_o}{k_o h_o} \left(\ln \frac{r_e}{r_w} + S_{pp} \right) \quad \text{.......(3.13)}$$

The potential of gravity forces is:

$$p_G = 0.433(\gamma_w - \gamma_o)(h_o - h_{op}) \quad (3.14)$$

When the total pressure drawdown is the same to the gravity difference, the water cone is stable, and the critical oil rate can be calculated by this equilibrium equation:

$$\Delta p_o = p_G \quad (3.15)$$

$$q_{oC} = \frac{0.003066(\gamma_w - \gamma_o)(h_o - h_{op})k_o h_o}{\mu_o B_o \left(\ln \frac{r_e}{r_w} + S_{pp} \right)} \quad (3.16)$$

The above equation is valid for the isotropic reservoir, and in the following sections of this chapter, it will be extended to anisotropic reservoir with detailed derivation.

3.3. Partial Penetration Skin

The skin factor caused by the partial penetration has been widely studied and many correlations have been developed. Papatzacos (1987) provided one of the most popular correlations to calculate this skin factor which has been used for many years. The well-reservoir system used in his model is shown in Figure 3.8 and his skin factor correlation is calculated as:

$$S_{pp} = \left(\frac{1}{h_{pD}} - 1 \right) \ln \frac{\pi}{2r_D} + \frac{1}{h_{pD}} \ln \left[\frac{h_{pD}}{2 + h_{pD}} \left(\frac{A-1}{B-1} \right)^{1/2} \right] \quad (3.17)$$

Where,

$$r_D = (r_w / h_o)(k_v / k_h)^{1/2} \quad (3.18)$$

$$h_{pD} = h_{op} / h_o \quad (3.19)$$

$$h_{1D} = h_1 / h_o \qquad (3.20)$$

$$A = 1/\left(h_{1D} + h_{pD} / 4\right) \qquad (3.21)$$

$$B = 1/\left(h_{1D} + 3h_{pD} / 4\right) \qquad (3.22)$$

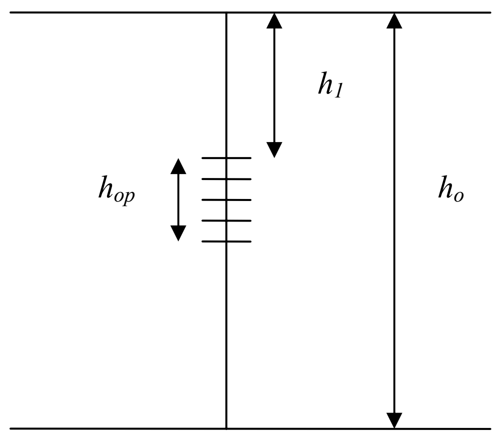

Figure 3.8 Partial penetration of a well

Where, h_1 is the distance from oil formation top to the penetration top, *ft*.

3.4. Anisotropic/Isotropic System Transformation

Most reservoirs in the real fields are anisotropic ($k_h \neq k_v$) where fluids flow in both horizontal and vertical directions. The vertical permeability effect is usually neglected when the well is fully penetrated and the horizontal permeability is much higher than the vertical permeability. Because at this situation, fluid moves in a horizontally radial flow which can be expressed as follows in steady state:

$$\frac{1}{r}\frac{d}{dr}\left(r\frac{dp}{dr}\right) = o \qquad (3.23)$$

But when the well is partially penetrated and the water drive of aquifer is strong, the vertical permeability effect cannot be ignored anymore (Kucuk and Brigham, 1979; Sheng, et al, 2006). The diffusivity equation should be modified as:

$$\frac{1}{r}\frac{\partial}{\partial r}\left(r\frac{\partial p}{\partial r}\right)+\frac{\partial^2 p}{\partial z^2}=o \quad (3.24)$$

Although only one item is added to the diffusivity equation, it is difficult to couple it. In order to solve this problem, several methods have been used:

1. Using numerical algorithm;
2. Using spherical flow model by anisotropy transformation;
3. Using radial flow model by anisotropy transformation.

Numerical algorithm is widely used with the widely applications of computer, but it is almost impossible to get a solution without the help of computer. Spherical flow model is easy to apply in anisotropic system; however, it needs to use superposition theory when there are no flow boundaries near the well. As a result, multiple sums are needed to get a solution. The process is time-consuming if there is no computer. The third method is more recent and easier to use than the former two (Besson, 1990; Spivey and Lee, 1999; Boughrara et al. 2007; Utama, 2008). By transforming the original problem with anisotropic permeability into an equivalent problem with isotropic permeability, the pressure response in an anisotropic system will be the same to that of an isotropic system (Spivey and Lee, 1999). As a relatively new method, the derivation process seems over-simplified in literature. In order to make this method clear, the derivation process is proposed as follows:

First, let's consider the flow in Cartesian coordinates for the purpose of convenience. The following assumptions are made:

1. The reservoir is anisotropic and homogeneous with uniform thickness. All formation properties are assumed to be independent of pressure;
2. The fluid is slightly compressible with constant viscosity in the reservoir.

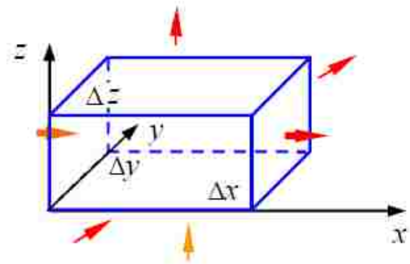

Figure 3.9 Basic control unit in reservoir

Take a small control unit (cube) from the reservoir as shown in Figure 3.9, which is small enough to ignore the gravity ($\Phi = P + \rho g z \approx P$).

Conservation of mass (in "x, y, z" directions):

Mass in: $\rho u_x\big|_x \Delta y \Delta z$, $\rho u_y\big|_y \Delta x \Delta z$, $\rho u_z\big|_z \Delta x \Delta y$

Mass out: $\rho u_x\big|_{x+\Delta x} \Delta y \Delta z$, $\rho u_y\big|_{y+\Delta y} \Delta x \Delta z$, $\rho u_z\big|_{z+\Delta z} \Delta x \Delta y$

Rate of accumulation in the control unit:

$$\Delta m = \Delta x \Delta y \Delta z \frac{\partial(\phi\rho)}{\partial t} \quad \text{.........(3.25)}$$

$$\sum_{x,y,z} m_{in} - \sum_{x,y,z} m_{out} = \Delta m \quad \text{.........(3.26)}$$

$$\begin{aligned}&(\rho u_x\big|_x - \rho u_x\big|_{x+\Delta x})\Delta y \Delta z + (\rho u_y\big|_y - \rho u_y\big|_{y+\Delta y})\Delta x \Delta z + \\ &(\rho u_z\big|_z - \rho u_z\big|_{z+\Delta z})\Delta y \Delta x = \Delta x \Delta y \Delta z \frac{\partial(\phi\rho)}{\partial t}\end{aligned} \quad \text{.........(3.27)}$$

$$\lim_{\Delta x, \Delta y, \Delta z \to 0} (Eqn.\,3.27) = -\frac{\partial}{\partial x}(\rho u_x) - \frac{\partial}{\partial y}(\rho u_y) - \frac{\partial}{\partial z}(\rho u_z) = \frac{\partial(\phi\rho)}{\partial t} \quad \text{.........(3.28)}$$

From Darcy's Law:

$$\begin{cases} u_x = \dfrac{-k_x}{\mu}\dfrac{\partial p}{\partial x} \\ u_y = \dfrac{-k_y}{\mu}\dfrac{\partial p}{\partial y} \\ u_z = \dfrac{-k_z}{\mu}\dfrac{\partial p}{\partial z} \end{cases} \quad \text{.......(3.29)}$$

$$\frac{\partial}{\partial x}(\rho\frac{k_x}{\mu}\frac{\partial p}{\partial x}) + \frac{\partial}{\partial y}(\rho\frac{k_y}{\mu}\frac{\partial p}{\partial y}) + \frac{\partial}{\partial z}(\rho\frac{k_z}{\mu}\frac{\partial p}{\partial z}) = \frac{\partial(\phi\rho)}{\partial t} \quad \text{.......(3.30)}$$

From the definition of compressibility, we can get the following formulas:

$$\because C = -\frac{1}{V}\frac{\partial V}{\partial P} \quad \text{.......(3.31)}$$

$$V = \frac{m}{\rho} \quad \text{.......(3.32)}$$

$$\Rightarrow \frac{\partial V}{\partial P} = \frac{\partial}{\partial P}(\frac{m}{\rho}) \quad \text{.......(3.33)}$$

$$\Rightarrow C = \frac{1}{\rho}\frac{\partial \rho}{\partial P} \quad \text{.......(3.34)}$$

$$\Rightarrow \rho C = \frac{\partial \rho}{\partial P} \quad \text{.......(3.35)}$$

Substitute Equation 3.35 into Equation 3.30:

$$\begin{aligned} &\frac{k_x}{\mu}(\frac{\partial \rho}{\partial x}\frac{\partial P}{\partial x} + \rho\frac{\partial^2 P}{\partial x^2}) + \frac{k_y}{\mu}(\frac{\partial \rho}{\partial y}\frac{\partial P}{\partial y} + \rho\frac{\partial^2 P}{\partial y^2}) + \\ &\frac{k_z}{\mu}(\frac{\partial \rho}{\partial z}\frac{\partial P}{\partial z} + \rho\frac{\partial^2 P}{\partial z^2}) = \frac{\partial(\phi\rho)}{\partial t} \end{aligned} \quad \text{.......(3.36)}$$

$$\begin{aligned} &\frac{k_x}{\mu}\left[\frac{\partial \rho}{\partial P}(\frac{\partial P}{\partial x})^2 + \rho\frac{\partial^2 P}{\partial x^2}\right] + \frac{k_y}{\mu}\left[\frac{\partial \rho}{\partial P}(\frac{\partial P}{\partial y})^2 + \rho\frac{\partial^2 P}{\partial y^2}\right] + \\ &\frac{k_z}{\mu}\left[\frac{\partial \rho}{\partial P}(\frac{\partial P}{\partial z})^2 + \rho\frac{\partial^2 P}{\partial z^2}\right] = \frac{\partial(\phi\rho)}{\partial t} \end{aligned} \quad \text{.......(3.37)}$$

$$\frac{k_x}{\mu}\left[\rho C(\frac{\partial P}{\partial x})^2\right]+\frac{k_y}{\mu}\left[\rho C(\frac{\partial P}{\partial y})^2\right]+\frac{k_z}{\mu}\left[\rho C(\frac{\partial P}{\partial z})^2\right]+$$
$$\frac{k_x\rho}{\mu}\frac{\partial^2 P}{\partial x^2}+\frac{k_y\rho}{\mu}\frac{\partial^2 P}{\partial y^2}+\frac{k_z\rho}{\mu}\frac{\partial^2 P}{\partial z^2}=\frac{\partial(\phi\rho)}{\partial t} \quad \text{...(3.38)}$$

Because “C” and pressure gradient are very small, they can be neglected. Equation 3.38 becomes:

$$\frac{k_x\rho}{\mu}\frac{\partial^2 P}{\partial x^2}+\frac{k_y\rho}{\mu}\frac{\partial^2 P}{\partial y^2}+\frac{k_z\rho}{\mu}\frac{\partial^2 P}{\partial z^2}=\frac{\partial(\phi\rho)}{\partial t} \quad \text{...(3.39)}$$

$$\frac{\partial(\phi\rho)}{\partial t}=\rho\frac{\partial\phi}{\partial t}+\phi\frac{\partial\rho}{\partial t}=\rho\frac{\partial\phi}{\partial t}+\phi\frac{\partial\rho}{\partial P}\frac{\partial P}{\partial t}=\rho\frac{\partial\phi}{\partial t}+\phi\rho C\frac{\partial P}{\partial t} \quad \text{.............................(3.40)}$$

Define:

$$C_f=\frac{1}{\phi}\frac{\partial\phi}{\partial P}\Rightarrow\phi C_f=\frac{\partial\phi}{\partial P} \quad \text{..(3.41)}$$

$$\frac{\partial(\phi\rho)}{\partial t}=\rho\phi C_f\frac{\partial P}{\partial t}+\phi\rho C\frac{\partial P}{\partial t} \quad \text{...(3.42)}$$

Define:

$$C_t=C_f+C\Rightarrow\frac{\partial(\phi\rho)}{\partial t}=\phi\rho C_t\frac{\partial P}{\partial t} \quad \text{..(3.43)}$$

Substitute Equation 3.43 to Equation 3.39, we can get the diffusivity equation in anisotropic reservoir:

$$k_x\frac{\partial^2 P}{\partial x^2}+k_y\frac{\partial^2 P}{\partial y^2}+k_z\frac{\partial^2 P}{\partial z^2}=\phi\mu C_t\frac{\partial P}{\partial t} \quad \text{..(3.44)}$$

Introduce a general coordinate transformation:

$$\begin{cases} x^{'}=a_x x \\ y^{'}=a_y y \\ z^{'}=a_z z \end{cases} \quad \text{...(3.45)}$$

Assume:

$$a_x a_y a_z = 1 \quad \text{.......(3.46)}$$

Substitute Equation 3.45 into Equation 3.44:

$$\Rightarrow a_x^2 k_x \frac{\partial^2 P}{\partial x'^2} + a_y^2 k_y \frac{\partial^2 P}{\partial y'^2} + a_z^2 k_z \frac{\partial^2 P}{\partial z'^2} = \phi \mu C_t \frac{\partial P}{\partial t} \quad \text{.......(3.47)}$$

Define:

$$\begin{cases} k_x' = a_x^2 k_x \\ k_y' = a_y^2 k_y \\ k_z' = a_z^2 k_z \end{cases} \quad \text{.......(3.48)}$$

Substitute Equation 3.48 into Equation 3.47, we can get the diffusivity equation under the new coordinates as:

$$k_x' \frac{\partial^2 P}{\partial x'^2} + k_y' \frac{\partial^2 P}{\partial y'^2} + k_z' \frac{\partial^2 P}{\partial z'^2} = \phi \mu C_t \frac{\partial P}{\partial t} \quad \text{.......(3.49)}$$

According to the mass conservation law, the volumetric flow rate through a small unit is the same in both coordinates. In original coordinates:

$$q = \vec{v} \cdot d\vec{A} = \frac{k_x}{\mu} \frac{\partial P}{\partial x} dydz + \frac{k_y}{\mu} \frac{\partial P}{\partial y} dxdz + \frac{k_z}{\mu} \frac{\partial P}{\partial z} dxdy \quad \text{.......(3.50)}$$

Substitute Equation 3.48 into Equation 3.50:

$$\begin{aligned} q = \vec{v} \cdot d\vec{A} &= \frac{k_x'}{\mu} \frac{\partial P}{\partial x'} dy' dz' + \frac{k_y'}{\mu} \frac{\partial P}{\partial y'} dx' dz' + \frac{k_z'}{\mu} \frac{\partial P}{\partial z'} dx' dy' \\ &= \vec{v}' \cdot d\vec{A}' \end{aligned} \quad \text{.......(3.51)}$$

In isotropic system:

$$k_x = k_y = k_z \quad \text{.......(3.52)}$$

In order to transform the original anisotropic system to equivalent isotropic system, the following relationship should be satisfied:

$$k_x^{'} = k_y^{'} = k_z^{'} \qquad (3.53)$$

$$\Rightarrow a_x^2 k_x = a_y^2 k_y = a_z^2 k_z \qquad (3.54)$$

Combine Equations 3.46 and 3.54, we can get the following formulas:

$$\begin{cases} a_x = \sqrt{\dfrac{\sqrt[3]{k_x k_y k_z}}{k_x}} \\ a_y = \sqrt{\dfrac{\sqrt[3]{k_x k_y k_z}}{k_y}} \\ a_z = \sqrt{\dfrac{\sqrt[3]{k_x k_y k_z}}{k_z}} \end{cases} \qquad (3.55)$$

$$\Rightarrow \overline{k} = k_x^{'} = k_y^{'} = k_z^{'} = \sqrt[3]{k_x k_y k_z} \qquad (3.56)$$

$$\begin{cases} x^{'} = \sqrt{\dfrac{\overline{k}}{k_x}} x \\ y^{'} = \sqrt{\dfrac{\overline{k}}{k_y}} y \\ z^{'} = \sqrt{\dfrac{\overline{k}}{k_z}} z \\ \Delta\rho^{'} = \sqrt{\dfrac{k_z}{\overline{k}}} \Delta\rho \end{cases} \qquad (3.57)$$

Simplify the above procedure, problem in 2-D Cartesian coordinates has the following transformation:

$$\begin{cases} a_x = \sqrt[4]{\dfrac{k_z}{k_x}} \\ a_z = \sqrt[4]{\dfrac{k_x}{k_z}} \end{cases} \quad \text{...} (3.58)$$

$$\Rightarrow \bar{k} = k_x^{'} = k_z^{'} = \sqrt{k_x k_z} \quad \text{...} (3.59)$$

$$\begin{cases} x^{'} = \sqrt{\dfrac{\bar{k}}{k_x}} x \\ z^{'} = \sqrt{\dfrac{\bar{k}}{k_z}} z \\ \Delta\rho^{'} = \sqrt{\dfrac{k_z}{\bar{k}}} \Delta\rho \end{cases} \quad \text{...} (3.60)$$

With the same process, diffusivity equation in 2-D Cylinder coordinates is:

$$\frac{k_r}{\mu}\frac{1}{r}\frac{\partial}{\partial r}\left(r\frac{\partial P}{\partial r}\right) + \frac{k_z}{\mu}\frac{\partial^2 P}{\partial z} = \phi C_t \frac{\partial P}{\partial t} \quad \text{..} (3.61)$$

Define:

$$\begin{cases} r^{'} = a_r r \\ z^{'} = a_z z \end{cases} \quad \text{...} (3.62)$$

Assume:

$$a_r a_z = 1 \quad \text{..} (3.63)$$

Substitute Equation 3.62 into Equation 3.61:

$$\Rightarrow \frac{a_r^2 k_r}{r^{'}}\frac{\partial}{\partial r^{'}}\left(r^{'}\frac{\partial P}{\partial r^{'}}\right) + a_z^2 k_z \frac{\partial^2 P}{\partial z^{'2}} = \phi\mu C_t \frac{\partial P}{\partial t} \quad \text{..} (3.64)$$

$$\Rightarrow \begin{cases} k_r^{'} = a_r^2 k_r \\ k_z^{'} = a_z^2 k_z \end{cases} \quad \text{...} (3.65)$$

$$\because q = \vec{v} \cdot d\vec{l} = \frac{k_r}{\mu}\frac{\partial P}{\partial r}dz + \frac{k_z}{\mu}\frac{\partial P}{\partial z}dr \quad \text{.........(3.66)}$$

$$\begin{aligned} \Rightarrow q &= \frac{1}{\mu}\left[\frac{1}{a_r a_z}\right]\left[k_r^{'}\frac{\partial P}{\partial r^{'}}dz^{'} + k_z^{'}\frac{\partial P}{\partial z^{'}}dr^{'}\right] \\ &= \frac{1}{\mu}\left[k_r^{'}\frac{\partial P}{\partial r^{'}}dz^{'} + k_z^{'}\frac{\partial P}{\partial z^{'}}dr^{'}\right] \quad \text{.........(3.67)} \\ &= \vec{v}^{'} \cdot d\vec{l}^{'} \end{aligned}$$

In order to transform the original anisotropic system to equivalent isotropic system, the following relationship should be satisfied:

$$k_r^{'} = k_z^{'} \quad \text{.........(3.68)}$$

$$\Rightarrow a_r^2 k_r = a_z^2 k_z \quad \text{.........(3.69)}$$

Combine Equations 3.63 and 3.69, we can get the following formulas:

$$\begin{cases} a_r = \sqrt[4]{\dfrac{k_z}{k_r}} \\ a_z = \sqrt[4]{\dfrac{k_r}{k_z}} \end{cases} \quad \text{.........(3.70)}$$

$$\Rightarrow \bar{k} = k_r^{'} = k_z^{'} = \sqrt{k_r k_z} \quad \text{.........(3.71)}$$

$$\begin{cases} r^{'} = \sqrt{\dfrac{\bar{k}}{k_r}}r \\ z^{'} = \sqrt{\dfrac{\bar{k}}{k_z}}z \\ \Delta\rho^{'} = \sqrt{\dfrac{k_z}{\bar{k}}}\Delta\rho \end{cases} \quad \text{.........(3.72)}$$

Applying to the same procedure to the spherical flow equations, we can get the following transformation factors:

$$\bar{k} = \sqrt[3]{k_x k_y k_z} \quad \text{.........(3.73)}$$

$$\begin{cases} x' = \sqrt{\dfrac{\bar{k}}{k_x}}x \\ y' = \sqrt{\dfrac{\bar{k}}{k_y}}y \\ z' = \sqrt{\dfrac{\bar{k}}{k_z}}z \\ \Delta\rho' = \sqrt{\dfrac{k_z}{\bar{k}}}\Delta\rho \end{cases} \qquad \text{...(3.74)}$$

After treating the anisotropic system by Equations 3.70 to 3.72, an equivalent isotropic system can be obtained. Equation 3.23 can be used instead of Equation 3.24 in water coning problem, which will make the task much easier to carry out. Notice that, the above derivation is based on the method presented by Spivey and Lee (1999), I just extended the method to get transformation factors for different flow models but I didn't use all of them in this study.

3.5. Modified Critical Oil Rate Correlation

After knowing how to address the partial penetration and anisotropy problems, the next step is to apply them to solve the water coning problem mentioned previously. Let's put more information on the system in Figure 3.1 which can be shown as Figure 3.10: a well is partially penetrated at the top of an anisotropic reservoir with bottom water, part of the parameters are shown in the figure. In order to determine the critical oil rate of this system, the following procedures are needed:

1. Transforming the anisotropic system to an equivalent isotropic system using Equations 3.70 to 3.72:

   Isotropic permeability:

$$\begin{cases} k' = k_h' = k_v' = \sqrt{k_h k_v} \\ k_o = k' k_{ro} \\ k_w = k' k_{rw} \end{cases} \qquad \text{...(3.75)}$$

Equivalent spatial and directional properties in isotropic system are shown in Equation 3.76;

$$\begin{cases} r_w' = \sqrt[4]{\dfrac{k_v}{k_h}} r_w \\ r_e' = \sqrt[4]{\dfrac{k_v}{k_h}} r_e \\ h_{op}' = \sqrt[4]{\dfrac{k_h}{k_v}} h_{op} \\ h_o' = \sqrt[4]{\dfrac{k_h}{k_v}} h_o \\ h_w' = \sqrt[4]{\dfrac{k_h}{k_v}} h_w \\ \Delta\rho' = \sqrt[4]{\dfrac{k_v}{k_h}} \Delta\rho \end{cases} \qquad \text{...(3.76)}$$

2. Determining the partial penetration skin factor using Papatzacos' method (Equations 3.17 to 3.22);
3. Calculating critical oil rate.

As indicated in many references (Schols 1972; Chaperon, 1986; Hoyland et al. 1989 and so on), the critical rate calculated from Equation 3.16 is always too conservative which is below the experimental and simulation results, and the equation needs to be amended. So, the dimensionless penetration ratio ($h_{pD} = h_{op} / h_o$) is combined into the equation as used by Hoyland et al. (1989). The final form of the equation for critical oil rate can be expressed as:

$$q_{oC} = \frac{0.003066\,(\gamma_w - \gamma_o)(h_o^{'} - h_{op}^{'})k_o h_o^{'}}{\mu_o B_o h_{pD}\left(\ln \frac{r_e^{'}}{r_w^{'}} + S_{pp}\right)} \quad \text{.......................................(3.77)}$$

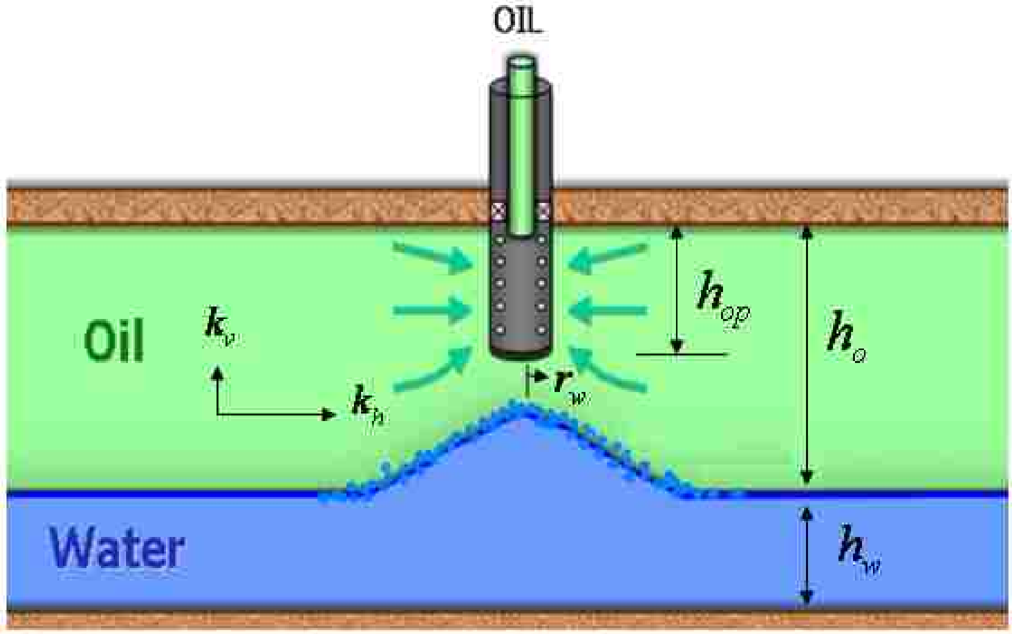

Figure 3.10 Schematic of a partial penetration well in an anisotropic reservoir with bottom water (Hernandez, 2007)

Critical oil rate in the bottom-water water reservoirs has been studied by several authors, who proposed different correlations (Meyer and Gardner, 1954; Schols 1972; Chaperon, 1986; Hoyland, Papatzacos and Skjaeveland, 1989 and so on). In order to verify Equation 3.77 in this study, the following four correlations are selected for comparison, as well as a numerical simulator --- CMG®:

Meyer and Gardner,

$$q_{MC} = \frac{0.001535 K_o (\rho_w - \rho_o)(h_o^2 - h_{op}^2)}{B_o \mu_o \ln \frac{r_e}{r_w}} \quad \text{...(3.78)}$$

Chaperon,

$$q_{CC} = \frac{4.888 \times 10^{-4} k_o h_o^2 (\rho_w - \rho_o)}{B_o \mu_o} \left[0.7311 + \frac{1.9434 h_o}{r_e \sqrt{\frac{k_v}{k_h}}} \right] \quad \text{.....................................(3.79)}$$

Schols,

$$q_{SC} = \frac{k_o (\rho_w - \rho_o)(h_o^2 - h_{op}^2)}{2049 B_o \mu_o} \left[0.432 + \frac{\pi}{\ln\left(\frac{r_e}{r_w}\right)} \right] \left(\frac{h_o}{r_e} \right)^{0.14} \quad \text{.......................................(3.80)}$$

Hoyland, Papatzacos and Skjaeveland,

$$q_{HC} = \frac{k_o (\rho_w - \rho_o)}{173.35 B_o \mu_o} \left[1 - \left(\frac{h_{op}}{h_o} \right)^2 \right]^{1.325} \left[\ln(r_e) \right]^{-1.990} h_o^{2.238} \quad \text{...............................(3.81)}$$

The properties of the well-reservoir system used in the comparison are listed in Table 3.1, Table 3.2 and Figure 3.11. Table 3.3 shows the grid division in simulation model, each grid has 0.5 ft and 1 ft height in vertical direction in oil zone and aquifer, respectively, and 0.05 ft width near the well in radial direction in both regions. Adopting the stratified random sampling method (Moser, 2009), the following ten cases (Table 3.4) are studied and the results are shown in Figure 3.12 to Figure 3.21.

Comparing to the simulation results, we can see that Meyer and Gardner's correlation usually gives lower outcomes, while Chaperon's correlation always gets higher values, and Equation 3.77 gives reasonable results which are similar to the simulation results in all of the ten cases, the relative errors are less than 15%. It means the method proposed in this chapter appears to be reasonable for critical oil rate calculation.

Table 3.1 Reservoir and well data

Data	Unit	Values
Datum depth	*ft*	15000
Thickness of oil zone	*ft*	50
Depth of WOC (original)	*ft*	15050
Thickness of water zone	*ft*	500
Reservoir pressure at datum depth	*ft*	6000
Position of top completion from formation top	*ft*	0
Thickness of top completion	*ft*	Vary
Horizontal permeability in oil zone (absolute)	*md*	80
Vertical permeability in oil zone (absolute)	*md*	Vary
Porosity in oil zone	*fraction*	0.3
Porosity in water zone	*fraction*	0.3
Well radius	*ft*	0.292
Outer radius	*ft*	1000
Total (rock + water) compressibility of the aquifer	*1/psi*	7.00E-06

Table 3.2 Fluid properties data

Data	Unit	Water	Oil	Rock
Reference pressure	*psi*	6000	6000	6000
Formation volume factor	*rb/stb*	1.02	1.26	
Compressibility	*1/psi*	0.000003	0.000015	0.000004
Viscosity	*cp*	0.4	0.8	
Surface density	*lb/cu-ft*	62.428	32.5	
Bubble point	*psi*		15	

Table 3.3 Grid division in simulation model for conventional well

Region	Direction	Grid Number
Oil Zone	**R**	50
	Θ	1
	Z	100
Aquifer	**R**	51
	Θ	1
	Z	500

Table 3.4 Cases studied for critical oil rate comparison

Cases / Ratios	1	2	3	4	5	6	7	8	9	10
Permeability ratio (k_v / k_h)	0.1	0.2	0.3	0.4	0.5	0.6	0.7	0.8	0.9	1.0
Penetration ratio (h_{op} / h_o)	0.1	0.3	0.9	0.4	0.6	0.4	0.5	0.8	0.5	0.7

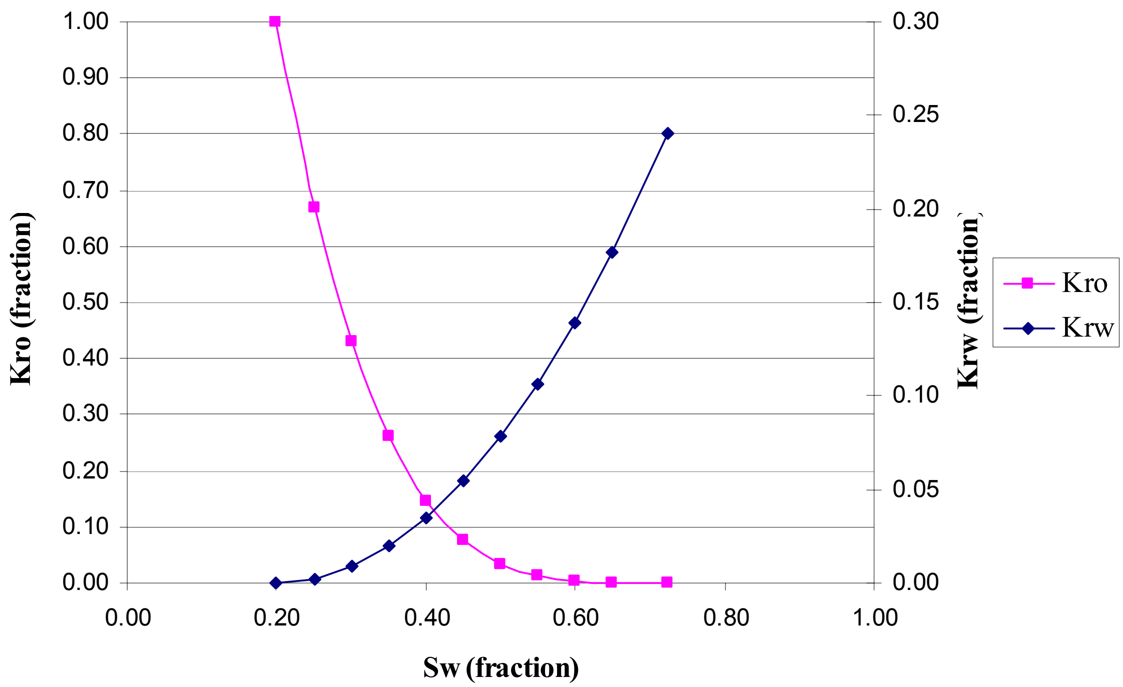

Figure 3.11 Relative permeability in simulation model for conventional well

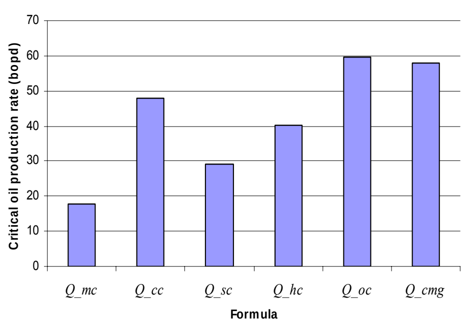

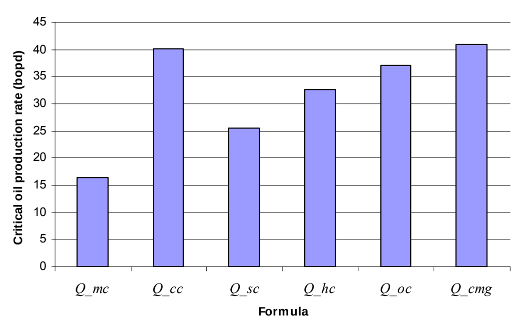

Figure 3.12 Case 1: k_v/k_h =0.1, h_{op}/h_o=0.1 **Figure 3.13 Case 2: k_v/k_h =0.2, h_{op}/h_o=0.3**

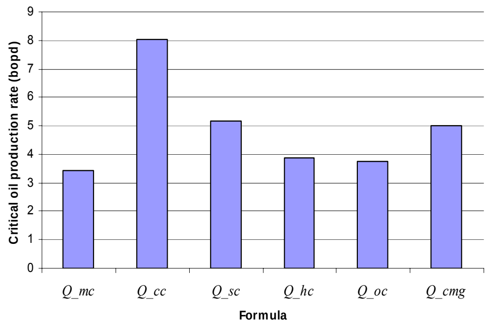

Figure 3.14 Case 3: k_v/k_h =0.3, h_{op}/h_o=0.9

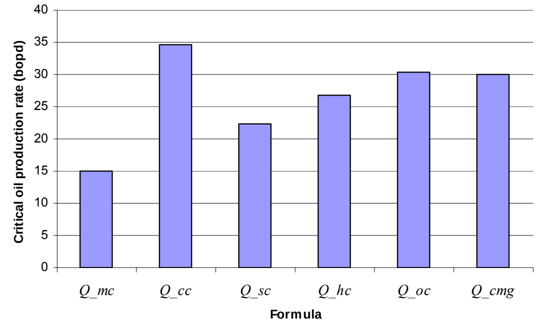

Figure 3.15 Case 4: k_v/k_h =0.4, h_{op}/h_o=0.4

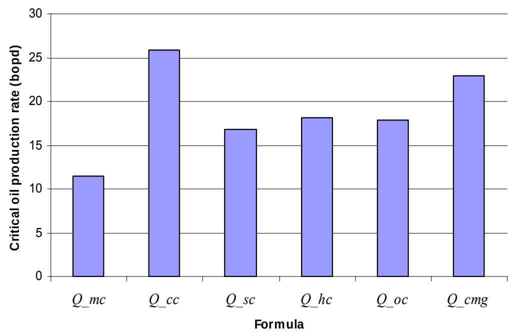

Figure 3.16 Case 5: k_v/k_h =0.5, h_{op}/h_o=0.6

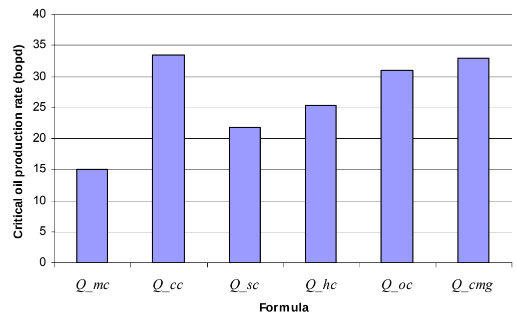

Figure 3.17 Case 6: k_v/k_h =0.6, h_{op}/h_o=0.4

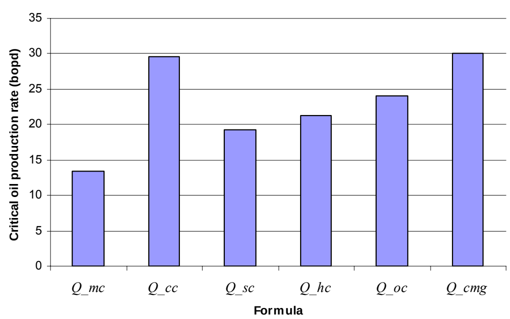

Figure 3.18 Case 7: k_v/k_h =0.7, h_{op}/h_o=0.5

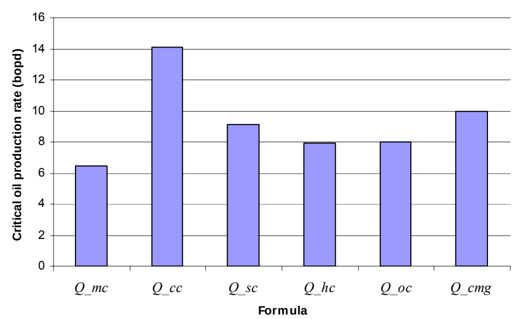

Figure 3.19 Case 8: k_v/k_h =0.8, h_{op}/h_o=0.8

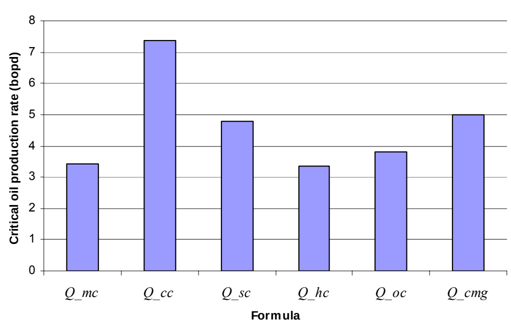

Figure 3.20 Case 9: k_v/k_h =0.9, h_{op}/h_o=0.5

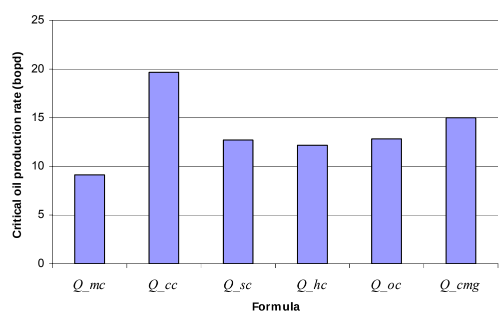

Figure 3.21 Case 10: k_v/k_h =1.0, h_{op}/h_o=0.7

3.6. Effect of Capillary Pressure on Critical Oil Rate

As mentioned in the beginning of this chapter, capillary pressure is ignored in most studies on water coning problems due to its small values relative to gravity and viscous effects. However, does it mean this small pressure should be neglected in critical oil rate calculation?

As we know, capillary pressure is the main reason of transition zone in oil reservoirs, where oil and water co-exist. The height of transition zone can be calculated by the following formula:

$$h_c = \frac{p_c}{0.433(\gamma_w - \gamma_o)} \quad (3.82)$$

Because the density difference between oil and water is usually small, a small capillary pressure can cause a considerable transition zone in the reservoir which makes it easier for water to breakthrough to the wells. As a result, the oil zone thickness in Equations 3.11 to 3.14 should be modified as:

$$h_{o\_CA} = h_o - h_c \quad (3.83)$$

And the critical oil rate with capillary pressure considered is:

$$q'_{oC} = \frac{0.003066(\gamma_w - \gamma_o)(h'_{o\_CA} - h'_{op})k_o h'_{o\_CA}}{\mu_o B_o h_{pD}\left(\ln\frac{r'_e}{r'_w} + S_{pp}\right)} \quad (3.84)$$

Using the same data to the previous example and assuming the capillary pressure is 4 psi as shown in Figure 3.22, the new critical oil rates can be shown as Figure 3.23 to Figure 3.32.

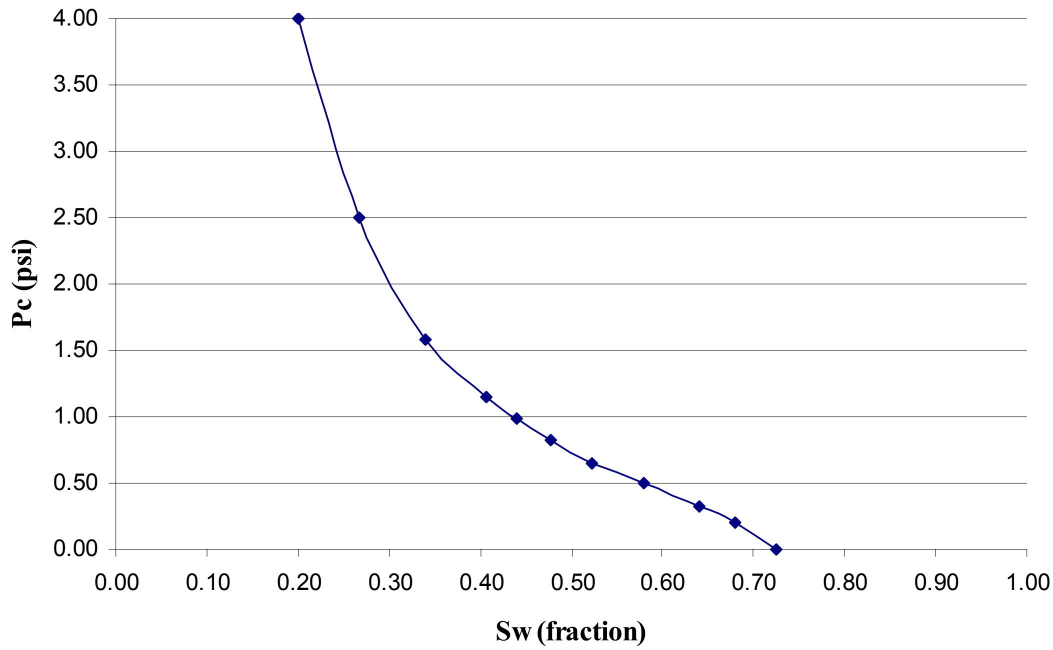

Figure 3.22 Capillary pressure distribution in simulation model

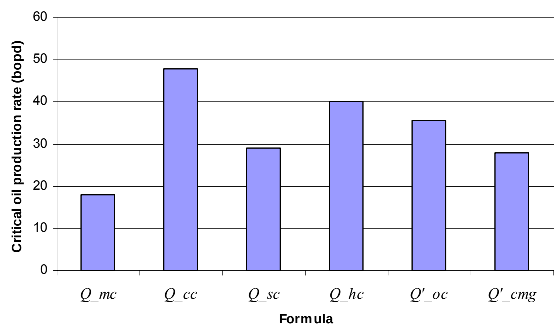

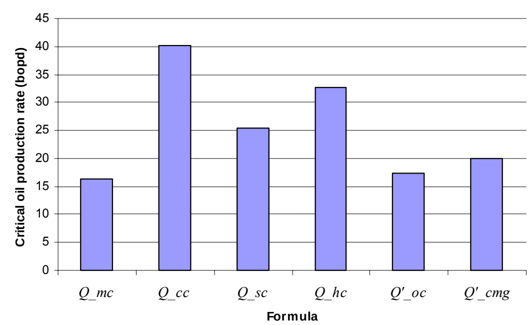

Figure 3.23 Case 1': k_v/k_h =0.1, h_{op}/h_o=0.1 Figure 3.24 Case 2': k_v/k_h =0.2, h_{op}/h_o=0.3

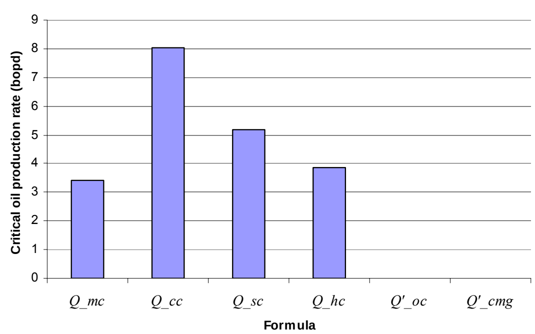

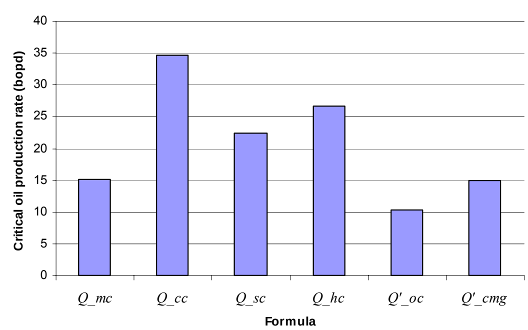

Figure 3.25 Case 3': k_v/k_h =0.3, h_{op}/h_o=0.9 Figure 3.26 Case 4': k_v/k_h =0.4, h_{op}/h_o=0.4

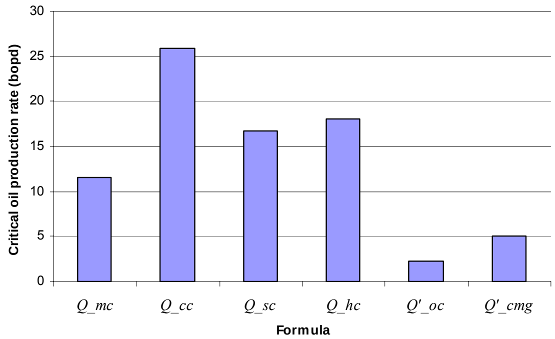

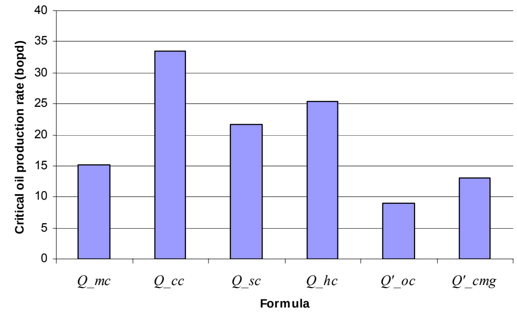

Figure 3.27 Case 5': k_v/k_h =0.5, h_{op}/h_o=0.6 Figure 3.28 Case 6': k_v/k_h =0.6, h_{op}/h_o=0.4

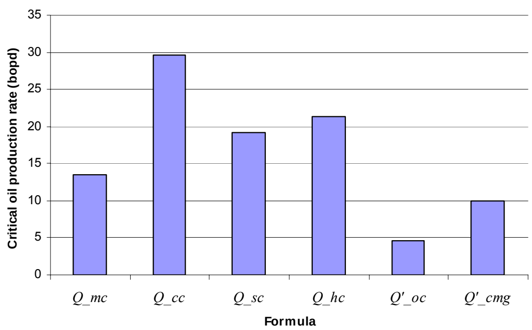

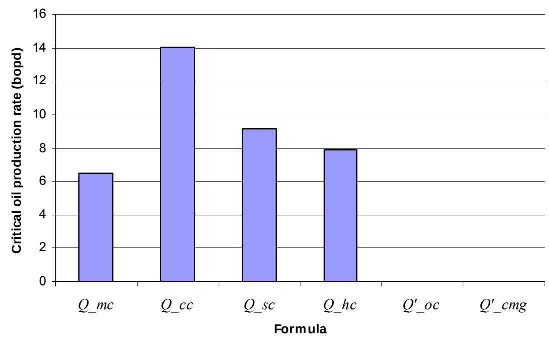

Figure 3.29 Case 7': k_v/k_h =0.7, h_{op}/h_o=0.5 Figure 3.30 Case 8': k_v/k_h =0.8, h_{op}/h_o=0.8

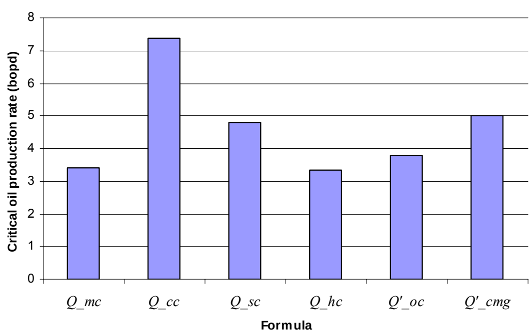

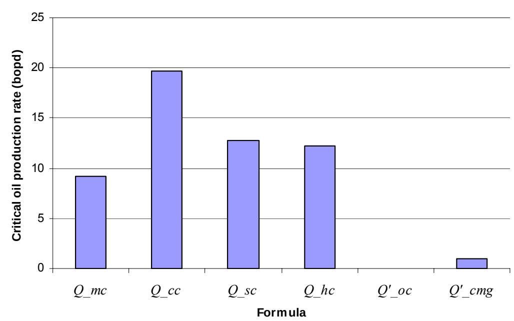

Figure 3.31 Case 9': k_v/k_h =0.9, h_{op}/h_o=0.5 Figure 3.32 Case 10': k_v/k_h =1, h_{op}/h_o=0.7

It is clear that, the critical oil rates are significantly reduced after considering the effect of capillary pressure and transition zone in the calculation. It is also obvious that, the critical oil rate approaches zero when the penetration of a well reaches the transition zone. Comparing with the previous example, the critical oil rate reduces more than 50% when the capillary pressure is considered, and in some cases, there is no critical oil rate or it is too small to see.

3.7. Discussion

The mechanisms of water coning problem in oil reservoirs with bottom water have been analyzed in this chapter, and a 2-phase, 2-D mathematical model has been developed to predict the critical oil rate with the given well-reservoir properties. The model includes the effects of partial penetration, anisotropy and capillary pressure in critical oil rate calculation. In most other similar studies, the capillary pressure is ignored. A method for anisotropy transformation is derived from material balance. The method can be used in cases where there is a need to evaluate the effect of reservoir anisotropy. Although, the value of capillary pressure is usually small, it has significant influence on the critical oil rate, especially when the thickness of oil zone is small or the penetration is close to the transition zone. As indicated by Abass and Bass(1988), if the vertical pressure gradient, capillary pressure, skin, and limited entry effects are considered, as it should be for many real cases, then there is no “critical oil rate”

CHAPTER 4. DOWNHOLE WATER LOOP (DWL) TECHNOLOGY FOR WATER CONING CONTROL

From the previous description, we have seen that, the main reason of water coning in oil well is the pressure drop caused by the oil production in oil zone. If put an equal pressure drop in the aquifer, water will not rise up and water coning can be controlled, then the drained water can either be lifted to the surface or be injected into the same aquifer at a deeper depth. The first method is known as Downhole Water Sink (DWS) technology which has been studied and applied for many years, while the second one is the Downhole Water Loop (DWL) technology which is relatively new comparing to DWS but showing beneficial advantages and potential to improve oil production.

4.1. DWL Well Completion Method and Mechanisms

In water coning, the dynamic OWC deforms upwards due to the pressure drop caused by oil production. Thus, an equal pressure drop in the water zone would keep the water from rising. Figure 4.1 depicts the mechanisms of controlling the DWL well system: a well is dually completed in the oil and water zones and the two completions are separated by a packer set inside the well at depth of the oil-water contact. Both the oil and water zone completions include a submersible pump. The top submersible pump lifts the oil to the surface while the bottom pump drains the formation water around the well and injects the water deeper into the same aquifer thus preventing the water cone from breaking through the oil column into oil-producing perforations.

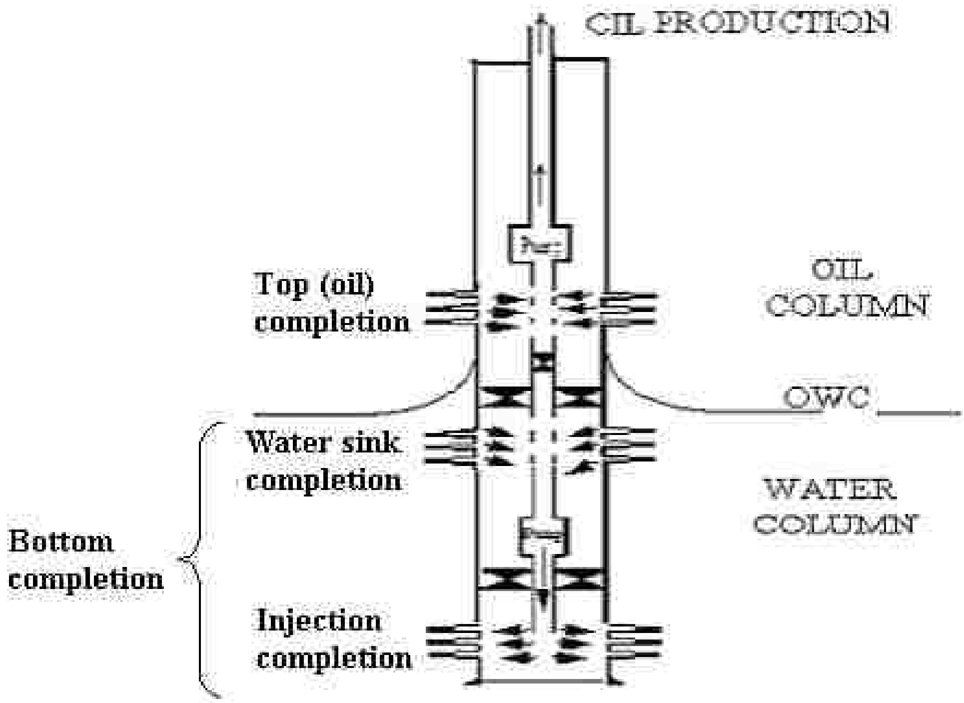

Figure 4.1 Downhole water loop (DWL) well completion

It is possible to use the flow potential theory to develop expressions for the streamlines and isopotential lines for a number of cases of 2D fluid flow in the DWL well system as shown in Figure 4.2. In a radial system, the change of pressure with respect to radius *dp/dr* is inversely proportional to the radius *1/r* (Smith and Pirson, 1963). It means that at large distance from the wellbore, pressure gradient would be extremely small. This pressure gradient is even smaller for the partial perforation. By reinjecting the produced water far away from the production interval, pressure interference is avoided and the water displacement mechanism is maintained. Also, supplementing the produced water reinjection with external water, in order to enhance the water displacement may additionally improve oil recovery (Myers, 1976; Kjos et al. 1995; Pang and Sharma, 1997; Singh, 2002).

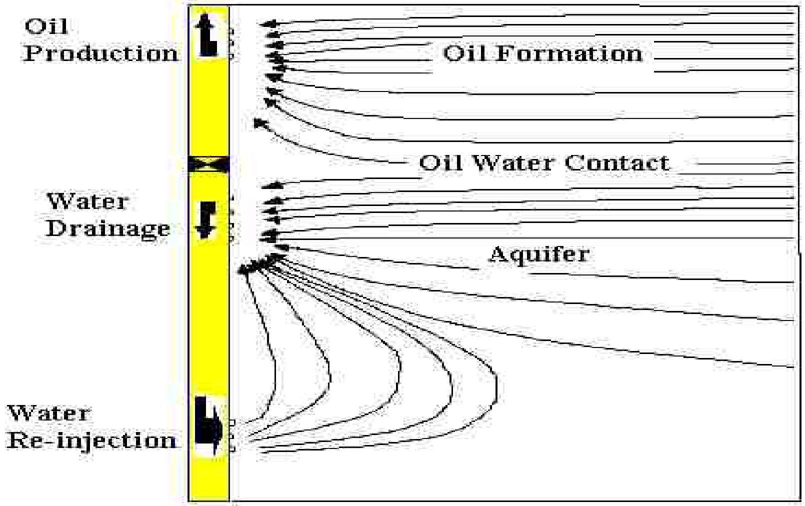

Figure 4.2 Flow streamlines from uniform source and point source to point sink in 2D system

4.2. DWS and DWL as Smart Completions

4.2.1. Comparison of DWS and DWL Wells

From the above description, we can see that the design of DWL is based on DWS and it can be treated as an improved version of DWS with more parts and functions. In well structure design, DWS has one packer, one pump and two completions, while DWL has two packers, two pumps and three completions. In well functions, DWS produces oil and water separately and lifts both of them to the surface. But there are some drawbacks with this method: it costs a lot of energy to pump so much water to the surface, especially when the well is deep and water coning is strong; it is expensive to treat so much water on the surface, especially in the offshore fields where facilities are limited by available space; it is harmful to the environment when a large quantity of produced water is disposed; the reservoir energy will be influenced when both oil and water are drained out of the formations, as a result, there may be no enough energy to drive the left oil to the well and it may reduce the final recovery. However, DWL can conquer these drawbacks:

it does not need to pump so much water to the surface, just needs a little pumping rate to inject the water back to the aquifer; water treatment is less than conventional well, because water coning is controlled and no much water is produced; it is an environment friendly way to keep the water in-situ; it does not deplete the energy in the reservoir, the aquifer pressure can be kept and the water drive can be maintained by injecting the water back to the water zone, as a result, the final oil recovery can be improved especially in the reservoir with small aquifer. So, it is clear that DWL has economical, operational and environmental advantages comparing with DWS.

4.2.2. DWS and DWL as "Smart" Wells

Smart or intelligent well technology is one of the most recent technologies that have been developed to improve the development of gas and oil filed. The main driver for this technology is the emergence of horizontal and multi-lateral wells around the world in the past 10 years. The main aspect of the smart well technology is the ability to control flow from many completions, laterals or zones utilizing down-hole control equipments.

The petroleum industry has clearly embraced the role of smart well in improving reservoir management since its successful field application (Glandt, 2005). With smart wells, one can accelerate production by getting more out of the well earlier, increase total recovery, improve water and/or gas injection efficiency, reduce cost on surface equipment and systems, decrease water production, reduce the operating expenses such as well interventions, and manage uncertainties better. Smart wells are particularly relevant for marginal fields, remote fields, high-volume wells and deep-water subsea wells. They are also suitable for highly deviated, horizontal and multilateral wells.

However, the definition of smart well is unclear in the industry, where different organizations have different opinions about what exactly the smart well is. The following are some typical definitions of smart well from well known petroleum companies:

Schlumberger's definition: "A well equipped with monitoring equipment and completion components that can be adjusted to optimize production, either automatically or with some operator intervention." (Schlumberger, 2009)

WellDynamics' definition: "A well that combines a series of components that collect, transmit and analyze completion, production and reservoir data, and enable selective zonal control to optimize the production process without intervention." (WellDynamics, 2009)

Intelligent Well Reliability Group's (IWRG) definition: "A well equipped with means to monitor specified parameters (e.g. fluid flow, temperature, pressure) and controls enabling flow from each of the zones to be independently modulated from a remote location (e.g. at the wellhead, or a nearby offshore platform, or a distant facility)." (Intelligent Well Reliability Group, 2009).

Baker Hughes' definition: "An intelligent well allows for monitoring and selective control of oil production, gas production, water injection or gas injection with the ability to remotely change the flow profile from/to individual zones without the need for intervention." (Baker Hughes, 2009)

So, which one is the best description of the smart well? Before answering this question, let's ask a more basic one: are the smart wells really intelligent? The answer is simply not yet. According to the Merriam-Webster dictionary, smart or intelligence is the ability to learn or understand or to deal with new or trying situations. The smart wells installed around the world have very significant advantages than regular completions but they can not learn nor deal with any situation yet.

Due to the smart well systems vary from site to site and can have different design, actuation and surveillance/monitoring processes—as individual as the field they are being installed in, as well as the divergence of its concept, more general definitions have been proposed to describe this technology based on its features:

Jansen (2001): Wells equipped with permanent downhole measurement equipment or control valves, and especially those with both, are nowadays known as smart or intelligent wells. The key question in the development of smart well technology is when the added functionality also adds value.

Ziebel (2009): "Really easy to describe it as complicated, but it is just a series of valves and sensors downhole that is powered and monitored from outside the wellhead."

There are many other names based on the different designs and functions of the smart well, such as intelligent completion, downhole instrumentation and control system (DIACS), active completion, high tech wells and so on (Ziebel, 2009).

Summarizing the various discussions in the literature, we can see that, a smart well is a system with one or more of the following features:

1. Has more than one completions, each completion provides production or injection control;
2. Equipped with permanent downhole measurement, monitoring or control equipment for data collecting, transmitting or analyzing;
3. Has the ability to detect any critical changes in downhole conditions and communicate these to a data collection and analysis centre, which allows the

operator to produce, monitor and control the production of hydrocarbons through remotely operated completion systems at or near real-time.

Comparing with the conventional well, it has the benefits of optimizing field production or injection programs, improving reservoir performance, achieving higher extraction ratios and reducing field development and intervention costs.

Figure 4.3 to Figure 4.7 show the popular smart wells used in field: smart well 1 has two completions, the top completion produces oil and water then separates them, the bottom completion injects the separated water back to a disposal zone, this technology is also known as Downhole Oil/Water Separation (DOWS) system; smart well 2 also has two completions, the bottom completion produces gas from a layer and the top completion injects the produced gas to another layer, to drive oil to an adjunct oil production well; smart well 3 employs three completions to carry out long-term production testing between a source (higher pressure) reservoir and a sink (depleted reservoir), it is a very environmentally friendly option which allows conducting long-term production testing without flowing to surface; smart wells 4 and 5 use multilateral braches to achieve different purposes and enhance oil production.

Similar to smart wells 1 to 3, both DWS and DWL wells have more than one completion, each completion provides production or injection control and equipped with downhole measurement, monitoring or control equipment for data collecting, transmitting or analyzing. According to the definition of smart well, both DWS and DWL wells belong to this category.

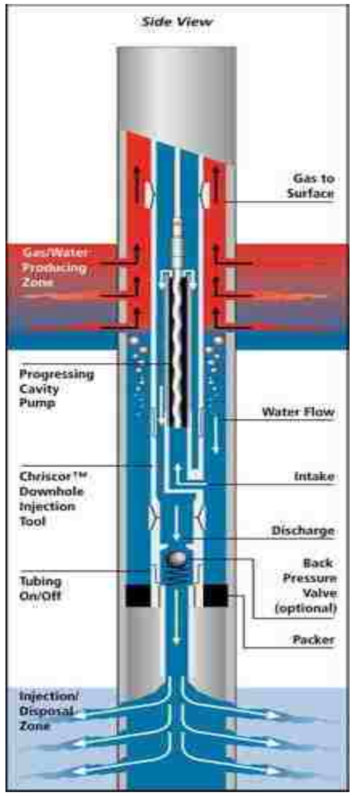

Figure 4.3 Smart well 1 (Conn and Themig, 2001)

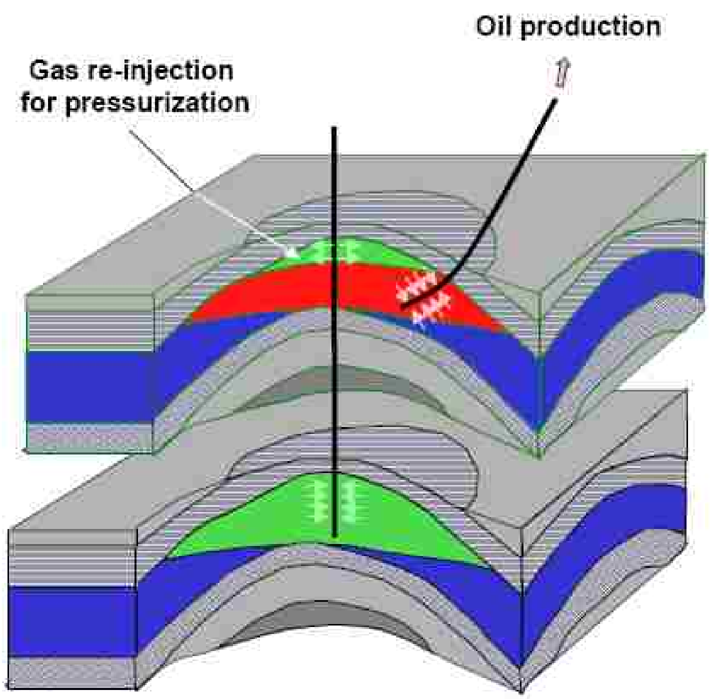

Figure 4.4 Smart well 2 (Jansen, 2001)

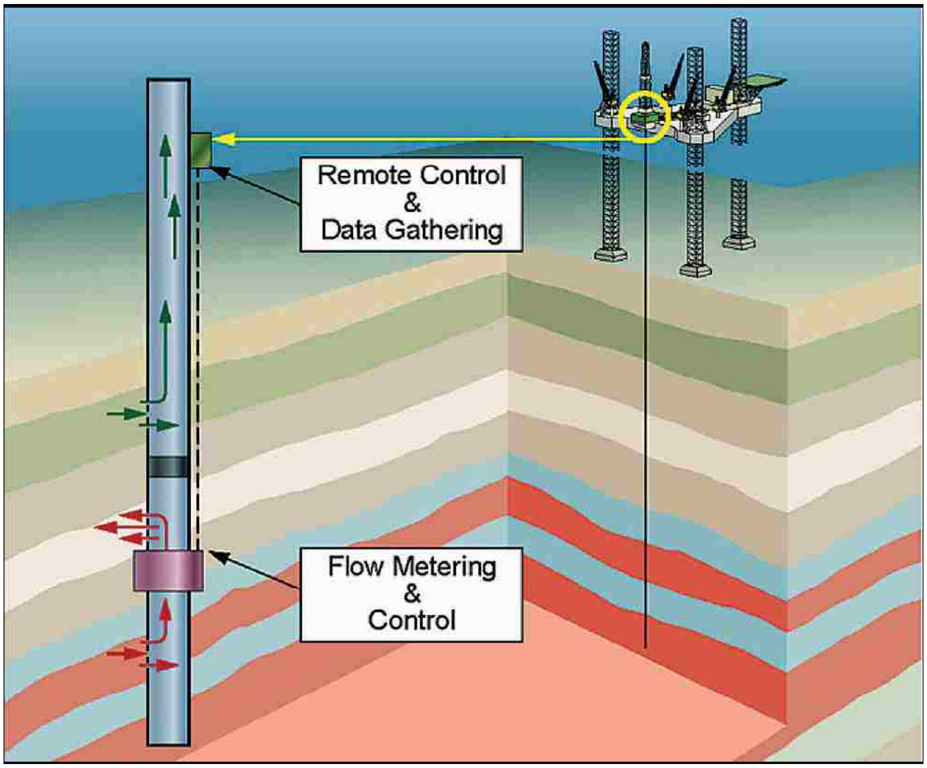

Figure 4.5 Smart well 3 (Glandt, 2005)

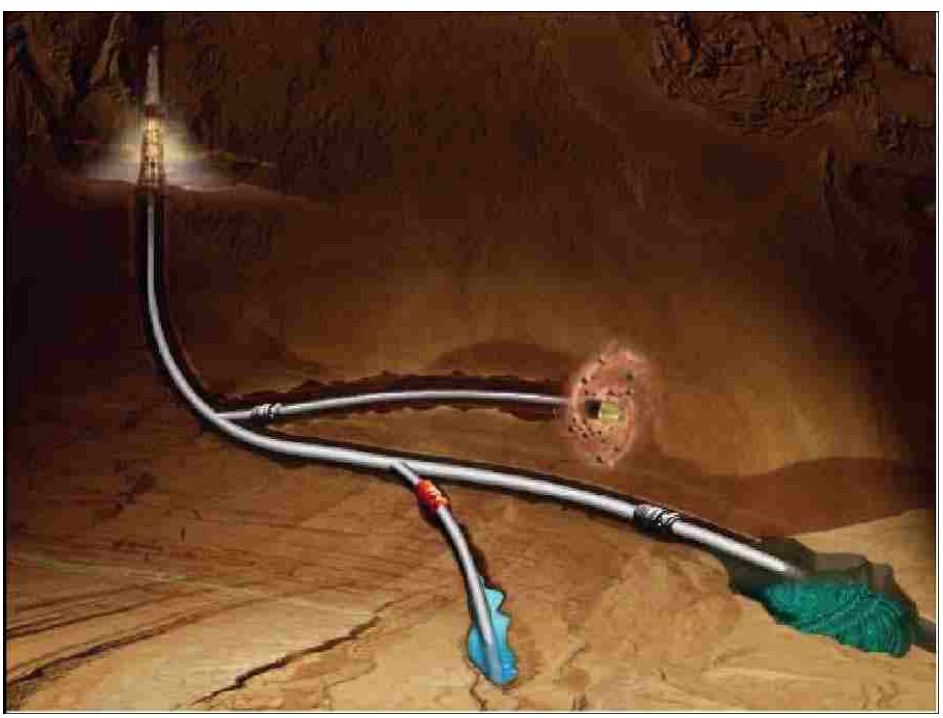

Figure 4.6 Smart well 4 (Saggaf, 2008)

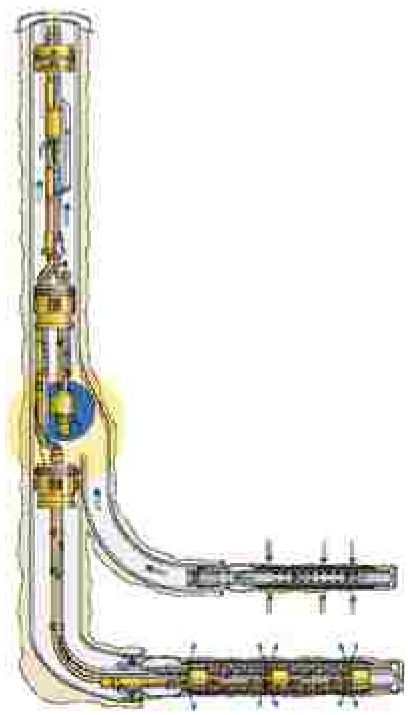

Figure 4.7 Smart well 5 (Baker Hughes, 2009)

CHAPTER 5. CRITICAL RATE MODELS FOR DWL

As conventional wells, there is a maximum oil rate for DWL system when the reservoir properties and well parameters are given. Determining the critical oil rate is still a main topic in DWL design. Numerical simulation is widely used in water coning problems because of its accuracy, however, it needs a lot of data and simulation cannot begin if there are not enough data. Also, it requires people to have knowledge about reservoir modeling and it is a very time-consuming process to find the critical oil rate for a well, especially when the well design is complex. Comparing to numerical simulation, analytical model needs much less data and easier to calculate the critical oil rate. So, before carrying out the complex and time-consuming simulation, an analytical model is necessary to predict the behavior of the DWL system. In the following sections, an analytical model for DWL will be developed first, and then a numerical simulation model will be built for further study of the system.

5.1. Analytical Model of DWL with Segregated Inflow of Oil and Water

In Chapter 3, we analyzed the water coning problem for a single well which produced oil in the top of the oil zone considering the effects of reservoir anisotropy and well partial penetration skin. An analytical model was derived to calculate the critical oil rate which indicated it was too small to be economical. Since the purpose of DWL system is to control water coning, determining the critical oil rate is one of the main topics in DWL design. Similar to critical oil rate, critical water drainage rate and D/I spacing are also important in designing DWS and DWL wells. Most of theoretical works focused on modeling the dynamic oil water contact (OWC) when calculating this rate. For example, Siemek and Stopa (2002) derived and solved a DWS differential equation for a flat (horizontal) oil water contact, and also derived a nonlinear equation describing the dynamic oil-water interface with no water breakthrough to oil completion. By solving this equation, critical oil production and water drainage rates were predicted by assuming extreme (top and bottom) positions of the interface line.

A simple way to calculate critical oil production and water drainage rates without modeling the whole oil-water interface line is to use vertical equilibrium and set an energy balance equation along vertical axis of the DWL well. The approach has been used in this study together with following definitions pertinent to DWL wells:

1. Critical oil rate " q_{opC} " is a maximum water-free oil rate at the top DWL completion with oil-free water drainage for a given D/I spacing. If the oil production rate is larger than this rate, water will break through the oil into the oil-producing completion and water coning will happen;
2. Critical water drainage rate " q_{wdC} " is a maximum oil-free water rate at the DWL drainage completion for a given D/I spacing. If the water drainage rate is bigger than this rate, oil would breaks into the water drainage completion and reverse oil coning will happen;
3. Critical D/I spacing " h_{diC} " is the minimum D/I spacing needed to avoid water coning. If the D/I spacing is bigger than this length, the production rate is practically constant (increases very slowly).

A DWL model has been built using the following simplifying assumptions:

1. The oil reservoir has bottom water;
2. The flow is radial and obeys Darcy's Law;

3. There is vertical equilibrium in the system;

4. Production is stabilized, i.e. there is a steady-state flow in the oil and water layers;

5. Permeability is constant in radial direction, i.e. $k_r = k_x = k_y$;

6. The oil production completion is at the top of the payzone;

7. There is no gas cap in the reservoir;

8. The lengths of water drainage and water re-injection completions are the same and are significantly smaller than the water layer thickness;

9. Water transition zone is ignored. (The effects of water transition zone and capillary pressure need detailed study after getting the correlations without considering their effects).

Before the detailed derivation, let's simplify the DWL system as shown in Figure 5.1: completion 1 produces oil from the oil zone, completion 2 drains water from the aquifer and completion 3 injects the drained water back to the same aquifer. In order to make the task easier, the anisotropic reservoir-well system should be transformed to an equivalent isotropic one by using the following transformations as shown in Equation 5.1 and Equation 5.2:

$$\begin{cases} \bar{k} = k' = k_r' = k_z' = \sqrt{k_r k_z} \\ k_o = k' k_{ro} \\ k_w = k' k_{rw} \end{cases} \quad \text{...(5.1)}$$

Partial penetration skins of three completions can be calculated from Equations 3.17 to 3.22. Suppose there is a small droplet at intersection between the OWC and vertical axis of the DWL well, water will breakthrough to the oil completion when this small droplet moves to the completion 1, on the other hand, oil will breakthrough to the water drainage completion when this small droplet moves to the completion 2. In practice, this would not be acceptable.

$$\begin{cases} r_w' = \sqrt[4]{\dfrac{k_z}{k_r}} r_w \\ r_e' = \sqrt[4]{\dfrac{k_z}{k_r}} r_e \\ h_o' = \sqrt[4]{\dfrac{k_r}{k_z}} h_o \\ h_{op}' = \sqrt[4]{\dfrac{k_r}{k_z}} h_{op} \\ h_w' = \sqrt[4]{\dfrac{k_r}{k_z}} h_w \\ h_{wo}' = \sqrt[4]{\dfrac{k_r}{k_z}} h_{wo} \\ h_{wd}' = \sqrt[4]{\dfrac{k_r}{k_z}} h_{wd} \\ h_{di}' = \sqrt[4]{\dfrac{k_r}{k_z}} h_{di} \\ h_{wi}' = \sqrt[4]{\dfrac{k_r}{k_z}} h_{wi} \\ \Delta\rho' = \sqrt[4]{\dfrac{k_r}{k_z}} \Delta\rho \end{cases} \qquad (5.2)$$

First, let’s consider the situations in the oil zone. A steady-state pressure drawdown will be formed with the production of oil, which can be expressed as:

$$\Delta p_{op} = \frac{141.2 q_o \mu_o B_o}{k_o h_o'} \left(\ln \frac{r_e'}{r_w'} + S_{pp\_op} \right) \qquad (5.3)$$

The potential of gravity force is:

$$p_{G\_op} = 0.433(\gamma_w - \gamma_o)(h_o' - h_{op}') \qquad (5.4)$$

The situation is similar in the aquifer. Water drainage by completion 2 causes a steady-state pressure drawdown as:

$$\Delta p_{wd} = \frac{141.2 q_{wd} \mu_w B_w}{k_w h_w^{'}} \left(\ln \frac{r_e^{'}}{r_w^{'}} + S_{pp\_wd} \right) \qquad (5.5)$$

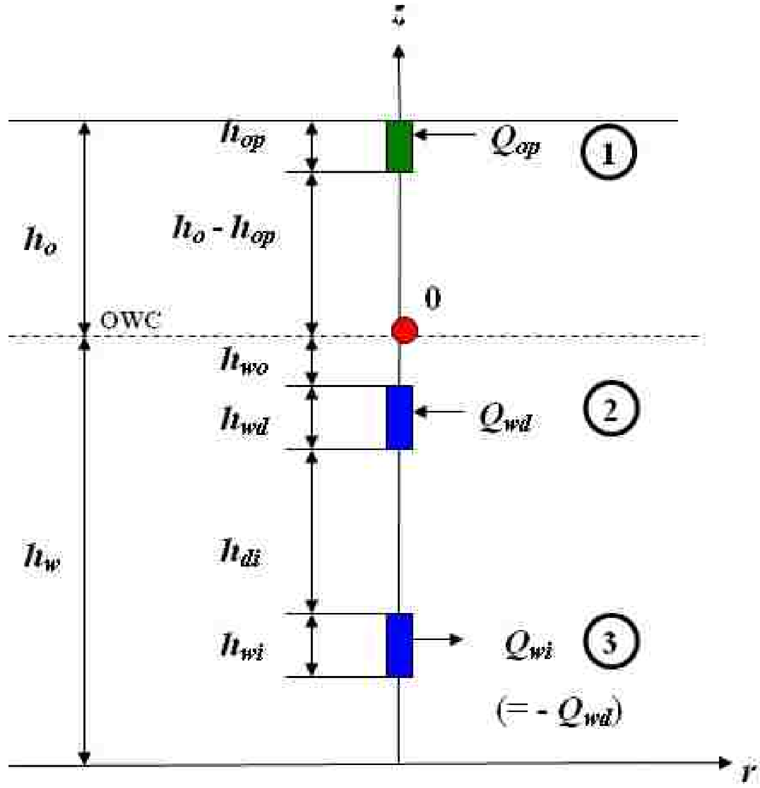

Figure 5.1 Simplified schematic of DWL system in reservoir with bottom water

Since oil is lighter than water, when this small droplet moves downward, it moves against the buoyancy force which can be approximated by a gravitational potential difference as:

$$F_{wd} = 0.433(\gamma_w - \gamma_o) h_{wo}^{'} \qquad (5.6)$$

A dimensionless injection number should be defined before analyzing the injection completion (Smith and Pirson, 1963):

$$D_{di} = \frac{h_{wo}'}{h_{wo}' + h_{di}'} \qquad (5.7)$$

Water injection by completion 3 causes a negative pressure drawdown as:

$$\Delta p_{wi} = -\frac{141.2 q_{wd} \mu_w B_w D_{di}}{k_w h_w'} \left(\ln \frac{r_e'}{r_w'} + S_{pp\_wi} \right) \qquad (5.8)$$

The movement of the small droplet should conquer the gravitational potential as:

$$p_{G\_wi} = 0.433 (\gamma_w - \gamma_o) D_{di} h_{wo}' \qquad (5.9)$$

With all three completions flowing, the dynamic OWC is stable when:

$$\Delta p_{op} + F_{wd} + \Delta p_{wi} = p_{G\_op} + \Delta p_{wd} + p_{G\_wi} \qquad (5.10)$$

Excluding the injection completion and skin factors, this expression is the same to the DWS models developed by Siemek and Stopa (2002) and Utama (2008), who considered the problem from different point of views.

Substituting Equations 5.3 ~ 5.9 into Equation 5.10, we get the following expressions for critical oil production and water drainage (re-injection) rates:

$$q_{opC} = \frac{q_{wd} B_w h_o'}{M B_o h_w'} \frac{\left[(1 - D_{di}) \ln\left(\frac{r_e'}{r_w'} \right) + S_{pp\_wd} - D_{di} S_{pp\_wi} \right]}{\ln\left(\frac{r_e'}{r_w'} \right) + S_{pp\_op}} +$$

$$\frac{0.003066 k_o h_o' (\gamma_w - \gamma_o)}{\mu_o B_o} \frac{\left[(D_{di} - 1) h_{wo}' + h_o' - h_{op}' \right]}{\ln\left(\frac{r_e'}{r_w'} \right) + S_{pp\_op}} \qquad (5.11)$$

$$q_{wdC} = \frac{q_{op} M B_o h_w'}{B_w h_o'} \frac{\ln\left(\frac{r_e'}{r_w'} \right) + S_{pp\_op}}{\left[(1 - D_{di}) \ln\left(\frac{r_e'}{r_w'} \right) + S_{pp\_wd} - D_{di} S_{pp\_wi} \right]} +$$

$$\frac{0.003066k_w h_w^{'}(\gamma_w-\gamma_o)}{\mu_w B_w}\frac{\left[h_{wo}^{'}-h_o^{'}+h_{op}^{'}-D_{di}h_{wo}^{'}\right]}{\left[(1-D_{di})\ln\left(\frac{r_e^{'}}{r_w^{'}}\right)+S_{pp\_wd}-D_{di}S_{pp\_wi}\right]} \text{............}(5.12)$$

Where M is the mobility ratio which is defined as:

$$M=\frac{k_w\mu_o}{k_o\mu_w} \text{..}(5.13)$$

Equations 5.11 and 5.12 are useful for practical applications: when the water drainage (re-injection) limitation is known (downhole pump size), Equation 5.11 determines the critical oil rate in the top completion; when the oil production limitation is known (nodal analysis), Equation 5.12 can be used to get the critical water drainage (re-injection) rate. Moreover, in order to know whether DWL installation is feasible for a reservoir, a critical water drainage/re-injection (D/I) spacing "h_{diC}" should be determined first. If the aquifer is thicker than the critical D/I spacing, the DWL system can be applied in this reservoir. The critical oil production or water drainage rates become insensitive to D/I spacing when it is larger than a certain "critical" value. Mathematically, this "critical" D/I spacing can be defined as:

$$\begin{cases} h_{diC}=\sqrt{\dfrac{\dfrac{h_{wo}^{'}q_{wd}B_w h_o^{'}}{MB_o h_w^{'}}\left(\ln\left(\dfrac{r_e^{'}}{r_w^{'}}\right)+S_{pp\_wi}\right)}{\left[\ln\left(\dfrac{r_e^{'}}{r_w^{'}}\right)+S_{pp\_op}\right]\dfrac{\partial Q_{opC}}{\partial h_{di}}}}- \\ \sqrt{\dfrac{0.003066h_{wo}^{'}k_o h_o^{'}h_{wo}^{'}(\gamma_w-\gamma_o)}{\mu_o B_o\left[\ln\left(\dfrac{r_e^{'}}{r_w^{'}}\right)+S_{pp\_op}\right]\dfrac{\partial Q_{opC}}{\partial h_{di}}}}-h_{wo}^{'} \\ 0<h_{diC}<0.8h_w \end{cases} \text{..}(5.14)$$

5.2. Verification of the Analytical Model with Field Data

By setting the D/I spacing infinitely large, the influence of completion 3 could be ignored to the system, so we reduced DWL well to the DWS well for which we had field data. Mathematically, " D_{di} "equals to zero when the D/I spacing is infinitely large, Equations 5.11 and 5.12 can be modified to calculate the critical oil production rate and critical water drainage rate for DWS well as follows:

$$q_{opC} = \frac{q_{wd} B_w h_o^{'}}{M B_o h_w^{'}} \frac{\left[\ln\left(\frac{r_e^{'}}{r_w^{'}}\right) + S_{pp\_wd} \right]}{\ln\left(\frac{r_e^{'}}{r_w^{'}}\right) + S_{pp\_op}} + \frac{0.003066 k_o h_o^{'} (\gamma_w - \gamma_o)}{\mu_o B_o} \frac{\left[h_o^{'} - h_{op}^{'} - h_{wo}^{'} \right]}{\ln\left(\frac{r_e^{'}}{r_w^{'}}\right) + S_{pp\_op}} \quad \text{...(5.15)}$$

$$q_{wdC} = \frac{q_{op} M B_o h_w^{'}}{B_w h_o^{'}} \frac{\ln\left(\frac{r_e^{'}}{r_w^{'}}\right) + S_{pp\_op}}{\left[\ln\left(\frac{r_e^{'}}{r_w^{'}}\right) + S_{pp\_wd} \right]} + \frac{0.003066 k_w h_w^{'} (\gamma_w - \gamma_o)}{\mu_w B_w} \frac{\left[h_{wo}^{'} - h_o^{'} + h_{op}^{'} \right]}{\left[\ln\left(\frac{r_e^{'}}{r_w^{'}}\right) + S_{pp\_wd} \right]} \quad \text{...(5.16)}$$

The model verification used the field performance data of a DWS well in the Nebo-Hemphill field in North Louisiana (Wojtanowicz et al, 1995; Utama, 2008). The properties of the field are shown in Table 5.1 and Figure 5.2. The big red points in Figure 5.3 and Figure 5.4 and data in first two columns of Table 5.2 are DWS production data from Nebo-Hemphill Field. It is clear that the model-calculated results approach the real data with the increase of D/I spacing, until they match it closely when the D/I spacing becomes infinite. Figure 5.3 and Figure 5.4 also show that, only a small D/I spacing can make the DWL system work in this field which indicates that DWL could be installed in reservoir with small aquifer; and also the water drainage/injection rate decreases dramatically with the increase of D/I spacing which means the thicker the aquifer, the better the results.

Table 5.1 DWS Production Data from Nebo-Hemphill Field (Wojtanowicz et al, 1995; Utama, 2008)

Parameter	**Value**	**Unit**
Horizontal permeability (k_r)	3500	*mD*
Vertical permeability (k_z)	3150	*mD*
End point water relative perm (k^*_{rw})	0.077	
End point oil relative perm (k^*_{ro})	0.107	
Well radius (r_w)	0.292	*ft*
Drainage radius (r_e)	850	*ft*
Oil zone thickness (h_o)	18	*ft*
Length of top completion (h_{op})	3	*ft*
Water zone thickness (h_w)	64	*ft*
Distance from water drainage perforation to OWC (h_{wo})	5	*ft*
Length of water drainage completion (h_{wd})	15	*ft*
Length of water injection completion (h_{wi})	15	*ft*
Water relative density (γ_w)	1.05	
Water viscosity (μ_w)	1	*cp*
Water volume factor (B_w)	1.02	*bbl/stb*
Oil relative density (γ_o)	0.93	
Oil viscosity (μ_o)	17	*cp*
Oil volume factor (B_o)	1.1	*bbl/stb*

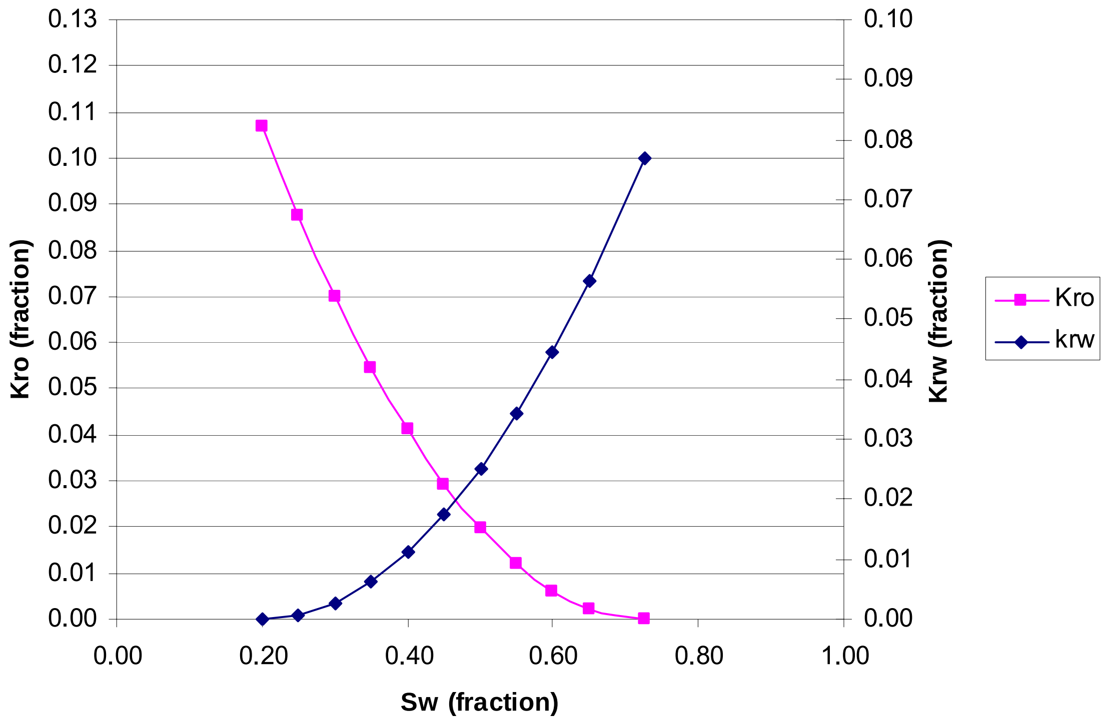

Figure 5.2 Relative permeability in simulation model of DWL well (Nebo-Hemphill Field)

Table 5.2 Comparison of DWS Production Data and DWL Model Results

Field data (DWS)		**Analytical Model (DWL)**	
Water drainage rate (*bwpd*)	Oil production rate (*bopd*)	Oil production rate (*bopd*) ($h_{di} = \infty\ ft$)	Water drainage rate (*bopd*) ($h_{di} = \infty\ ft$)
1500	32.8	31.98	1548.04
1700	35-45	36.23	1760.58
2000	40	42.61	1900.60
2500	54	53.25	2535.22
2600	55-60	55.37	2629.23

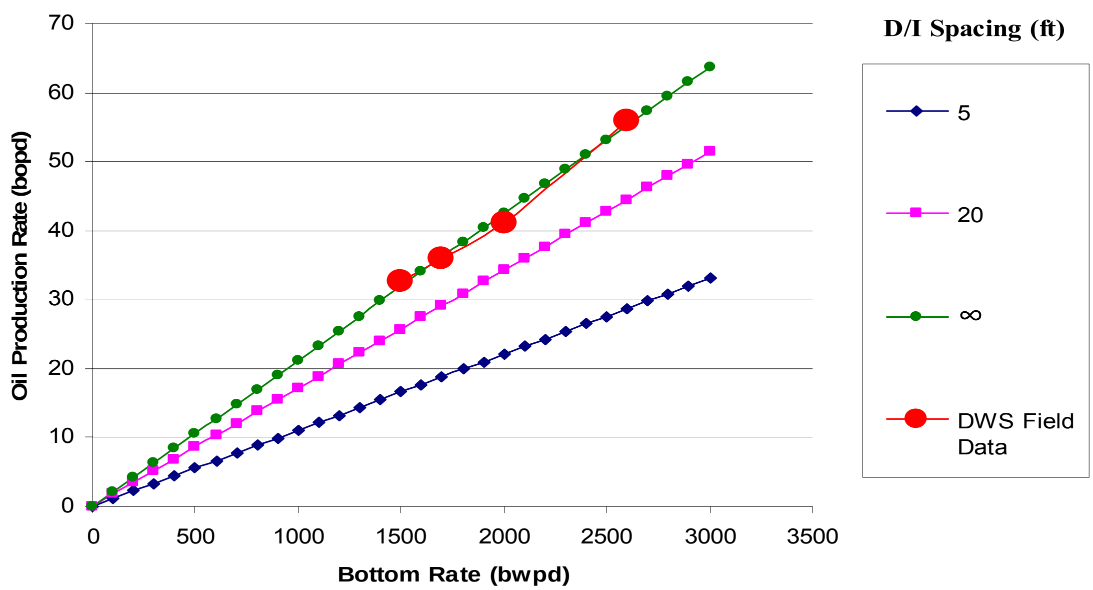

Figure 5.3 Water-free oil rate increases with bottom rate

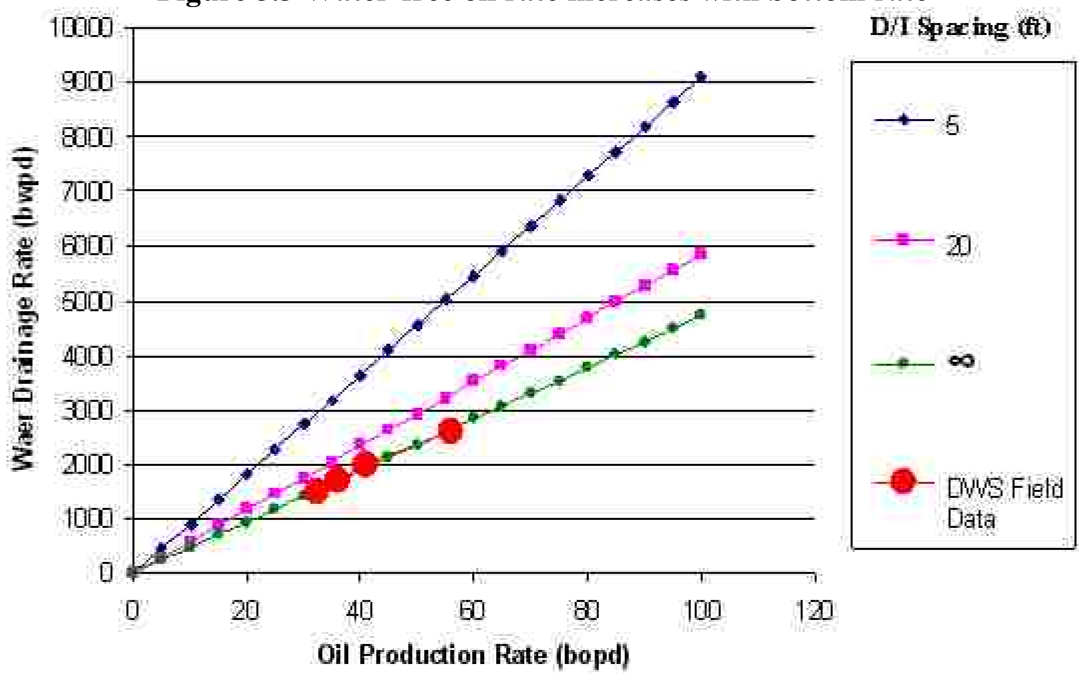

Figure 5.4 Oil-free water rate increases with top rate

5.3. Comparison of the DWL Analytical and Numerical Models

Since numerical simulators can model multiphase flow interactions more accurately when the model is carefully calibrated with proper grids, a numerical model is necessary to study the behavior of DWL in detail. Kurban (1999) built one of the earlier DWS well models using the numerical reservoir simulator ECLIPSE. In order to eliminate the volumetric (material balance) effects and verify the analytical results of DWS which are stabilized in nature, Kurban used three approaches to build the steady-state model: putting an aquifer influx in the grid edges; assigning an infinite porous cell at the boundary and re-injection of produced fluids. He concluded that re-injection of produced fluids achieves the stabilized flow conditions better than the other two methods. Kjos et al (1995) also concluded that, the reservoir pressure will decrease very fast unless the water drive is very strong, so re-injection of the produced fluids is necessary in the simulation model. Hernandez (2007) systematically studied different aquifer models and concluded that concentric cylinder aquifer can represent real situations better than the Fetkovich aquifer model. In the former studies of DWS model, the grid number in the vertical direction is always fixed and the grid size in aquifer is coarse. However, it is not suitable for the DWL model, where the location of injection completion has important effects on the system.

Based on the well-studied DWS models, a 2-D (R-Z) radial-cylindrical is built for DWL using the reservoir simulator "IMEX" as shown in Figure 5.5 and Table 5.3: each grid has 0.5 *ft* and 1 *ft* height in vertical direction in oil zone and aquifer, respectively, and 0.05 *ft* width near the well in radial direction in both regions. The aquifer model is concentric cylinder aquifer rather than the Fetkovich aquifer. The produced oil and water are injected back to the oil zone and aquifer at their outer boundaries, respectively to keep the stabilized state. The structure of well settings in the simulation model is shown in Figure 5.6: well "P1" produces oil and water in the oil zone, "I1" injects the oil from

“P1” back to the oil zone at its outer boundary, “I2” injects the water from “P1” back to the aquifer at its outer boundary, “P2” drains water in the aquifer and “I3” injects this water back to the aquifer in the inner boundary.

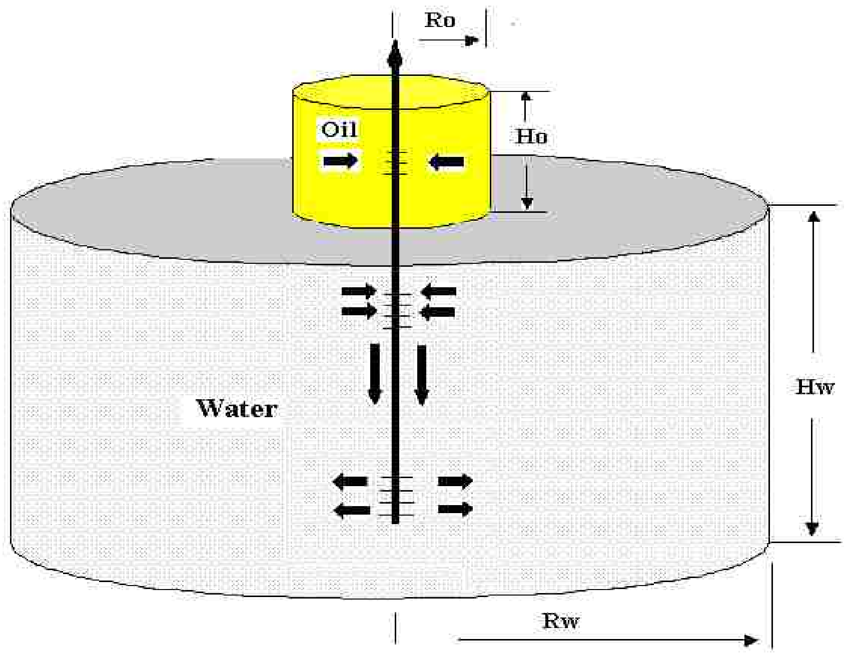

Figure 5.5 2-D radial-cylindrical simulation model of DWL well-reservoir system

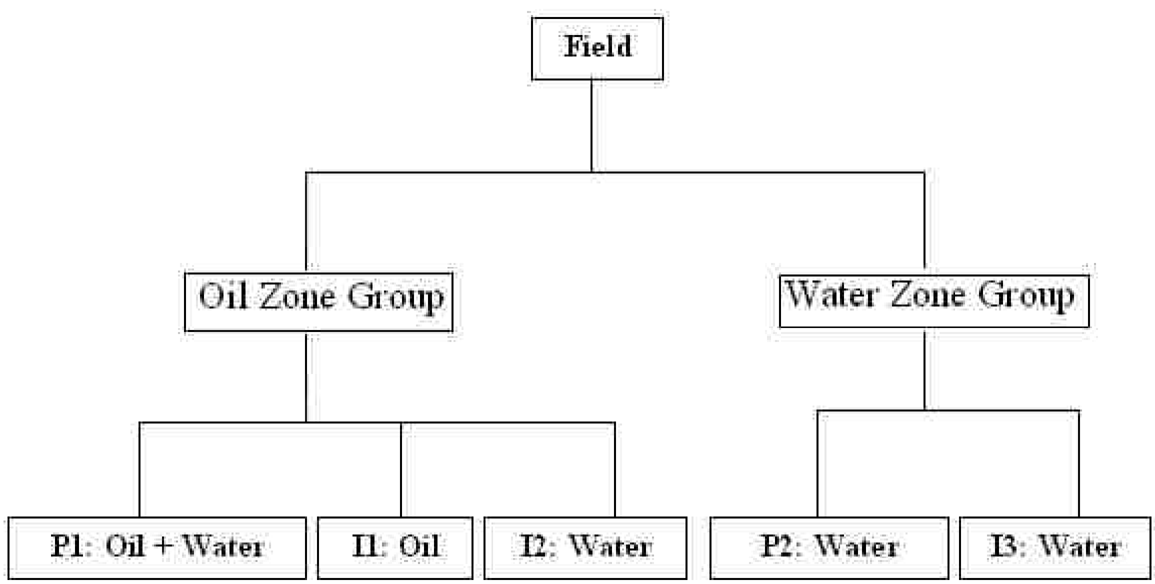

Figure 5.6 Structure of well settings in the simulation model

Table 5.3 Grid division in simulation model for DWL well

Region	Direction	Grid Number
Oil Zone	**R**	50
	Θ	1
	Z	$h_o / 0.5$
Aquifer	**R**	51
	Θ	1
	Z	$h_w / 1$

Using the data from Table 3.1 and Table 3.2, the development of water cut and bottom-hole flowing pressure of "P1" well can be shown in Figure 5.7 and Figure 5.8, which show that the model may reach equilibrium condition after a considerably long time.

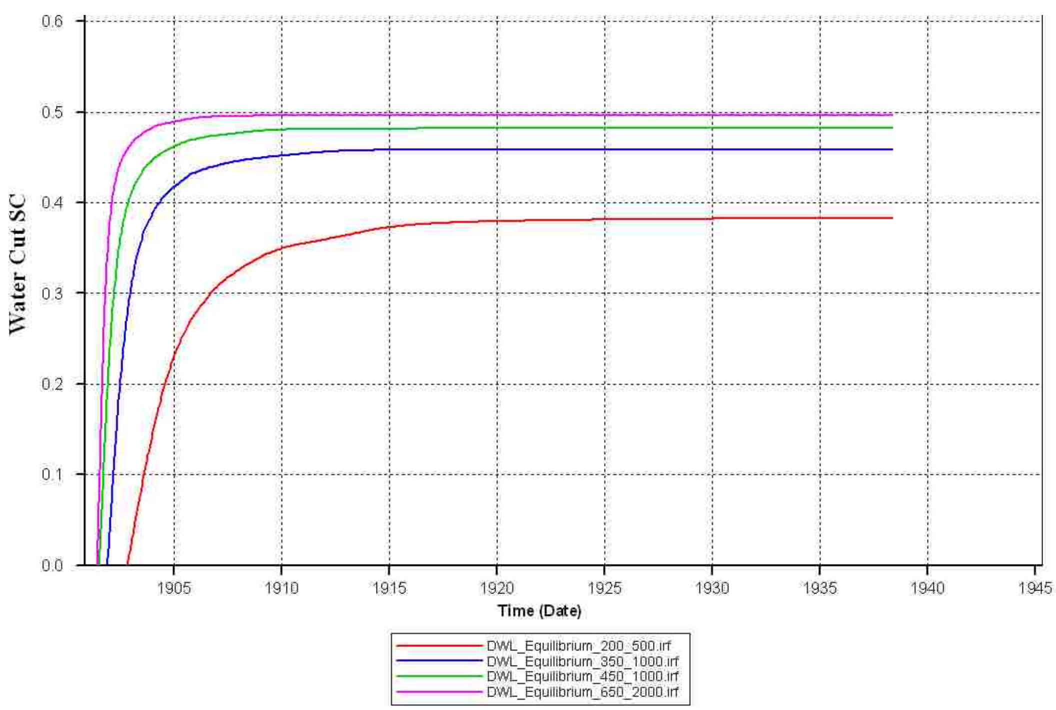

Figure 5.7 Water coning stabilization process with equilibrium water cut

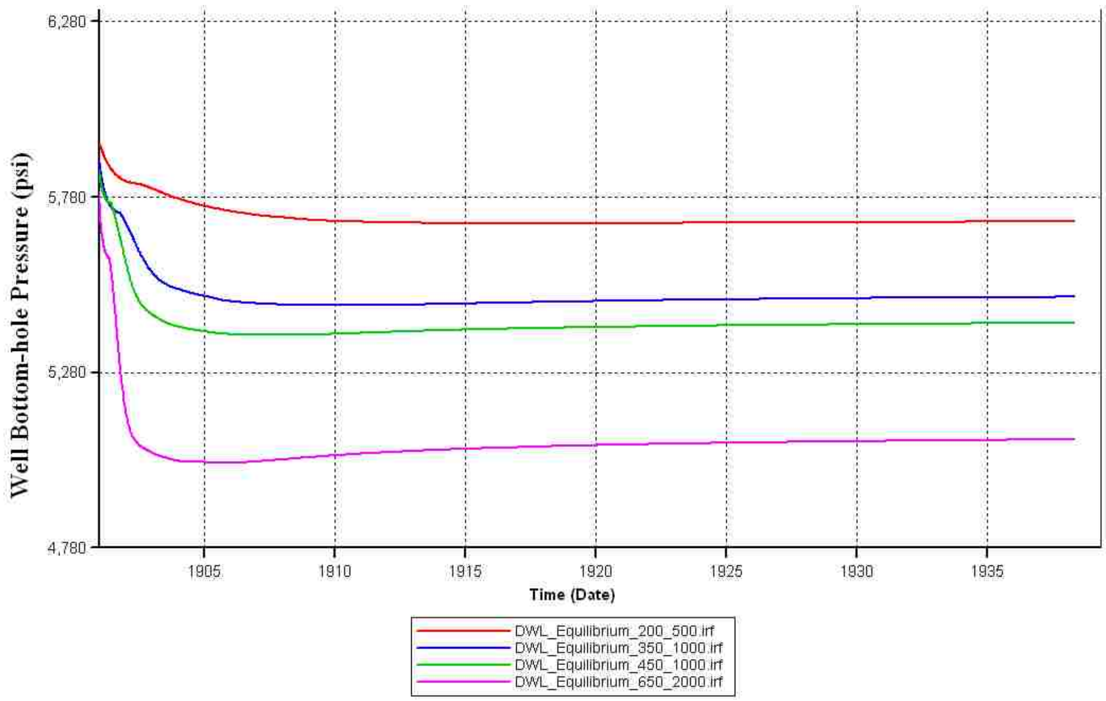

Figure 5.8 Stabilization of bottom-hole flowing pressure

The reasons of a long stabilizing time needed in the model might be explained as follows:

1. The pressure change between water drainage completion and water injection completion is severe when the water drainage/injection rate is high;
2. The aquifer size in the model is big, it needs a long time for the pressure change in the well to reach the outer boundary of the aquifer;
3. In a two-phase flow model, water and oil flow simultaneously and the pressure balance at OWC needs a long time to reach.

Since critical rates cannot be calculated directly in the simulator, the following steps are used to find the values of each critical rate. Take critical oil rate for example:

1. Input well and reservoir properties to the simulator, set fixed values for water drainage/injection rate and D/I spacing;

2. Guess an initial oil production rate which is small enough to prevent water breakthrough;

3. Run the simulator and monitor the water cut and bottom hole pressure in the top completion;

4. If the bottom hole pressure is stable for enough long time and water cut remains zero, then record the oil production rate as "q_{op1}";

5. Change the oil production rate to a bigger value and go to step 3;

6. Repeat step 3 to step 5 until the water cut becomes a non-zero value, then stop simulation and the latest "q_{op1}" is the critical oil rate.

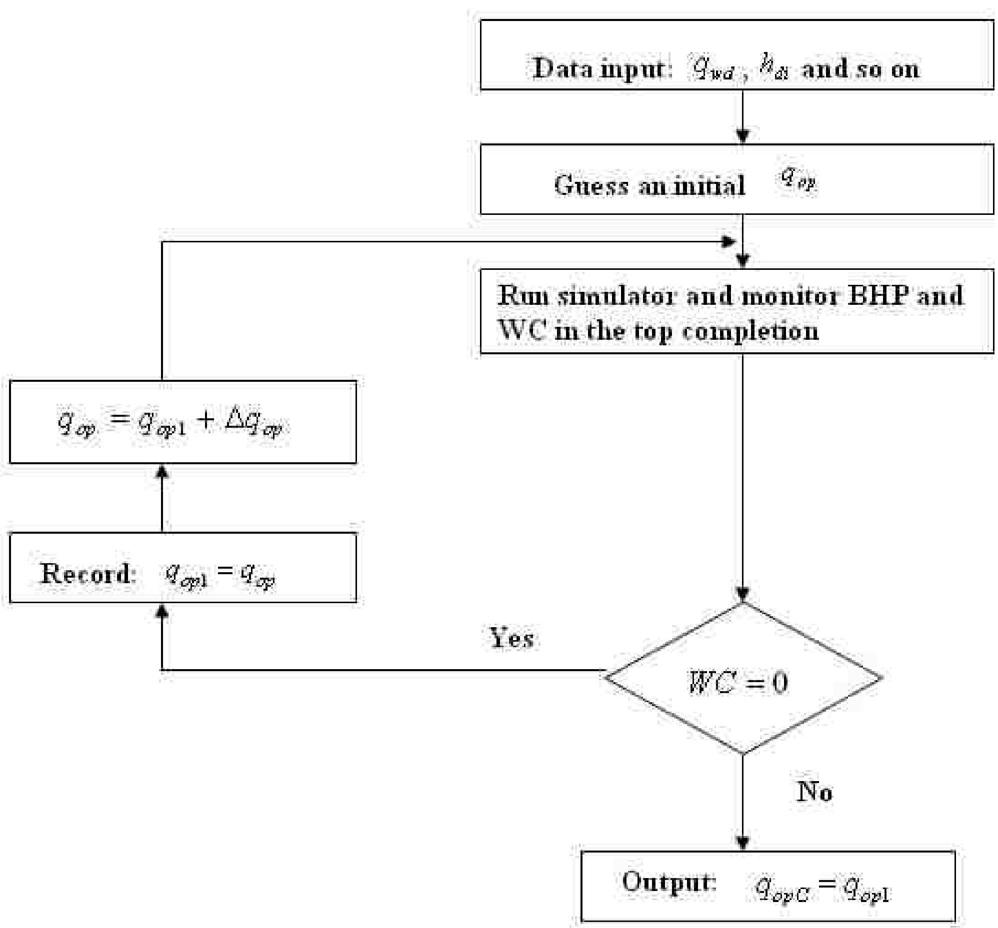

Figure 5.9 Steps to find critical oil rate

Using the data of Nebo-Hemphill field and setting the bottom rate as 1000 *bwpd* and D/I spacing as 5 *ft*, the critical oil rate can be found as 12 *bopd* as shown in Figure 5.10 and Figure 5.11. Critical water drainage/injection rate and D/I spacing can be found using the same procedure.

Figure 5.12 depicts the comparison of the critical oil rate obtained from analytical and numerical models when the water drainage/injection rate is fixed at 1000 *bwpd*. It shows that the critical oil rate increases fast at the initial beginning of D/I spacing and then becomes stable after a certain value, which is called critical D/I spacing. When D/I spacing decreases to zero, DWL system reduces to conventional well as shown in the figure, it is obvious that critical rate is too low to be economic in this field. However, DWL well can give much higher critical oil rate with a proper amount of drained water.

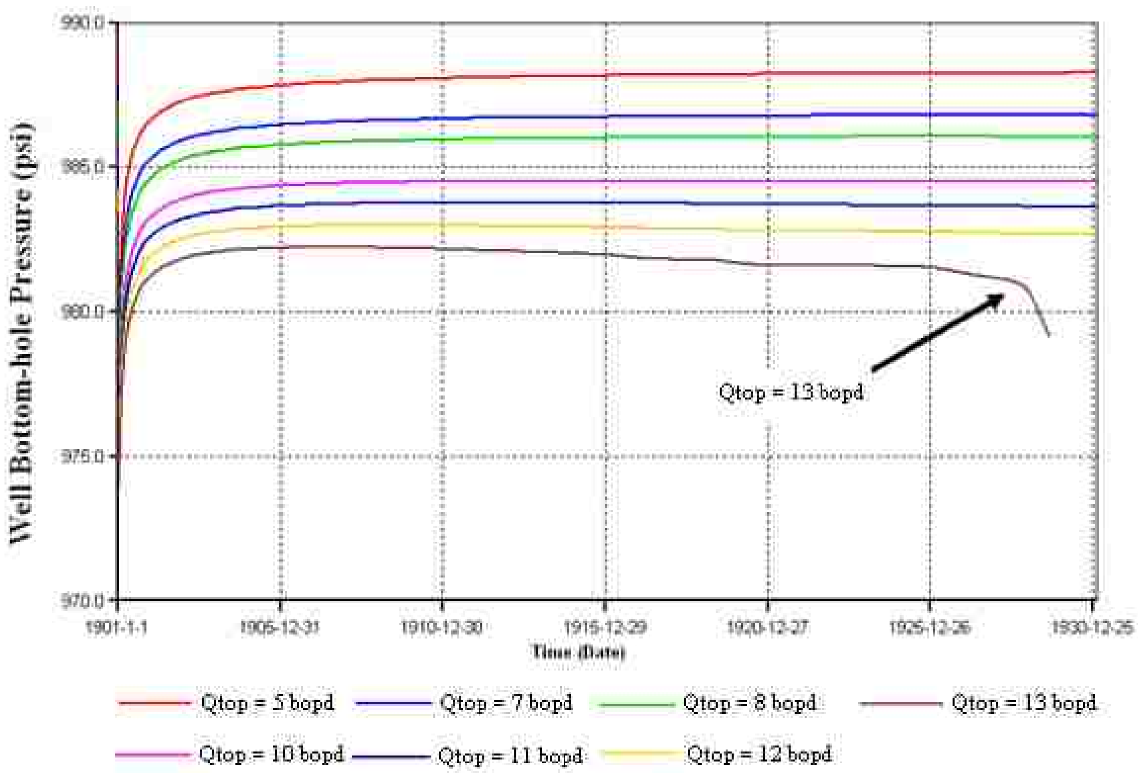

Figure 5.10 Top completion bottom-hole pressure changes with different oil rate for case $q_{wd} = 1000$ bwpd, $h_{di} = 5$ ft

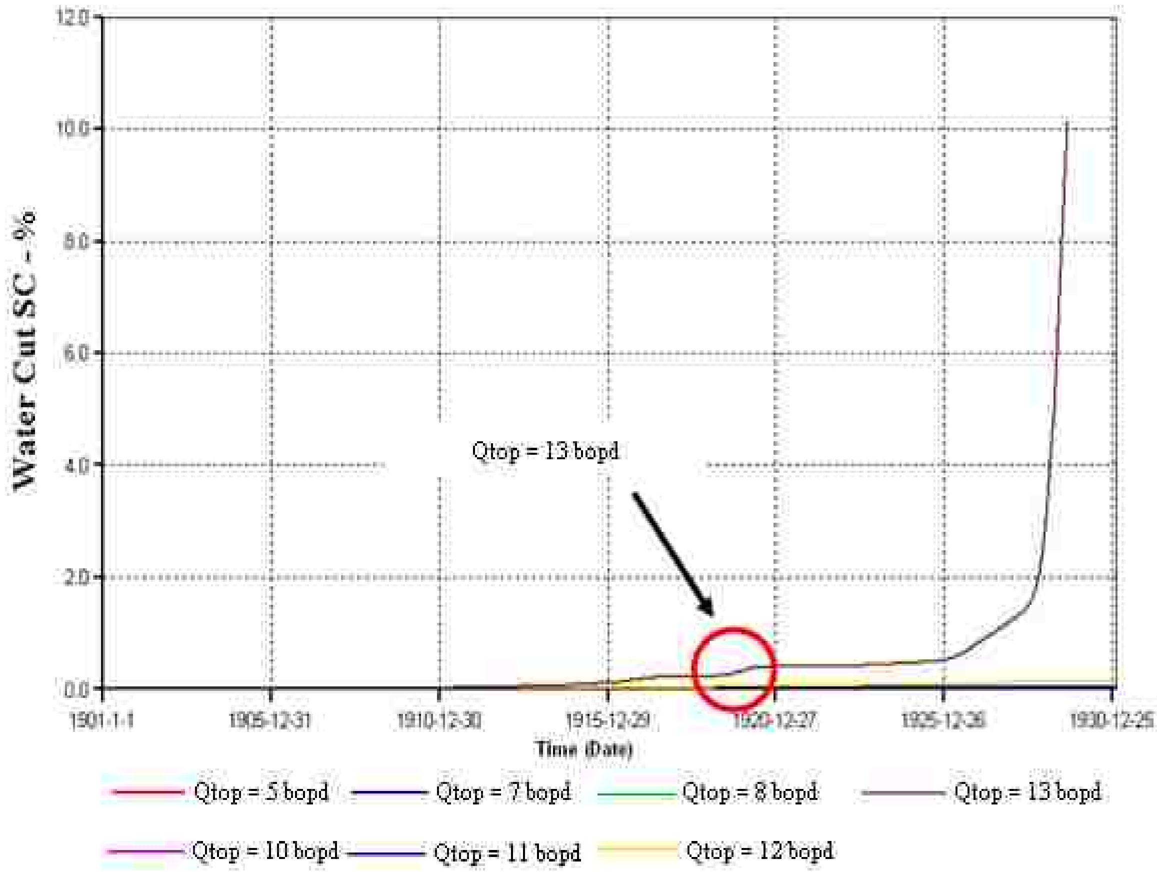

Figure 5.11 Top completion water cut changes with different oil rate for case $q_{wd} = 1000$ bwpd, $h_{di} = 5$ ft

Figure 5.13 shows the water drainage/injection rate needed to produce water-free oil at 10 *bopd* in the top completion with different D/I spacing. It is clear that the critical water drainage/injection rate decreases fast at first, and then becomes stable after a certain D/I spacing. Large quantity of water is drained to produce a limited amount of clean oil when the D/I spacing is short, which indicates that longer D/I spacing is preferred when the aquifer is thick enough. Both figures show that the differences between analytical and numerical models are around 10%. It means that the analytical model can roughly estimate the performance of DWL in an acceptable range.

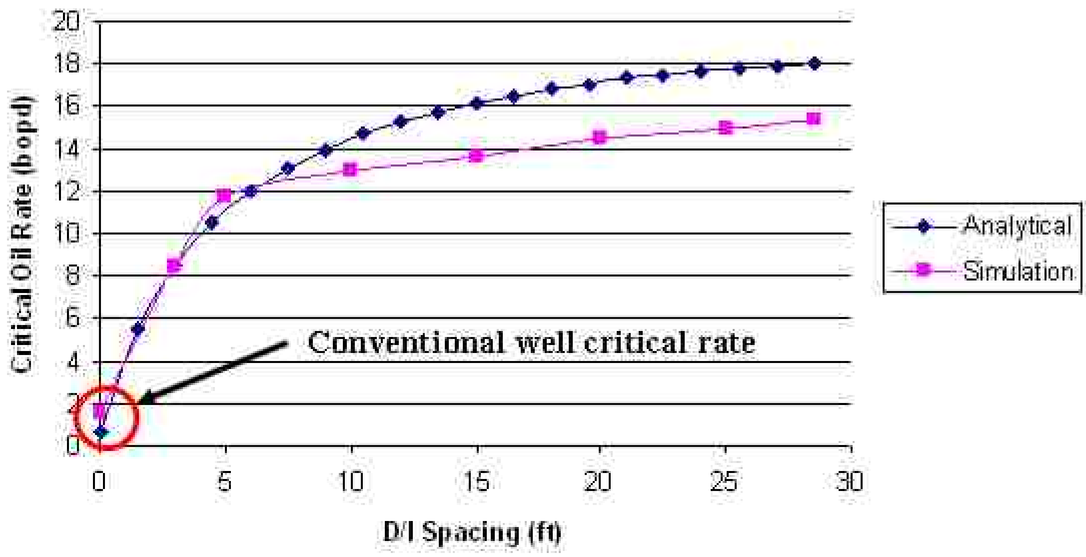

Figure 5.12 Critical oil rate changes with D/I spacing ($Q_{wd} = 1000$ bwpd)

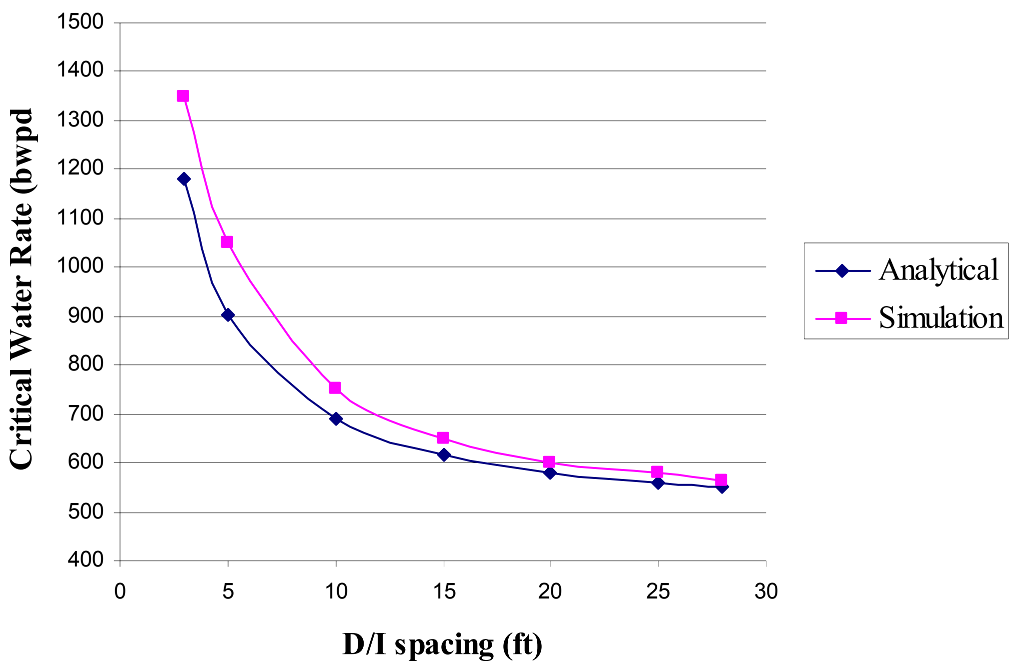

Figure 5.13 Critical water rate changes with D/I spacing ($Q_{op} = 10$ bopd)

5.4. Use of DWL Model for Determining the Critical D/I Spacing

From Figure 5.12 and Figure 5.13 we can see that, the critical D/I spacing is important to DWL system, too short D/I spacing will make the production uneconomical, on the other hand, too long D/I spacing will also add drilling and completion cost. Equation 5.14 indicates that some algorithm is needed to calculate this rate, because the skin factor of the injection completion "S_{pp_wi}" relates to the D/I spacing which is unknown. The steps shown in Figure 5.14 are used to get the skin factor:

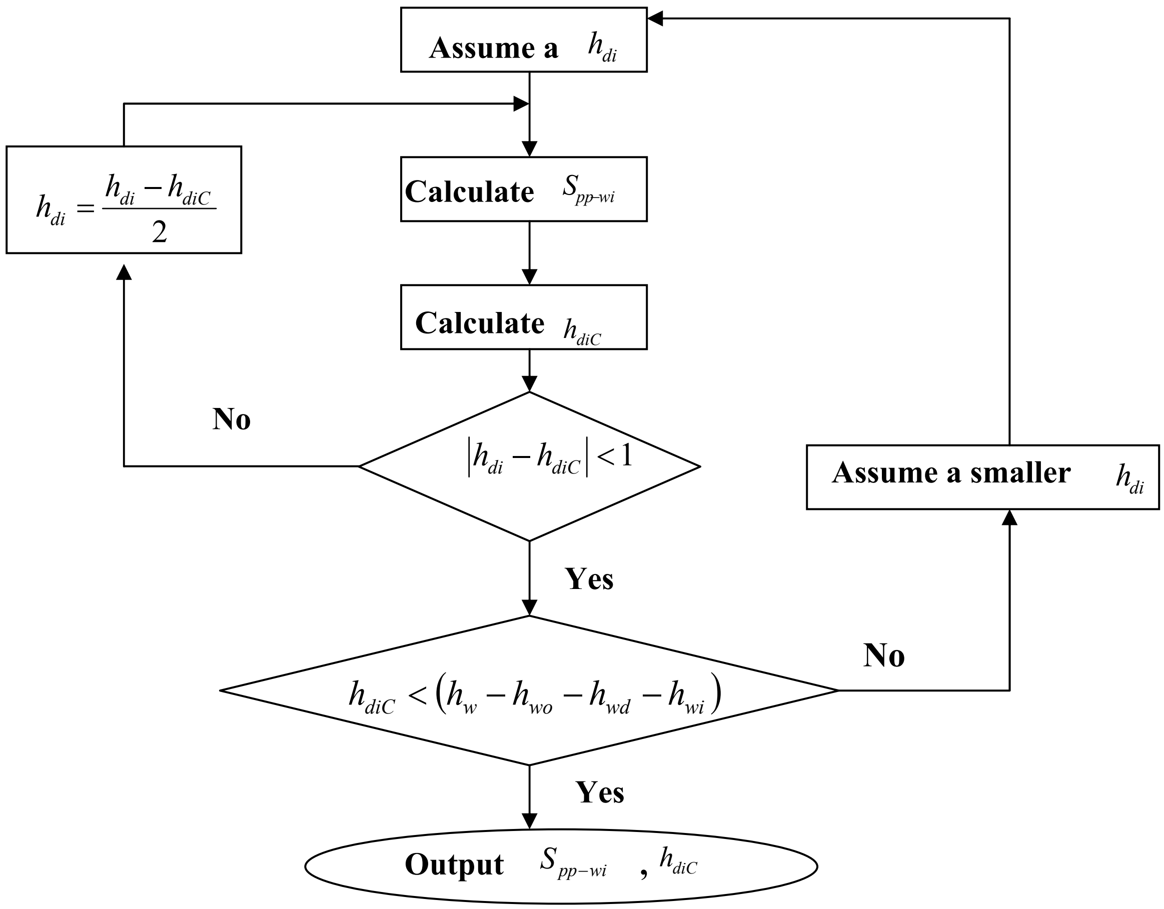

Figure 5.14 Steps to calculate injection completion skin and critical D/I spacing

1. Assume a D/I spacing "h_{di}";

2. Calculate the injection completion skin factor "S_{pp-wi}" using this D/I spacing;

3. Calculate the critical D/I spacing "h_{diC}" by Equation 5.14;

4. Check the value of "$\left|h_{di} - h_{diC}\right|$", if it is bigger than 1, then calculate the D/I spacing using "$h_{di} = \frac{h_{di} - h_{diC}}{2}$" and go to step 2; if it is less than 1, then go to step 5;

5. Check whether "$h_{diC} <= (h_w - h_{wo} - h_{wd} - h_{wi})$", if it is not, which means the D/I spacing exceeds the limitation of aquifer thickness, then assume a smaller D/I spacing and go to step 1, repeat the process until find the critical D/I spacing; if it is true, then go to step 6;

6. Output the injection completion skin factor and critical D/I spacing.

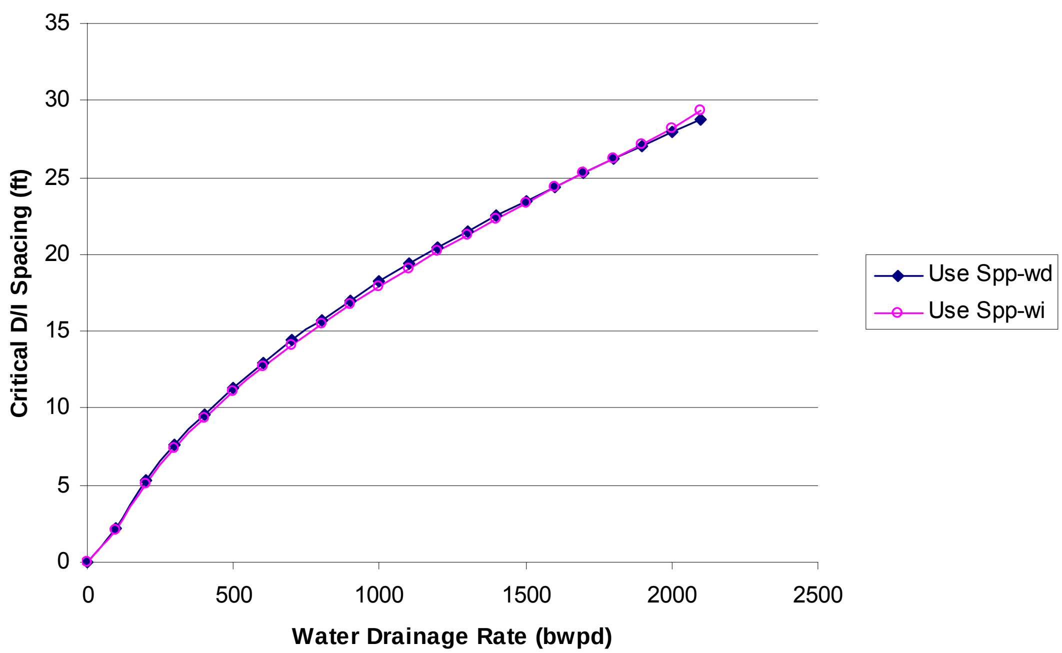

Figure 5.15 Critical D/I spacing calculated by different methods

The above process usually finishes within 10 iterations. However, a more simplified method can be used to get the critical D/I spacing. Notice that, the difference between water drainage completion skin and water injection completion skin is small when their penetration lengths are the same. So, it indicates that the skin factor of water drainage completion may be used instead of the injection skin to calculate the critical D/I spacing.

Using the same data in Table 5.1, the critical D/I spacing calculated by different methods is shown in Figure 5.15. It shows that the difference between the two methods is very small which means that drainage completion skin could be used to estimate the critical D/I spacing when there is no computer available. Also, we can see that the D/I spacing increases with water drainage/injection rate from this figure.

5.5. Discussion

By analyzing the mechanism of water coning control with DWL installation and applying the energy balance equation at intersection between the OWC and vertical axis of the DWL well, an analytical model has been built for DWL with segregated inflow of oil and water. The model, then has been verified by comparing with field data and numerical simulator. The results of the model show good match with both field data and simulation results. From the above study, it is clear that:

1. The model can estimate the performance of DWL in reservoirs fast and give reasonable results;
2. The critical oil rate can be increased dramatically by using DWL well compare to the conventional wells;
3. D/I spacing has significant influence on both critical oil production rate and critical water drainage/injection rate: small values of D/I spacing rapidly increase the critical oil production rate and reduce the critical water drainage/injection rate. Hence, the DWL system could work even in reservoirs with small bottom water.

CHAPTER 6. PERFORMANCE ANALYSIS OF DWL IN RESERVOIR WITH BOTTOM WATER

In the previous sections, we have seen that the critical oil rate of conventional well is too low to be economical, although DWL well can improve critical oil production rate significantly, it is still not the best solution in practice because of the large amount of water drainage/injection rate to get a relatively low critical oil rate increase. In fact, oil zone gets thinner with the production of oil, water will breakthrough to the oil well sooner or later, which means production of water is unavoidable in reservoir with bottom water. Water cut increases dramatically after water breakthrough in conventional wells, if it is not controlled properly, water will soon occupy all the perforations and a lot of oil will be bypassed. So, water cut control after breakthrough is more important in real practice. In the following parts of this chapter, the performance of DWL well will be discussed under situations of before and after water breakthrough.

6.1. DWL Well Performance before Water Breakthrough

To produce oil at a higher rate while avoiding oil in injection water, an Inflow Performance Window (IPW) similar to that of DWS well (Swisher and Wojtanowicz, 1995) can be developed for different combinations of the top and bottom rates as shown in Figure 6.1. Data in Table 3.1 and Table 3.2 are used with vertical to horizontal permeability ratio equals to 0.6 and different D/I spacing as shown in the figure.

In the figure, there are three (q_{bot} $vs.$ q_{top}) plots, each of them being an "envelope" representing different D/I spacing: 10 *ft,* 30 *ft* and 60 *ft*. The top boundary of each envelope represents maximum oil-free water drainage rate, while the lower boundary corresponds to maximum top rate of oil with no water. (Points inside the envelopes represent such combination of rates that the oil is water-free and drainage water contains no oil --- i.e. segregated production.) It is evident that with the injection point approaching the water drainage completion, the performance window of the DWL system moves into the area of larger water rates and smaller oil production. It is important to see that the DWL water re-injection technology would work even for a very close distance between drainage and injection completions (small D/I spacing). It means that the DWL system does not require drilling deep or deviated wells to inject produced water. Moreover, the system would not reduce the water-drive ability of the aquifer (reservoir pressure) while giving a low-water-cut oil production.

It is also evident that the system provides a limited control of the oil production rate. The upper blue line (*fo_bot*=0*, D/I*= 10 *ft*) in Figure 6.1 represents the maximum rate of water drainage/injection without oil breakthrough, while another blue line (*fw_top*=0*, D/I*= 10 *ft*) means the minimum water rate to prevent water breakthrough into the oil production completion when the D/I spacing is fixed at 10 *ft*. These two lines intercept at the point (98, 300), which stands for the maximum practical stable performance of the system. When the D/I spacing is fixed at 10 *ft*, oil can be produced at 98 *bopd* with 300 *bwpd* water drainage/injection rate, at this point, the top completion only produces oil and the bottom completions only drain/inject water. Production at the maximum performance point results in a very small margin of stability, only a small increase of oil or water rate will make the water or oil breakthrough, which is called flip-flop condition. This point moves right down with the increase of D/I spacing, which means more clean oil could be produced with less water drainage/injection rate.

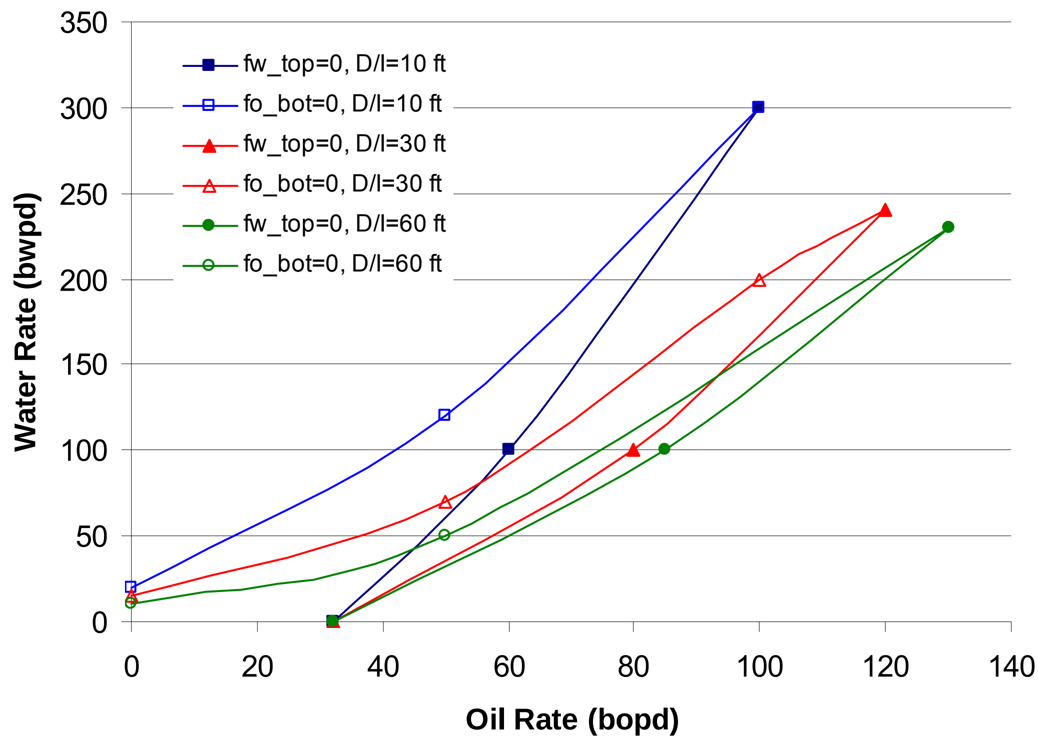

Figure 6.1 Inflow performance windows for DWL system with various D/I spacing

6.2. DWL Well Performance after Fluid Breakthrough

6.2.1. Prevent Oil Breakthrough into the Bottom Completions

If the drainage-injection water contains some oil, not only the aquifer will be polluted, but also the injection completion will be damaged. (Even small oil content in injection water would deposit residual oil-saturated skin zone around the injection completion thus reducing permeability to water and injectivity of the completion.) So, it is important to avoid oil in the injection water.

Let's consider the oil content limit in the injection water. Figure 6.2 shows that oil content in injection water changes with D/I spacing and injection rate. When the top rate is high, bottom rate is low or the D/I spacing is short, there will be little oil in the injection water. These results correspond to the drainage completion located 10 *ft* below the oil water contact. Note also that if the drainage completion is placed 20 *ft* below the OWC or the top oil production rate is increased above 1700 *bopd*, there will be no oil in the injection water for all these cases. It indicates that, in order to prevent oil breakthrough, the water drainage completion should not be placed too close to the OWC, and the oil production rate should not be too small.

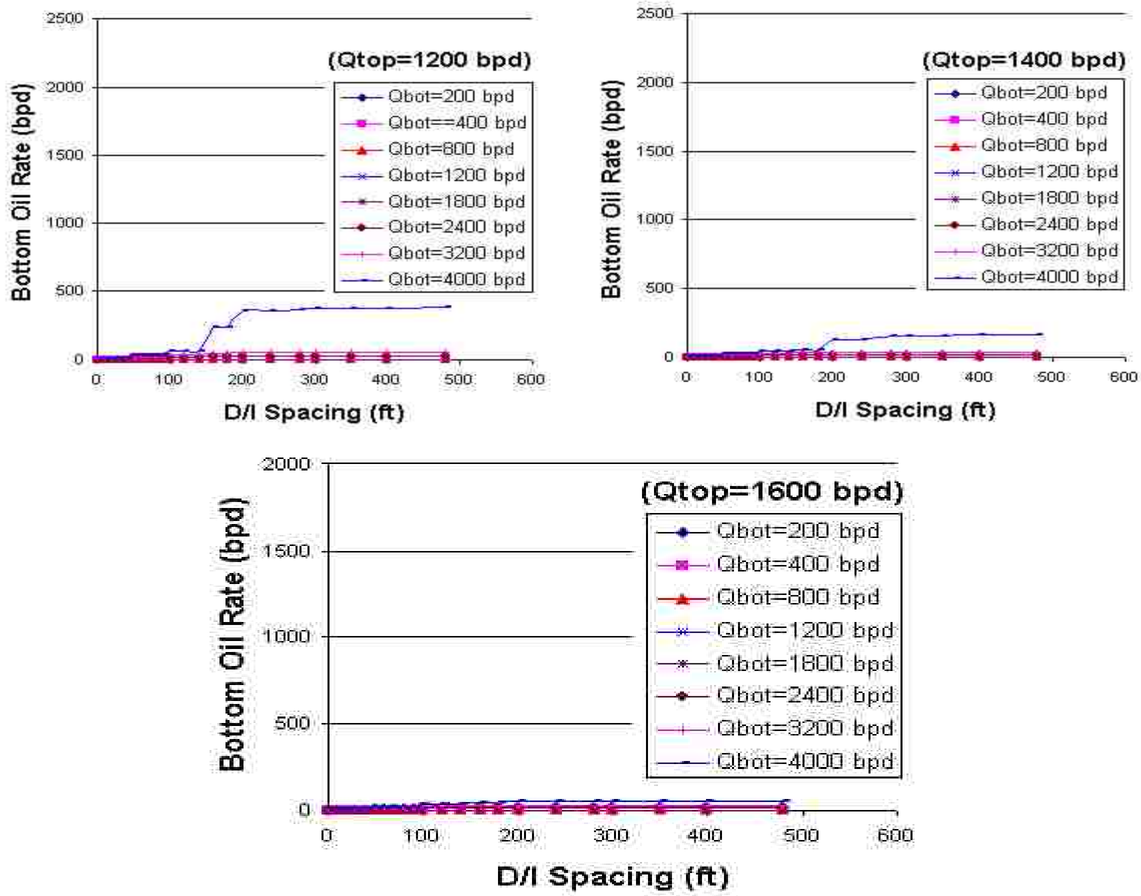

Figure 6.2 Oil content in injection water depends upon D/I spacing and combination of production and drainage rate

6.2.2. Water Cut Development after Water Breakthrough

From section 5.1 we can see that, DWL well can improve critical oil production rate significantly comparing to the conventional well, but it is still not the best solution in practice because of the large amount of water drainage/injection rate to get a relatively low critical oil rate increase and it is difficult to get the stable segregated fluids flow due to the narrow IPW. In fact, oil zone gets thinner with the production of oil, water will breakthrough to the oil well sooner or later, which means production of water is unavoidable in reservoir with bottom water.

In conventional wells, water cut develops fast after water breakthrough, if it is not controlled properly, water will soon occupy all the perforations and the well has to be shut in. As a result, a lot of oil will be bypassed and the total recovery will be reduced. So, water cut control after breakthrough is more important in real practice.

Based on the early studies of water coning theory (Sobocinski and Cornelius, 1965, Bournazel and Jeanson, 1971), Kuo and DesBrisay (1983) developed one of the most widely-used models to predict water cut performance in conventional wells after breakthrough:

$$WC = WC_D \times WC_{ul} \qquad (6.1)$$

Where,

$$WC_{ul} = \frac{Mh_w}{Mh_w + h_o} \qquad (6.2)$$

$$\begin{cases} WC_D = 0 & \text{for} \quad t_D < 0.5 \\ WC_D = 0.94 \log t_D + 0.29 & \text{for} \quad 0.5 < t_D < 5.7 \\ WC_D = 1 & \text{for} \quad t_D > 5.7 \end{cases} \qquad (6.3)$$

$$t_D = \frac{t}{t_{BT}} \qquad (6.4)$$

$$t_{BT} = \frac{\mu_o \phi h_o (t_D)_{BT}}{0.00137(\rho_w - \rho_o)k_v(1+M)} \qquad (6.5)$$

Where, $\alpha = 0.5$ for $M < 1$, and $\alpha = 0.6$ for $1 < M < 10$.

$$(t_D)_{BT} = \frac{z}{3 - 0.7z} \quad (6.6)$$

$$z = \frac{0.0037(\rho_w - \rho_o)k_h h_o (h_o - h_{op})}{\mu_o q_o B_o} \quad (6.7)$$

Shirman (1998) experimentally verified this model by Hele-Shaw model as shown in Figure 6.3. Using the data in Table 3.1 and Table 3.2, the water cut calculated by Kuo and DesBrisay's model is 0.7963 and the simulation results vary from 0.765 to 0.798 as shown in Figure 6.4. The good matching of the experimental and calculation results means that Kuo and DesBrisay's model can be used to predict the water cut performance of conventional wells in real reservoirs after breakthrough.

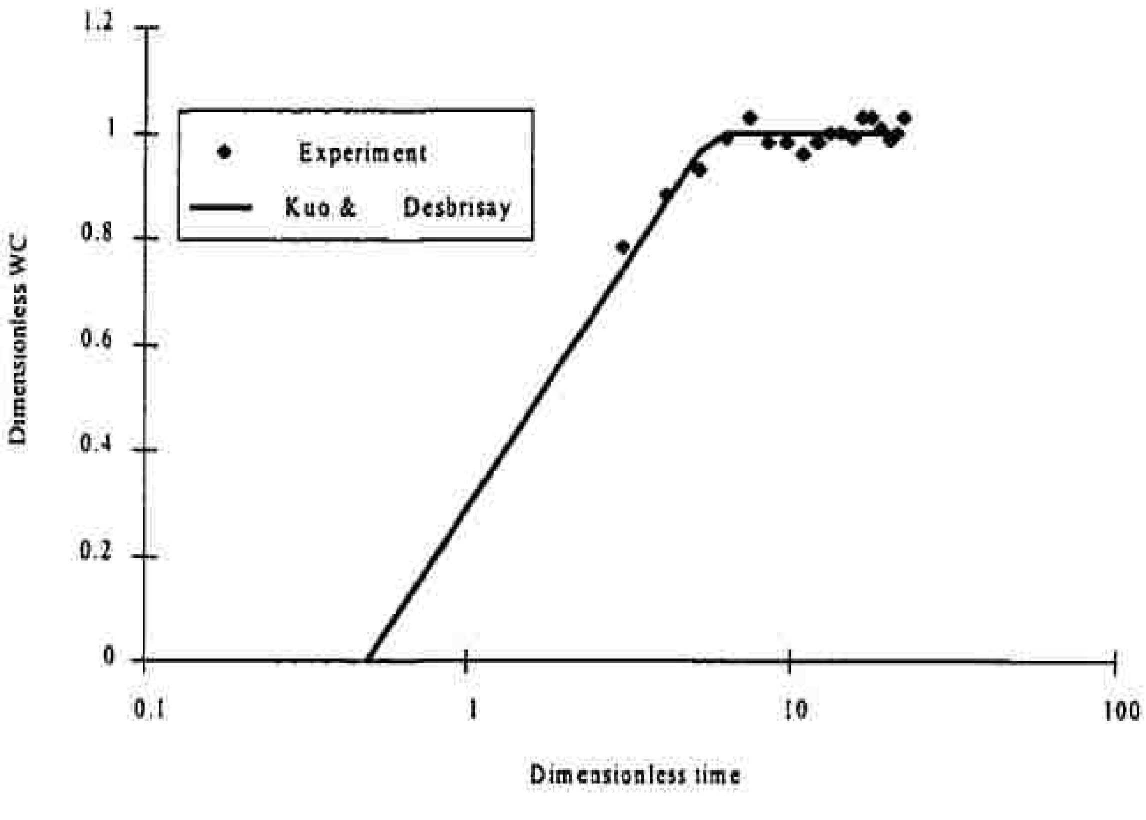

Figure 6.3 Matching of water cut performance from experiments and Kuo and DesBrisay's model (Shirman, 1998)

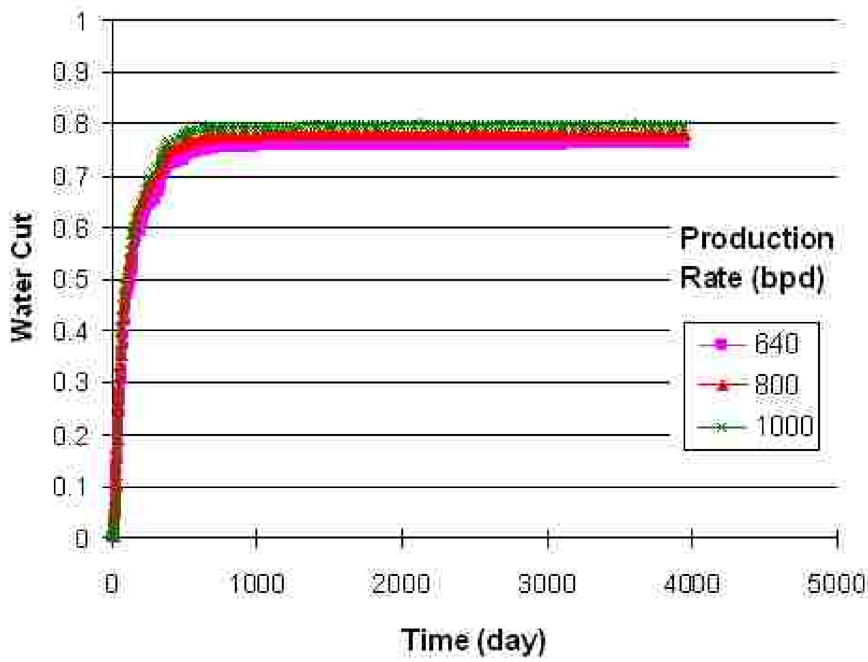

Figure 6.4 Water cut changes with production rate in conventional wells

According to Kuo and DesBrisay's model, water cut will be equal to an ultimate value (Equation 6.2) after the stabilization of the water cone. The reason is that, with the increasing of water encroachment, the water cone covers a larger area of the oil completion and more water is then produced. Under this situation, the height of the water cone decides the water cut. As discussed previously, there are two main factors determine the development of water cone: viscous force and gravitational force. When the production rate is high, the viscous force will be much greater than the gravitational force and become the main factor of cone shape. After the system reaching equilibrium condition, the production rate does not change anymore, the cone height will be fixed at a certain point. At this point, the fluid mobility and reservoir geometry determine the final value of water cut. Because the oil production rate is always high enough to make the viscous force much greater than the gravitational force, the fluid mobility and reservoir geometry determine the ultimate water cut in real practice.

However, it is not always the case for DWL well. As shown from Figure 6.5 and Figure 6.6, DWL well with different D/I spacing or bottom water rate has different water cut. It is clear that, water cut decreases with bottom water rate or D/I spacing when the top production rate is fixed at 800 *bpd*. Comparing to the conventional well, DWL well reduces the water cut from 0.7963 to 0.361 with 4000 *bwpd* bottom water rate and 200 *ft* D/I spacing. Unlike conventional well, the force balance is more complex in DWL well. There are another two viscous forces from the aquifer, one is generated by water drainage and the other is caused by water injection. Because of the water drainage rate is always very high and the viscous force caused by it tends to balance the force generated by oil production. Another viscous force caused by water injection decreases fast with the increase of D/I spacing, it becomes very small when the D/I spacing is long. In this case, the resultant force of viscous forces caused by oil production, water drainage and injection determines the shape of water cone. As a result, the more water drainage rate and longer D/I spacing lead to lower cone height and water cut.

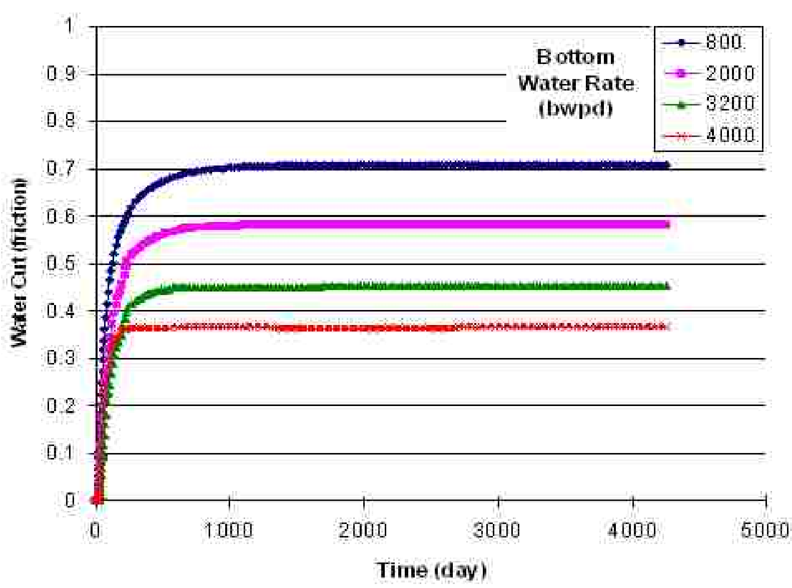

Figure 6.5 Water cut changes with bottom water rate in DWL wells (Top rate equals to 800 *bpd*, D/I spacing equals to 200 *ft*)

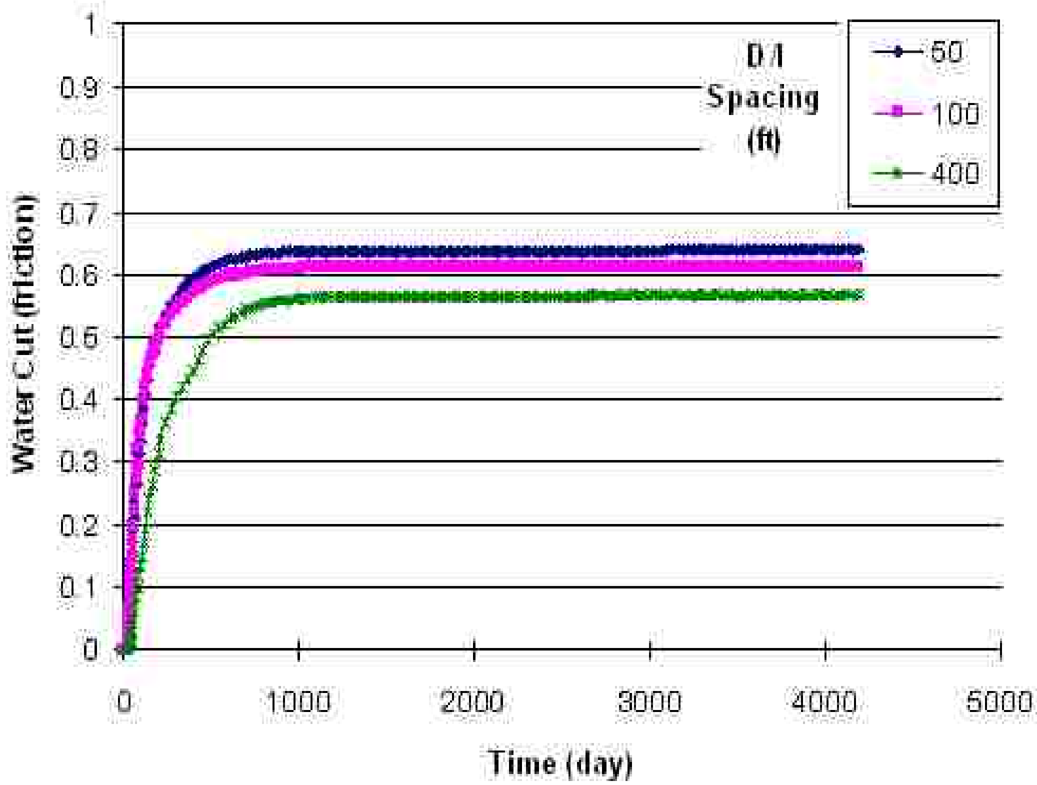

Figure 6.6Water cut changes with D/I spacing in DWL wells (Bottom rate equals to 2000 *bwpd*, top rate equals to 800 *bpd*)

In conventional wells, with a maximum liquid production rate the increased water cut means less oil produced --- a common problem in production practices. Therefore, the main advantage of DWL is lower water cut and higher oil rate. As shown from Figure 6.5 to Figure 6.8, larger bottom water rate and D/I spacing dramatically improves well performance by reducing water cut and increasing oil rate. At long D/I spacing, the effect of water drainage on well performance is very strong: as shown in Figure 6.7, a 60-percent and 100-percent increase of water drainage would increase oil production by 55% and 80%, respectively. For a given D/I spacing, an effective increase of oil production requires synchronized increases in production and drainage rates --- Figure 6.8. A sole increasing of the top production rate is not so effective.

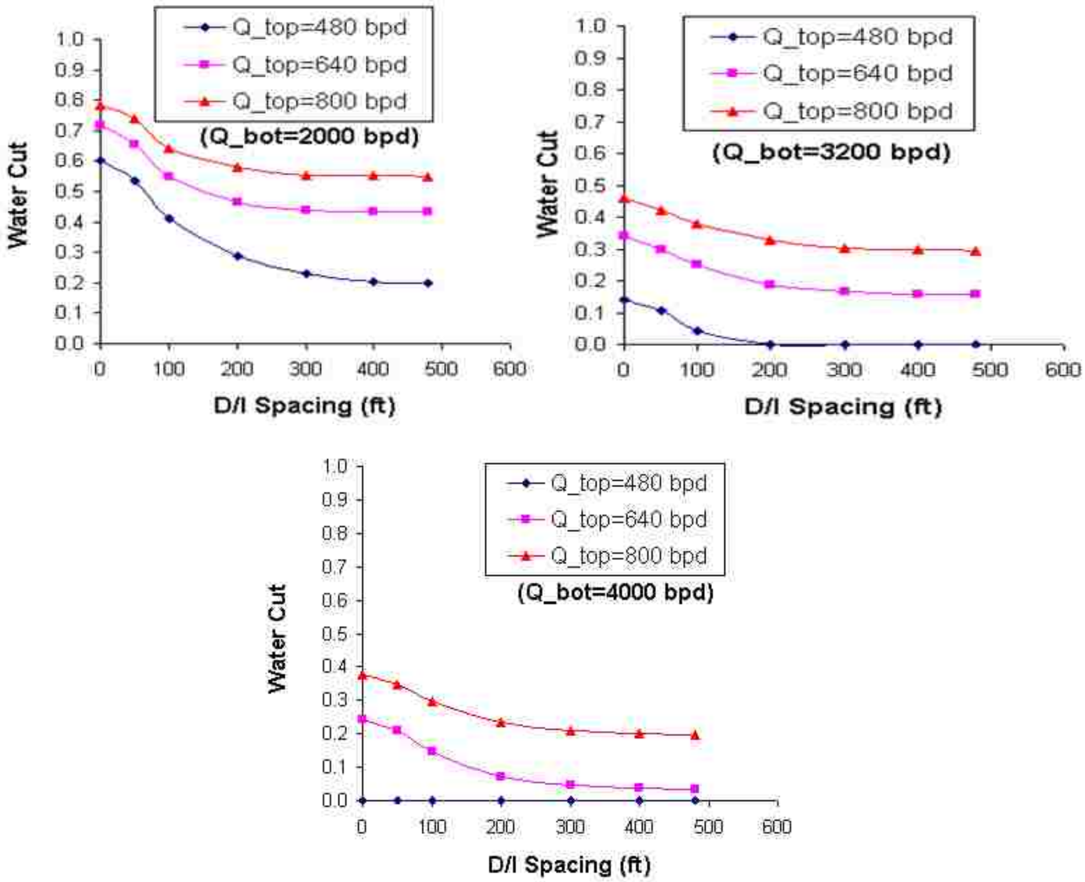

Figure 6.7 Water cut changes with top rate and D/I spacing at various bottom rate

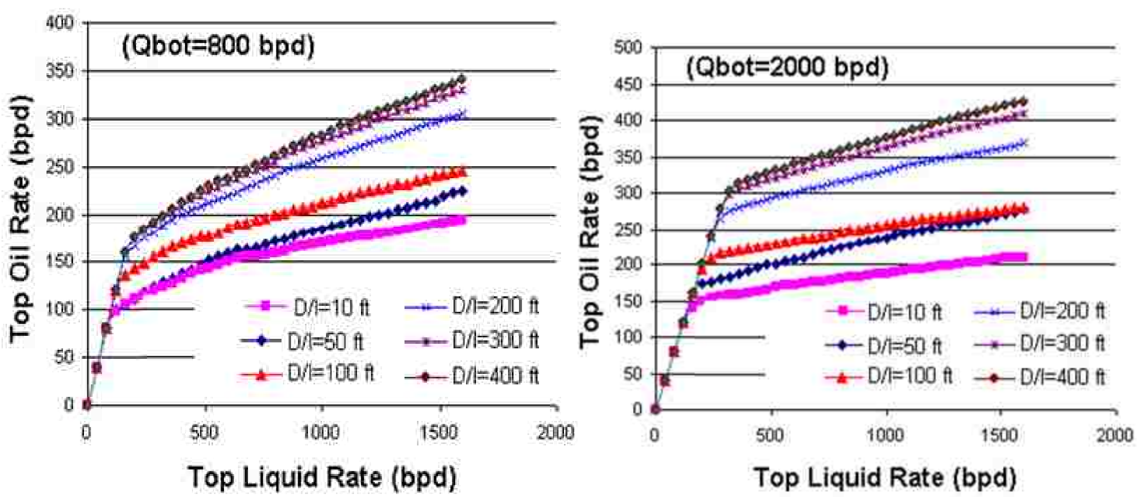

Figure 6.8 Top completion oil rate changes with top completion liquid rate at various D/I spacing and bottom rate

6.3. DWL Well Performance (Nodal) Analysis

Production systems (Nodal) analysis method seeks the highest oil or gas production rate. The method's name comes from imposition of consistent pressures and rates at key interfaces or nodes in the reservoir-well-flowline system (e.g., the node at the bottom of a well couples the tubing and inflow performance). Valid solution corresponds to the tubing and inflow performance curves intercept that complies the bottomhole flowing pressure with production rate. This production optimization technique requires a representative inflow model. Inflow performance curves are generated either using analytical or empirical models or by reservoir simulators.

Similar to DWS wells, the rates for the three completions in DWL wells are adjusted to reduce or completely eliminate water from the top completion while the drained water (not contaminated with oil) is injected back into the aquifer without further processing. Arslan et al (2004, 2005) applied nodal analysis method to DWS wells. They pointed out that oil wells would be generally produced at their highest possible rate to maximize the cash flow. However, the maximum allowable pressure drawdown was a limiting factor due to the practical considerations such as well integrity, sand control, gas liberation, etc. This limit should also be considered in inflow models. The nodal analysis for DWS wells was based on the following operational principles:

1. Produce at maximum possible top rate (economic goal);
2. Maintain a pressure drawdown below or equal to the maximum allowable pressure drawdown for both completions (completion limit);
3. Maintain a water drainage rate below the flip-flop line for any top rate (No reverse coning.) (An environmentally imposed limit);

4. Set the top and drainage rates that can flow to surface (TPR limit);
5. Limit drainage rate according to maximum allowable injection limit possible (Disposal limit).

A nodal analysis solution would result from an inflow model representing reservoir properties at a given time. Then, the calculated production rate from the model was employed to predict the incremental recovery for a period of interest. Using this incremental recovery, the change in the average reservoir properties at different stages of depletion was estimated from material balance. Future rates were predicted successively in this manner. By using this method, it was concluded that the DWS technology could increase oil production rate more than twofold compared with conventional wells.

Qin and Wojtanowicz (2007) extended DWS nodal analysis method in bottom water drive heavy oil reservoir to study the dynamics of productivity loss in wells. They considered varying water cut during the production and the ways to control it: reducing well's pressure drawdown, assessing the operational range of bottom hole flowing pressure and increasing the bottom water drainage. They found out that the operational range of production rates with variable water cut was very small for heavy oil; pressure drawdown in heavy oil was very sensitive to the rate; increasing water drainage rate could stimulate natural flow of heavy oil without a need for oil lifting; a considerable improvement in water control and well productivity could be achieved by using DWS in heavy oil reservoir.

Due to the similarity between DWS and DWL wells, DWS nodal analysis method could be extended to DWL wells by evaluating the pressure versus flow rate relationship for the top completion for a range of bottom rates and D/I spacings. As an additional constraint, oil should be eliminated from injection water, so the water is oil-free. This constraint is added to the DWL well performance plots, as shown in Figure 6.9 and Figure 6.10 for bottom water rates 4000 *bwpd* and 7200 *bwpd*, respectively (using the reservoir properties in Table 3.1and Table 3.2). In the plots, several upward lines represent tubing performance relationship (TPR) with variable water cut --- each line for different D/I spacing. The numbered intercepts (1, 2 …) indicate the rate/pressure conditions of natural flow at the top completion. It is clear that DWL increases production rate and reduces water cut comparing to conventional well. The results also show that larger D/I spacing improves DWL performance until D/I optimum value is reached.

In Figure 6.9 and Figure 6.10, lines AB and A'B' represent the limit of oil-free water drainage. For each D/I spacing and drainage rate, there is a minimum production rate (q_{top}) needed to prevent oil drainage. Figure 6.9 shows a case when the oil-free drainage limit is met for all values of D/I spacing. When the drainage rate (q_{bot}) is 4000 *bwpd*, the oil-free injection limitation line AB is below the IPR line, it means that reservoir energy is enough to sustain the natural flow rates. In this case, 850 *bpd* with water cut 0.75, the DWL well's production rate is 1050 *bpd* with water cut 0.56 for the D/I spacing 50 *ft*. Moreover, the DWL production rate would increase to 1280 *bpd* with water cut reduced to 0.31 for the D/I spacing 480 *ft*. For the two D/I spacings, the oil rates would increase by 54% and 76% comparing to the conventional well's production rate, respectively.

Figure 6.10 shows a case when the D/I spacing restricted by the oil-free drainage limit. When the drainage rate is 7200 *bpd*, the oil-free injection limitation line A'B' is across the IPR, it means that if D/I spacing is bigger than 100 *ft*, the reservoir energy is not enough to lift the natural flow rate to the surface, a pump should be added in the top completion to maintain the production rate, or else oil will be injected to the aquifer.

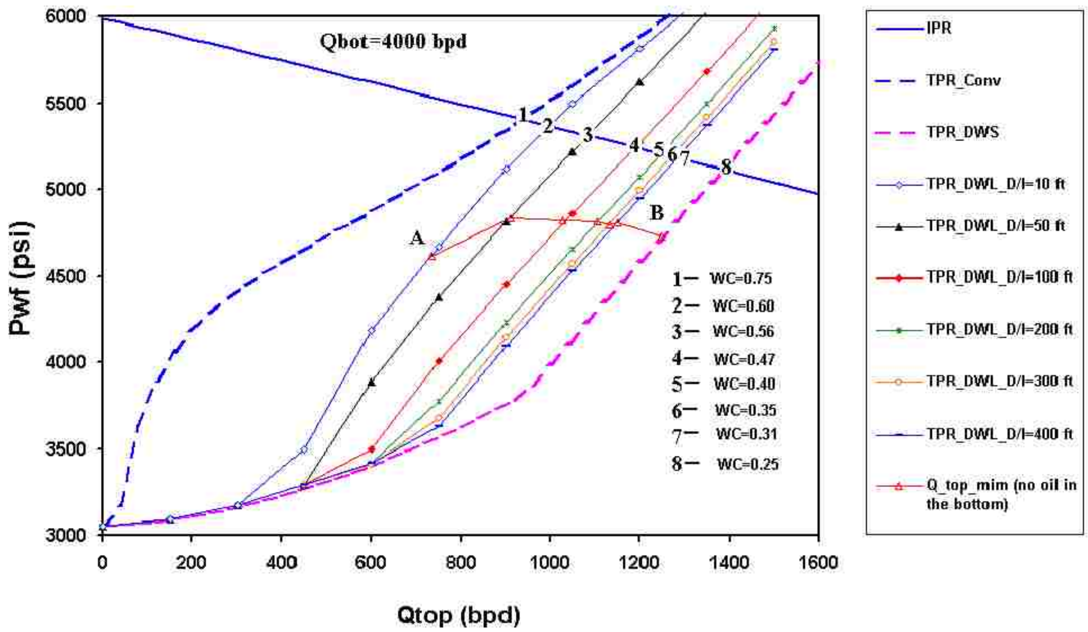

Figure 6.9 Nodal analysis for DWL wells for water drainage-injection rate 4000 *bwpd*

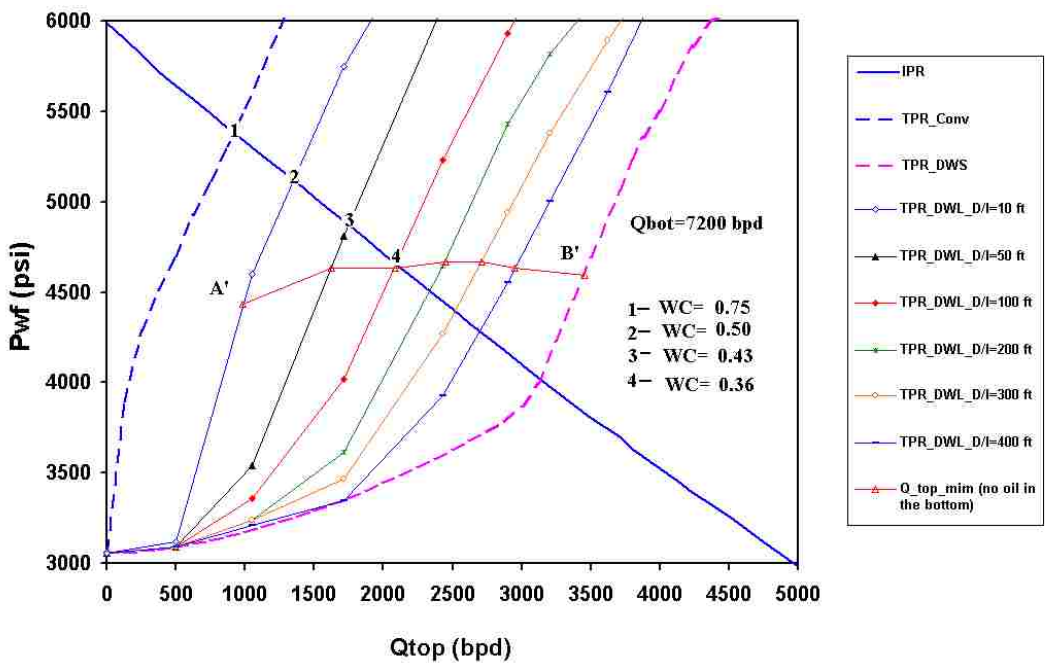

Figure 6.10 Nodal analysis for DWL wells for water drainage-injection rate 7200 *bwpd*

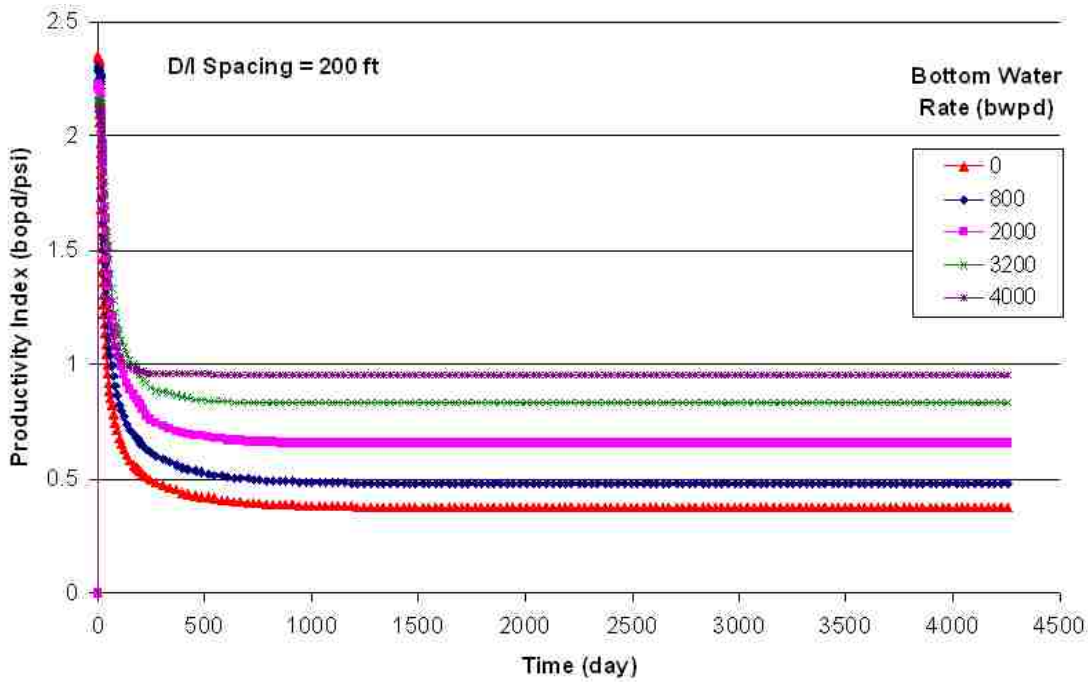

Figure 6.11 Productivity index comparison of conventional well and DWL well with various bottom water rate

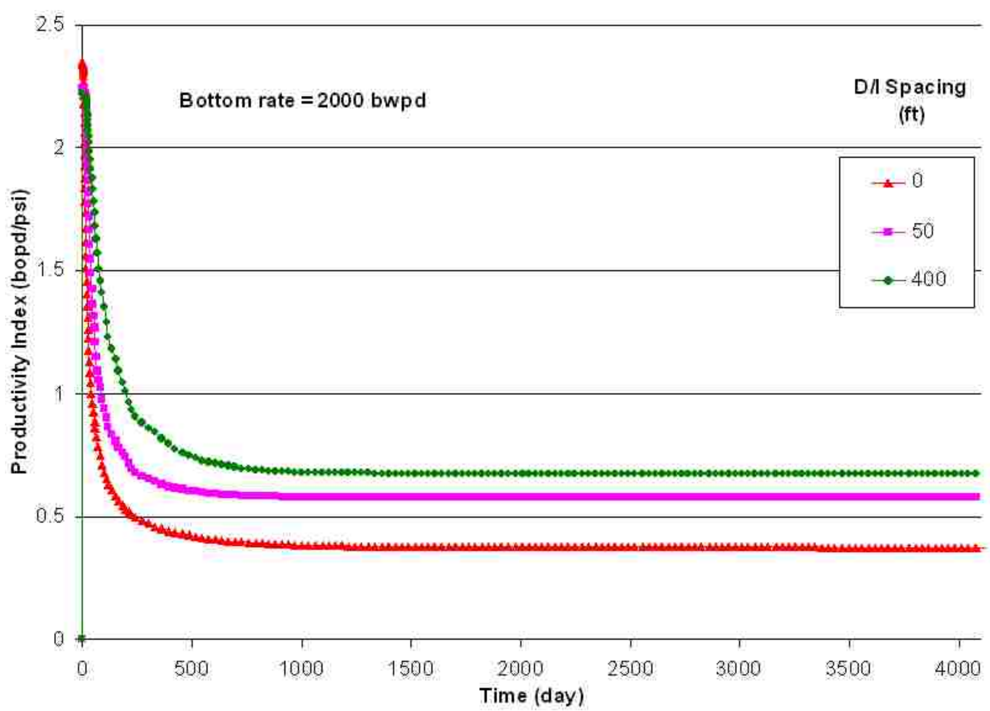

Figure 6.12 Productivity index comparison of conventional well and DWL well with various D/I spacing

Productivity index (oil production per unit pressure drop) is significant to an oil production well, it shows the quality of a well and the performance of a well can be evaluated from it. Reservoir engineers always seek ways to improve the productivity index. Figure 6.11 and Figure 6.12 show the productivity index comparison of conventional well and DWL well with various bottom water rate and D/I spacing.

It is evident that DWL well and conventional well have similar productivity indexes at the beginning of the production, however, conventional well cannot maintain the value stable for a long time and DWL well has higher productivity index with the production goes on. It means DWL well can produce oil in a stable rate and more cost-effective.

6.4. Discussion

The performance of DWL well has been analyzed both before and after water breakthrough to the top completion: an Inflow Performance Window (IPW) has been developed for different combinations of top and bottom rates with various D/I spacing before water breakthrough; a DWS nodal analysis method has been modified and used to analyze DWL well performance after water breakthrough. Effects of DWL operational parameters: D/I spacing, production and drainage-injection rates have been studied for a selected well-reservoir system. Also studied was the effect of the oil-free water drainage limit on DWL performance design. The study leads to the following conclusions:

1. DWL well provides limited control region before water breakthrough, production at the maximum performance point results in a very small margin of stability, only a small increase of oil or water rate will make the water or oil breakthrough.

This point moves right down in IPW with the increase of D/I spacing, which means more clean oil could be produced with less water drainage/injection rate;

2. The water cut performance in DWL well is quite different from that of conventional well, the method good for conventional well may not be used for DWL well;
3. Both D/I spacing and water drainage/injection rate have significant influence on the water cut performance in the top completion: larger D/I spacing or water drainage/injection rate improves well performance by reducing water cut and increasing oil rate;
4. For a given D/I spacing, an effective increase of oil production requires synchronized increases in production and drainage rates. A sole increasing of the top production rate is not effective as it would result in higher water cut;
5. Nodal analysis model of DWL well with variable water cut and oil-free water drainage limit has practical merit. The method would help to design the D/I spacing and decide if one or two downhole pumps were needed for the system;
6. The higher productivity index of DWL well also shows that it is more cost-effective to install DWL well in reservoirs with bottom water than conventional well.

CHAPTER 7. CONCLUSIONS AND RECOMMENDATIONS

7.1. Conclusions

In this work, the mechanism of water coning control with DWL installation was analytically analyzed, and a simplified analytical model has been built using the flow potential distribution theory combining with transformation factors and skin factors to consider both reservoir anisotropy and well partial penetration effects. The model, then has been verified by comparing with field data and numerical simulator. It shows that the results of the model are accurate enough. The performance of conventional well and DWL well has been compared and the results show that DWL well has higher oil production rate and lower water cut than conventional well, DWL well also provides more flexibility for reservoir engineers to control water coning in reservoir with bottom water. The higher productivity index of DWL well also shows that it is more cost-effective to install DWL well in reservoirs with bottom water than conventional well. We also studied the effects of DWL operational parameters: D/I spacing, production and drainage-injection rates have been studied for a selected well-reservoir system. Also studied was the effect of the oil-free water drainage limit on DWL performance design. A DWS nodal analysis method has been modified and used to analyze DWL well performance. From the above study, it follows that:

1. A simplified analytical model is proposed to estimate the performance of DWL under segregated production domain, it can evaluate the reservoir candidates fast and give reasonable results;

2. Critical oil rate can be increased dramatically by using DWL well compare to the conventional wells;
3. Small values of D/I spacing rapidly increase the critical oil production rate. Hence, the DWL system could work even in reservoirs with thin aquifer;
4. A numerical model is developed to simulate the performance of DWL under water control domain, the model is useful in evaluate the water cut control effects of DWL;
5. Water cut in DWL well could be controlled effectively by either increasing D/I spacing or water drainage rate;
6. Oil rate in DWL well is higher and more stable since the water cut could be controlled by adjusting the water drainage rate;
7. A Modified Nodal Analysis model of DWL is proposed to find the best combination of D/I spacing and water drainage rate to get the highest oil rate. The method would also help to design the D/I spacing and decide if one or two downhole pumps were needed for the system.

7.2. Recommendations

1. Due to the large number of parameters involved in DWL analysis and experimental design, dimensionless groups that control the system should be found to simplify the work. More detailed study involving different modeling, reservoir properties, and production conditions should be done to get a better understanding of DWL operations in various reservoirs;
2. More in-depth study of water cut development after water breakthrough in DWL wells should be carried out. Since it is unavoidable to produce some water in

reservoirs with bottom water, water cut control is more realistic than just improve the critical oil rate;

3. Recovery and economical comparisons of different type of wells such as conventional well, DWS well and DWL well should be done to maximize the profits of real fields;
4. More detailed study involving different modeling, reservoir properties, and production conditions should be done to get a better understanding of DWL operations in reservoir with bottom water. Optimized operational strategy of DWL is needed before field practice;
5. Injectivity decline analysis of the water injection completion should be done to predict the long time performance of DWL;
6. Optimized operational strategy of DWL is needed before field practice.

NOMENCLATURE

a_x, is the general coordinate transformation factor in x direction, dimensionless;

a_r, is the general coordinate transformation factor in r direction, dimensionless;

a_y, is the general coordinate transformation factor in y direction, dimensionless;

a_z, is the general coordinate transformation factor in z direction, dimensionless;

a_D, is the dimensionless injection constant;

$a_n b_n$, is the depth of a hypothetical flux element of density a_n extending from the top of the sand to the point $z = b_n$, *ft*^{2};

B_o, is the oil formation factor, *rb/stb*;

C, is the compressibility, *1/psi*;

c_1, is the system total compressibility of the invaded zone, *1/psi*;

c_2, is the system total compressibility of the invaded zone, *1/psi*;

D_b, is the distance from OWC to the bottom of the perforation interval, *ft*;

F_η, is the diffusivity ratio of water and oil;

G, is the gravity force, *psi*;

h_1, is the distance from oil formation top to the penetration top, *ft*.

h_c, is the height of the transition zone, *ft*;

h_{cb}, is the height of completion bottom from top of formation, *ft*;

h_{ct}, is the height of completion from top of formation, *ft*;

h_o, is the oil formation thickness, *ft*;

h_{oC}, is the critical cone height, *ft*;

h_{op}, is the length of partial penetration, *ft*;

h_w, is the aquifer thickness, *ft*;

h_{wi}, is the thickness of the water injection zone, *ft*;

$\bar{k}$, is the average permeability in isotropic reservoir, *md*;

k_h, is the horizontal permeability in reservoir, *md*;

k_v, is the vertical permeability in reservoir, *md*;

k_x, is the permeability in x direction, *md*;

k_y, is the permeability in y direction, *md*;

k_z, is the permeability in z direction, *md*;

k_r, is the permeability in r direction, *md*;

k_o, is the effective permeability of oil phase, *md*;

k_{wr}, is the effective permeability of water in horizontal direction, *md*;

k_{wz}, is the effective permeability of water in vertical direction, *md*;

k_{or}, is the effective permeability of oil in horizontal direction, *md*;

k_{oz}, is the effective permeability of oil in vertical direction, *md*;

$p(t,x,y)$, is the pressure at point (x,y) of the reservoir at time t, *psi*;

p_c, is the capillary pressure, *psi*;

p_{oi}, is the bottom hoe injection pressure, *psi*;

Δp_o, is the total pressure drawdown in oil formation, *psi*;

Δp_{op}, is the pressure drawdown in oil formation caused by oil production, *psi*;

Δp_S, is the pressure drawdown in oil formation caused by the skin factor, *psi*;

q_i, is the water injection rate, *stb/d*;

q_o, is the oil production rate, *bpd*;

q_{oC}, is the critical oil rate calculated by the correlation derived in this thesis, *bopd*;

q_{opC}, is the critical oil rate for DWL well, *bopd*;

q_{CC}, is the critical oil rate calculated by Chaperon's correlation (1986), *bopd*;

q_{MC}, is the critical oil rate calculated by Meyer and Gardner's correlation (1954), *bopd*;

q_{SC}, is the critical oil rate calculated by Schols' correlation (1972), *bopd*;

q_{HC}, is the critical oil rate calculated by Hoyland et al.' correlation (1989), *bopd*;

q_{cmg}, is the critical oil rate simulated by CMG®, *bopd*;

q_{bot}, is the water drainage/injection rate in DWL, *bwpd*;

q_{top}, is the fluids production rate of the top completion in DWL, *bpd*;

q_{wdC}, Critical water drainage/injection rate, *bwpd*;

r_A, is the radius of drainage area, *ft*;

r_e, is the radius of reservoir, *ft*;

r_w, is the radius of well, *ft*;

S_{pp}, is the skin factor caused by the partial penetration, *dimensionless*;

S_{wi}, is the skin factor of the water injection well, *dimensionless*.

Z_S, is the distance between point source and apex of the water cone, *ft*;

$Z_{\min}$, is the critical D/I spacing, *ft*;

Greek:

α_p, is the linear poro-elastic expansion coefficient;

α_w, is the overall hydraulic diffusivity coefficient which combines both the formation and fluid properties;

μ, is the fluid viscosity, *cp*;

μ_o, is the viscosity of oil, *cp*;

μ_w, is the viscosity of water, *cp*;

Δm, is the rate of mass accumulation, *lbm*;

$\Delta\rho$, is the density difference of water and oil, *lbm/ft³*;

γ_w, is the relative gravity of water, *fraction*;

γ_o, is the relative gravity of oil, *fraction*;

ψ_w, is the water dimensionless function;

ϕ , is the porosity of the reservoir, fraction;

Φ, is the fluid potential in the reservoir, *psi*;

υ, is the Poisson's ratio;

∇^2, is the Laplace operator.

REFERENCES

Abass, H.H. and Bass, D.M. The Critical Production Rate in Water-Coning System. SPE 17311, *Proceedings of the SPE Permian Basin Oil and Gas Recovery Conference, Midland, TX, Mar. 10-11, 1988.*

Abbaszadeh, M. and Kmal, M. Pressure-Transient Testing of Water-Injection Wells, *SPE 16744, SPE Reservoir Engineering, February, 1989.*

Abou-Sayed, A.S. et al, A Mechanistic Model for Formation Damage and Fracture Propagation During Water Injection, *SPE 94606, Proceedings of SPE European Formation Damage Conference, Scheveningen, Netherland, May 25-27, 2005.*

Addington, D.V. An Approach to Gas-Coning Correlations for a Large Grid Cell Reservoir Simulator. *JPT , November, 1981.*

Afaleg, N.I. et al. Design and Deployment of Maximum Reservoir Contact Wells with Smart Completion in the Development of a Carbonate Reservoir. *SPE 93138, Proceedings of the SPE Pacific Oil and Gas Conference and Exhibition, Jakarta, Apr. 5-7, 2005.*

Ahmed, S.A. et al, Produced Water Management Strategy and Water Injection Best Practices: Design, Performance, and Monitoring. *SPE 108238, Proceedings of the International Petroleum Technology Conference, Doha, Qatar, November 21-23, 2005.*

Ahmed, T. Reservoir Engineering Handbook. *3rd Edition, Elsevier Press, Burlington, MA, 2006.*

Ajayi, A. and Konopczynski, M. Intelligent-Well Technology Reduced Water Production in a Multilateral Oil Producer. *SPE 102982, Proceedings of SPE ATCE, San Antonio, Sep. 24-27, 2006.*

Alikhan, A.A. and Farouq, A.S.M. State-of-the-Art of Water Coning Modeling and Operation.. *SPE 13744, Proceedings of the SPE Middle East Oil Technical Conference and Exhibition, Bahrain. Mar. 11-14 1985.*

Al-Amoudi, S.M. and Dogru, A.H. Water Coning in High Permeability Sandstone Reservoirs in Gulf. *SPE 37726 Proceedings of the Middle East Oil Show and Conference, Bahrain, Mar. 15-18 1997.*

Ambrose, A.W. Analysis of Oil-field Water Problems. *AIME, Vo. 65, p. 245-268, 1921.*

Armenta, M. Mechanisms and Control of Water Inflow to Wells in Gas Reservoirs with Bottom-Water Drive, *Ph.D dissertation, Louisiana State University, Baton Rouge, 2003.*

Arslan. O. et al. Nodal Analysis for Oil Wells with Downhole Water Sink Completions, *CIPC 2004-242, Proceedings of the Canadian International Petroleum Conference, Calgary, Canada, June 8-10, 2004.*

Arslan, O. Optimal Operating Strategy for Wells with Downhole Water Sink Completions to Control Water Production and Improve Performance, *Ph.D dissertation, Louisiana State University, Baton Rouge, 2005.*

Babu, D.K. and Odeh, A.S. Productivity of a Horizontal Well. *SPE Reservoir Engineering, Nov. 1989.*

Baker Hughes. Intelligent Production Systems. *http://www.bakerhughesdirect.com/cgi/bot/resources/ExternalFileHandler.jsp?bookmarkable=Yes&path=private/BOT/public/intelligent_wells/index.html&channelId=-546906632, July, 2009.*

Baker Hughes. Intelligent Well Systems™. *http://www.bakerhughes.com/ bakerhughes/water_management/completion_IWS.htm, July, 2009.*

Barkve, T. An Analytical Study of Reservoir Pressure During Water- Injection Well Tests. *SPE 15791, paper available from SPE, Richardson, TX, 1985.*

Bear, J. Dynamics of Fluids in Porous Media. *Elsevier Publishing Co., Inc. p. 665−727, New York, 1972.*

Beggs, H.D. Production Optimization Using NODAL Analysis. *OGCI and Petroskills Publications, Tulsa, OK, 1991.*

Besson, J. Performance of Slanted and Horizontal Wells in an Anisotropic Medium. *SPE 20965, Proceedings of the SPE European Petroleum Conference, The Hague, Oct. 21-24, 1990.*

Boughrara, A.A. et al. Approximate Analytical Solutions for the Pressure Response at a Water-Injection Well. *SPEJ, Mar. 2007.*

Bournazel, C., and Jeanson, B. Fast Water Coning Evaluation Method. *SPE 3628, Proceedings of the SPE 46th ATCE, New Orleans, Oct. 3–6, 1971.*

Bowlin, K.R. et al. Field Application of In-situ Gravity Segregation to Remediate Prior Water Coning. *SPE 38296, Proceedings of the SPE Western regional Meeting, Long Beach, CA, Jun. 25-27, 1997.*

Bratvold, R.B. and Horne, R.N. Analysis of Pressure-Falloff Tests Following Cold Water Injection. *SPEFE Vo. 5, No. 3, 1990.*

Brigham, W.E. Discussion of Productivity of a Horizontal Well. *SPERE Vo. 5, No. 2, 1990.*

Brock, W.R. Application of Intelligent-Completion Technology in a Triple-Zone Gravel Packed Commingled Producer. *SPE 101021, Proceedings of SPE ATCE, San Antonio, TX, Sep. 24-27, 2006.*

Brown, K.E. and Beggs, H.D. The Technology of Artificial Lift Methods. *PennWell Books, Tulsa, OK, 1977.*

Brons, F. and Marting, V.E. The Effect of Restricted Fluid Entry on Well Productivity. *JPT, 1322-G, 1960.*

Buckingham, E. On Physically Similar Systems; Illustrations of the Use of Dimensional Equations. *Phys. Rev. 1914, 4, 345.*

Byrne, W.B. Jr. and Morse, R.A. The Effects of Various Reservoir and Well Parameters on Water Coning Performance. *SPE 4287, Proceedings of the 3rd Numerical Simulation of Reservoir Performance Symposium of SPE in Houston, TX, Jan. 10-12, 1973.*

Calhoun, J. Fundamentals of Reservoir Engineering. *The University of Oklahoma Press. Norman, OK, 1960.*

Carpenter, C. W., Jr., Bail, P. T., Bobek, J. E. A Verification of Waterflood Scaling in Heterogeneous Communicating Flow Models. *Soc. Pet. Eng. J. 1962, 2, 9−12.*

Caudle, B.H. and Silberberg, I.H. Laboratory Models of Oil Reservoirs Produced By Natural Water Drive. *SPEJ, Vo. 5, No. 1, March, 1965.*

Caudle, D. D. Produced Water Regulations in the United States: Then, Now and in the Future. *SPE 77389, Proceedings of the SPE ATCE, San Antonio, TX, Sep. 29 – Oct. 2, 2002.*

Chaney, P. E. et al. How to Perforate Your Well to Prevent Water and Gas Coning. *OGJ, May 1956, p. 108.*

Chaperon, I. Theoretical Study of Coning Toward Horizontal and Vertical Wells in Anisotropic Formations: Subcritical and Critical Rates. *SPE 15377, Proceedings of the SPE 61st ATCE, New Orleans, LA, Oct. 5–8, 1986.*

Chappelear, J.E and Hirasaki, G.J. A Model of Oil-Water Coning for Two-Dimensional, Areal Reservoir Simulation. *SPEJ, Vo. 16, No. 2, April, 1976.*

Chen, H-K. Performance of Horizontal Wells, Safah Field, Oman. *SPE 25568, Proceedings of the SPE Middle East Oil Show, Bahrain, Apr. 3-6, 1993.*

Chierici, G. L. et al. A Systematic Study of Gas and Water Coning by Potentiometric Models. *JPT, Aug. 1964.*

Chugbo, A.I. et al. Thin Oil Columns Most People Think Horizontal Wells, Obagi Field Case Suggests the Contrary. *SPE 19599, Proceedings of the SPE ATCE, San Antonio, TX, Oct. 8-11, 1989.*

Conejerosa, R. and Lenoachb, B. Model-based Optimal Control of Dual Completion Wells. *JPSE, Vo. 42, p. 1 – 14, 2004.*

Conn, T and Themig, D. A Common Sense Approach to Intelligent Completions through Improved Reliability and Lower Costs. *PROMORE 002, Nov. 2001.*

Craig, F. F., Sanderlin, J. L., Moore, D. W., Geffen, T. M. A Laboratory Study of Gravity Segregation in Frontal Drives. *Trans. AIME, 210, 1957.*

Craig, F.F., Jr. The Skin Effect and Its Impediment to Fluid Flow into a Wellbore. *Trans. AIME, Vo. 198, p. 171, 1971.*

Croes, G. A., Schwarz, N. Dimensionally Scaled Experiments and the Theories on the Water-Drive Process. *Trans. AIME 1955, 204, 35−42.*

Dake, L.P. Fundamentals of Reservoir Engineering. *Elsevier Scientific Publishing Co., New York, 1978.*

Detienne, J.L. et al, Produced Water Re-Injection on a Low Permeability Carbonaceous Reservoir, SPE 78482, *Proceedings of the 10th Abu Dhabi International Petroleum Exhibition and Conference, October 13-16, 2002.*

Driscoll, V.J. Multiple Producing Intervals to Suppress Coning. *US Patent No. 3638731, Feb. 1, 1972.*

Djuro N. Numerical Reservoir Characterization Using Dimensionless Scale Numbers with Application In Upscaling. *Ph.D Dissertation, Louisiana State University, August, 2002.*

Dutta, V.K. and Arnold, M.D. Permeability Scaling in a Numerical Coning Model. *Proceedings of the Fall Meeting of the Society of Petroleum Engineers of AIME, New Orleans, LA, Oct. 3-6, 1971.*

Ehlig-Economides, C.A. et al. Production Enhancement Strategies for Strong Bottom Water Drive Reservoirs. *SPE 36613, Proceedings of the SPE ATCE, Denver, CO, Oct. 6-9, 1996.*

Elkins, L.F. Fosterton Field An Unusual Problem of Bottom Water Coning and Volumetric Water Invasion Efficiency. *Trans. AIME, Vo. 216, 1959.*

Erlandsen, S. M. Production Experience from Smart Wells in the Oseberg Field. *SPE 62953, presented in the 2000 SPE Annual Technical Conference and Exhibition, Dallas, TX, Oct. 1-4, 2000.*

Fortunati, F. Water coning at the bottom of the well. *SPE 544, Technical Note, 1 – 9, 1962.*

Gai, H. A Method to Asses the Value of Intelligent Wells. *SPE 77941, Proceedings of the SPE Asia Pacific Oil and Gas Conference and Exhibition, Melbourne, Oct. 8-10, 2002.*

Geertsma, J., Croes, G. A., Schwarz, N. Theory of Dimensionally Scaled Models of Petroleum Reservoirs. *Trans., AIME, Vo. 207, 1956.*

Gharbi, R, Peters, E, Elkamel, A. Scaling Miscible Fluid Displacements in Porous Media. *Energy Fuels, Vo. 12, No. 4, p. 810-811, 1998.*

Giger, F.M. Analytic Two Dimensional Models of Water Cresting before Breakthrough for Horizontal Wells. *SPE Reservoir Engineering Journal, 409– 416 (Nov.), 1989.*

Gilman, J. R. et al. Application of Short Radius Horizontal Borehole in Naturally Fractured Yates Field. *SPE Reservoir Engineering,* February, 1995.

Gilbert, W.E. Flowing and Gas-Lift Well Performance. *Drilling & Prod. Proc. API, No. 801-30H, Dallas, 1954.*

Glandt, C.A. Reservoir Management Employing Smart Wells: A Review. *SPE Drilling & Completion Journal, Vo. 20, No. 4, p. 281-288, Dec. 2005.*

Golan, M. and Whitson, C.H. Well Performance. *International Human Resources Development Corporation, Boston, 1986.*

Gordeyev, Y.N. and Entov, V.M. The Pressure Distribution around a Growing Crack. *J. Appl. Maths. Mechs. Vo. 51, No. 6, p. 1025–1029, 1997.*

Gringarten, A.C. et al. Unsteady-State Pressure Distribution Created by a Well with a Single Infinite-Conductivity Vertical Fracture. *SPEJ. p. 347, Aug. 1974.*

Gringarten, A.C. and Ramey, H.J. Jr. An Approximate Infinite Conductivity Solution for a Partially Penetrating Line-Source Well. *SPEJ. p. 140, Apr. 1975.*

Gunning, J. et al. Coning in dual completed systems. *JPSE, Vo. 23, p. 27–39. August, 1999.*

Guo, B. and Lee, R.L-H. A Simple Approach to Optimization of Completion Interval in Oil/Water Coning Systems. *SPEREE, Vo. 8, No. 4, Nov. 1993.*

Harris, M.H. The Effect of Perforating Oil Well Productivity. *JPT, Vo. 18, No. 4, April, 1966.*

Haug, B.T. et al. Horizontal Wells in the Water Zone: The Most Effective Way of Tapping Oil From Thin Oil Zones? *SPE 22929, Proceedings of the SPE ATCE, Dallas, TX, Oct. 6-9, 1991.*

Hawkins, M.F. A Note on the Skin Effect. Trans. *AIME, Vo. 207, p. 356, 1956.*

Hazebroek, P. et al. Pressure Fall-Off in Water Injection Wells. *Trans. AIME, Vo. 213, p. 250-260, 1958.*

Henley, D.H. et al. A Scale-Model Study of Bottom-Water Drives. *JPT, Vo. 13, No. 1, January, 1961.*

Hernandez, J.C. Oil Bypassing By Water Invasion to Wells Mechanisms and Remediation, *Ph.D dissertation, Louisiana State University, Baton Rouge, 2007.*

Hernandez, J.C., Wojtanowicz, A.K. Prediction of Oil Bypassing in Bottom Water Systems Using Dimensionless Groups. *CIPC 2007-064. Canadian International Petroleum Conference. Calgary, Alberta, Canada, June 12 – 14, 2007.*

Hoyland, L. A. et al. Critical Rate for Water Coning: Correlation and Analytical Solution. *SPERE, Nov. 1989.*

Inikori, S.O. Numerical Study of Water Coning Control with Downhole Water Sink (DWS) Well Completions in Vertical and Horizontal Wells, *Ph.D dissertation, Louisiana State University, Baton Rouge, 2002.*

Inikori, S.O. Wojtanowicz, A.K. Contaminated Water Production in Old Oil Fields with Downhole Water separation Effects of Capillary Pressures and Relative Permeability Hysteresis. *SPE 66536, Proceedings of the SPE/EPA/DOE Exploration and Production Environmental Conference, San Antonio, TX, Feb. 26-28, 2001.*

Inikori, O.S. et al. Water Control in Oil Wells with Downhole Oil-Free Water Drainage and Disposal. *SPE 77559, Proceedings of the SPE ATCE, San Antonio, TX, Sep. 29-Oct. 2, 2002.*

Intelligent Well Reliability Group. http://www.proneta.co.uk/smartwell.htm. *July, 2009.*

Jansen, J.D. *Contribution to the "Jaarboek" of the "Mijnbouwkundige Vereeniging", Feb. 2001.*

Jin, L. Wojtanowicz, A.K. Performance Analysis of Wells with Downhole Water Loop (DWL) Installation for Water Coning Control. *CIPC 2008-173, Canadian International Petroleum Conference. Calgary, Alberta, Canada, Jun. 17-19 2008.*

Jin, L. Wojtanowicz, A.K, Hughes, R.G. An Analytical Model for Water Coning Control Installation in Reservoir with Bottom Water. *CIPC2009-098, Canadian International Petroleum Conference. Calgary, Alberta, Canada, 16-18 June 2009.*

Jøranson, H. et al. Better Reservoir Management through Improved Water-Injection Methods with Data Analysis and Detailed Fracture/Reservoir Modeling. *SPE 110329, Proceedings of the SPE ATCE, Anaheim, CA, Nov. 11-14, 2007.*

Joshi, S. Augmentation of Well Productivity Using Slant and Horizontal Wells. *JPT, June 1988.*

Joshi, S. Horizontal Well Technology. *Pennwell Publishing Company, Tulsa, OK. 1991.*

Ju, B. et al, An Effective Method To Improve Recovery of Heavy Oil Reservoir with Bottom Water Drive, *International Petroleum Technology Conference held in Doha, Qatar, November 21–23, 2005.*

Kabir, C.S. et al. Understanding Coning Performance in a High-Anisotropy Reservoir: The Burgan Reservoir Case Study. *SPE 62993, Proceedings of the SPE ATCE, Dallas, TX, Oct. 1-4, 2000.*

Karcher, B. et al. Some Practical Formulas to Predict Horizontal Well Behavior. *SPE 15430, Proceedings of the SPE 61st ATCE, New Orleans, Oct. 5–8, 1986.*

Karp, J.C. et al. Horizontal Barriers for Controlling Water Coning. *JPT, p. 783– 790 July, 1962.*

Kasap, E. et al. Formation-Rate-Analysis Technique: Combined Drawdown and Buildup Analysis for Wireline Formation Test Data. *SPEREE Vo. 2, No. 3, p. 271, 1999.*

Kazemi, H. and Seth, S.M. Effect of Anisotropy and Stratification on Pressure Transient Analysis of Wells with Restricted Flow Entry. *JPT. p. 639, May 1969.*

Khan, A.R. and Caudle, B.H. Scaled Model Studies of Thin Oil Columns Produced by Natural Water Drive. *SPEJ, Vo. 9, No. 3, September, 1969.*

Khan, A.R. A Scaled Model Study of Water Coning. *JPT, Vo. 22, No. 6, June, 1970.*

Kirby, R.H., et al. Characterization of a Vertically Compartmentalized Reservoir in a Supergiant Field, Burgan Formation, Greater Burgan Field, Kuwait, Part 1: Stratigraphy and Water Encroachment. *SPE 49214, Proceedings of the SPE ATCE, New Orleans, LA, Sept. 27-30, 1998.*

Kisman, K.E. et al. Water-wetting Treatment for Reducing Water Coning in an Oil Reservoir. *U.S. Patent No15,060,730, Oct.29, 1991.*

Kisman, K.E. et al. Treatment for Reducing Water Coning in an Oil Reservoir. *U.S. Patent No.5,062,483, Nov. 5, 1992.*

Kjos, T. et al. Down-Hole Water-Oil Separation and Water Reinjection through Well Branches, *SPE 030518, Proceedings of SPE Annual Meeting held in Dallas, Texas, October 22-25, 1995.*

Konieczek, J. The Concept of Critical Rate in Gas Coning and Its Use in Production Forecasting. *SPE 20722 Proceedings of the SPE ATCE, New Orleans, LA, Sept. 23-26, 1990.*

Koning, E. J. L. Fractured Water Injection Wells – Analytic Modelling of Fracture Propagation. *SPE 14684, paper available from SPE, Richardson, TX, 1985.*

Konopczynski, M. and Ajayi, A. Design of Intelligent Well Downhole Valves for Adjustable Flow Control. *SPE 90664, presented SPE ATCE, Houston, Sept. 26-29, 2004.*

Kucuk, F and Brigham, W.E. Transient Flow in Elliptical System. *SPEJ, Dec. 1979.*

Kuo, C. T. and DesBrisay, C. L. A Simplified Method for Water Coning Predictions. *SPE 12067, Proceedings of the 58th ATCE, San Francisco, Oct. 5–8, 1983.*

Kurban, H. Numerical Simulation of Downhole Water Sink Production System Performance. *MS Thesis, Louisiana State University, Baton Rouge, LA, 1999.*

Lee, S.H. and Tung, W.B. General Coning Correlations Based on Mechanistic Studies. *SPE 20742, Proceedings of the SPE ATCE, New Orleans, LA, Sept. 23-26, 1990.*

Leverett, M.C. et al. Dimensional-Model Studies of Oil-Field Behavior. *Trans. AIME, 146, 175−193, 1942.*

Letkeman, J.P and Ridings, R.L. A Numerical Coning Model. *SPEJ, Vo. 10, No.4, December, 1970.*

Liu, X. and Ortoleva, P. A Coupled Reaction and Transport Model for Assessing the Injection, Migration and Fate of Waste Fluids. *SPE 36640, Proceedings of the SPE ATCE, Denver, CO, Oct. 6-8, 1996.*

MacDonald, R.C. and Coats, K.H. Methods for Numerical Simulation of Water and Gas Coning. *SPEJ, Vo. 10, No. 4, December, 1970.*

Matthews, C.M. et al. Application of Downhole Oil/Water Separation Systems in the Alliance Field. *SPE 35817, Proceedings of the 3rd International Conference on Health, Safety & Environment in Oil & Gas Exploration and Production, New Orleans, LA, Jun. 9-12, 1995.*

Mattax C. and Dalton, R.: Reservoir Simulation. *SPE Monograph Volume 13, Richarson, Texas, 1990.*

Mech, J. et al. A nodal Approach for Applying Systems Analysis to the Flowing and Artificial Lift Oil or Gas Well. *SPE 8025, available from the SPE Book Order Dept., Mar. 5, 1979.*

Menouar, H.K. and Hakim, A.A. Water Coning and Critical Rates in Vertical and Horizontal Wells. *SPE 29877, SPE Middle East Oil Conf. Bahrein, March 11 – 14, 1995.*

Meyer, H. I., and Garder, A. O. Mechanics of Two Immiscible Fluids in Porous Media. *J. Applied Phys., No. 11, p. 25, Nov. 1954.*

Meyer, H.I. and Searcy, D.F. Analog Study of Water Coning. *JPT, Vo. 8, No. 4, April, 1956.*

Miller, R. T. and Rogers, W. L. Performance of Oil Wells in Bottom Water Drive Reservoirs. *SPE 4633, Proceedings of the 48th Annual Fall Meeting of the Society of Petroleum Engineers of AIME held in Las Vegas, NV, Sep. 30-Oct. 3, 1973.*

Moreno, J.M.M. et al. Well Impairment Upscaling Applied to Water Injection above Fracture Pressure Simulation. *Proceedings of the XXVII Iberian Latin American Congress on Computational Methods in Engineering, Belem, Para, Sep. 3 – 6, 2006.*

Moser, E.B. Fundamental Sampling Techniques. *Department of Experimental Statistics, Louisiana State University, Baton Rouge, LA, 2009.*

Mungan, N. A Theoretical and Experimental Coning Study. *SPEJ, Vo. 15, No. 3, June, 1975.*

Muskat, M. and Wyckoff, R.D. An Approximate Theory of Water-coning in Oil Production. *Trans. AIME, Vo. 114, 1935.*

Muskat, M. The Effect of Casing Perforations on Well Productivity. *Trans. AIME, Vo. 151, 1943.*

Muskat, M. The Performance of Bottom Water-drive Reservoirs. *Trans. AIME, Vo. 170, 1947.*

Muskat, M. The Effect of Permeability Stratification in Complete Water-Drive Systems. *Trans. AIME, Vo. 189, 1950.*

Myers, D.L. Mini-Injection Tests Provide Inflow Performance Characteristics for Oil wells, *SPE 6040, Proceedings of the 51st Annual Fall Technical Conference and Exhibition of SPE of AIME, New Orleans, October 3-6, 1976.*

Naldrett, G. and Ross, D. When Intelligent Wells are Truly Intelligent, Reliable, and Cost Effective. *OTC 17999, Proceedings of the 2006 Offshore Technology Conference held in Houston, TX, May. 1–4, 2006.*

Nielsen, R. L., Tek, M. R. Evaluation of Scale-Up Laws for Two-Phase Flow Through Porous Media. *Soc. Pet. Eng. J. 1963, June, 164−176.*

Offeringa, J., van der Poel, C. Displacement of Oil from Porous Media by Miscible Liquids. *Trans. AIME, 201, 310−315. 1954.*

Ould-amer, Y. et al. Attenuation of water coning using dual completion technology. *JPSE, Vo. 45, p. 109– 122. 2004.*

Outmans, H.D. Effect of Coning on Clean Production Rate of Well in Heterogeneous Reservoir. *SPE 893, Proceedings of 39th Annual Fall Meeting SPE, Houston, TX, October 11 – 14, 1964.*

Ozkan, E., and Raghavan, R. Performance of Horizontal Wells Subject to Bottom Water Drive. *SPE 18545, Proceedings of the SPE Eastern Regional Meeting, Charleston, West Virginia, Nov. 2–4, 1988.*

Paige, R.W. et al, Optimising Water Injection Performance, *SPE 29774, Proceedings of the Middle East Oil Show, Bahrain, March 11 – 14, 1995.*

Papatzacos, P. Approximate Partial-Penetration Pseudoskin for Infinite-Conductivity Wells. *SPE Reservoir Engineering, May, 1987.*

Papatzacos, P. et al. Cone Breakthrough Time for Horizontal Wells. *SPE 19822, Proceedings of the SPE 64th ATCE, San Antonio, TX, Oct. 8–11, 1989.*

Pang, S. and Sharma, M.M. A Model for Predicting Injectivity Decline in Water-Injection Wells, *SPE 28489, Proceedings of the SPE Annual Technical Conference and Exhibition, New Orleans, September 25-28, 1997.*

Parker, R.K. Water Coning --- A System for Predicting WOR Performance. *SPE 6978, Unsolicited material in SPE eLibrary, 1977.*

Patzek, T and Silin, D.B. Water Injection into a Low-Permeability Rock - 1: Hydrofracture Growth. *Transport in Porous Media, Vo. 43, p. 537–555, 2001.*

Paul, J.M. and Strom, E.T. Oil Reservoir Permeability Control using Polymeric Gels. *Canadian Patent No. 1,264,856, Dec.20, 1988.*

Peres, A.M.M. and Reynolds, A.C. Theory and Analysis of Injectivity Tests on Horizontal Wells. *SPEJ Vo. 8, No. 2, 2003.*

Permadi, P. et al. Horizontal Well Completion with Stinger for Reducing Water Coning Problems. *SPE 37464, Proceedings of the SPE Production Operations Symposium, Oklahoma City, OK, Mar. 9-11, 1997.*

Perkins, F. M., Collins, R. E. Scaling Laws for Laboratory Flow Models of Oil Reservoirs. *Trans. AIME 219, p. 383−385, 1960.*

Pirson, S.J. and Mehta, M.M.. A Study of Remedial Measures for Water-Coning By Means of a Two-Dimensional Simulator. *SPE 1808, Fall Meeting of the Society of Petroleum Engineers of AIME, New Orleans, LA, Oct. 1-4, 1967.*

Pirson, S. J. Oil Reservoir Engineering. *Robert E. Krieger Publishing Company, Huntington, NY, 1977.*

Pollock, C.B., and Shelton, J.L. Method for Decreasing Water production by Gas Injection in a Single Well Operation. *Canadian Patent No.866, 573, March 23, 1971.*

Qin, W. and Wojtanowicz, A.K. Well Performance Analysis for Heavy Oil with Water Coning, *CIPC 2007-162, Proceedings of the Canadian International Petroleum Conference, Calgary, Canada, June 12-14, 2007.*

Rapoport, L. A. Scaling Laws for Use in Design and Operation of Water−Oil Flow Model. *Trans. AIME, 204, 143−150, 1955.*

Rapoport, L. A., Leas, W. J. Properties of Linear Waterfloods. *Trans. AIME, 198, 139−148, 1953.*

Recham, R. et al. Effects of Water Coning on the Performance of Vertical and Horizontal Wells-A Reservoir Simulation Study of Hassi R'mel Field, Algeria. *SPE 65506, Proceedings of the SPE/CIM International Conference on Horizontal Well Technology, Calgary, Canada, Nov. 6-8, 2000.*

Reynolds, A.C. et al. Pseudoskin Factor Caused by Partial Penetration. *JPT. p. 2197, Dec. 1984.*

Richardson, J.G. and Blackwell, R.J. Use of Simple Mathematical Models for Predicting Reservoir Behavior. *JPT, Vo. 23, No. 9, September, 1971.*

Richardson, J.G. et al. Coning. *JPT, Vo. 39, No.8, August, 1987.*

Romero-Juarez, A. Characteristic of Oil Production Related to Water Coning. *SPEREE, p. 1 – 34, 1964.*

Ruark, A.E. Inspectional Analysis: A Method Which Supplements Dimensional Analysis. *J. Elisha Mitchell Sci. Soc., 51, 127−132. 1935.*

Russel, T.J., Larry, W.L., Arnaud, M.D. Prediction of capillary fluid interfaces during gas or water coning in vertical wells. *SPE 77772, Proceedings of the SPE ATCE, San Antonio, TX, Sept. 29– Oct. 2, 2002.*

Saggaf, M.M. A Vision for Future Upstream Technologies. *JPT, Vo. 60, No. 3, Mar. 2008.*

Sakowski, S.A. et al. Impact of Intelligent Well System on Total Economics of Field Development. *SPE 94672, presented in the SPE Hydrocarbon Economics and Evaluation Symposium, Dallas, TX, Apr. 3-5, 2005.*

Saleri, N.G. Haradh III: A Milestone for Smart Fields. *JPT, Vo. 58 No. 11, Nov. 2006.*

Saleri, N.G. Technology Tomorrow: The Next Trillion: Anticipating and Enabling Game-Changing Recoveries. *JPT, Vol. 58 No. 4, Apr. 2006.*

Schlumberger. Oil Field Glossary. *http://www.glossary.oilfield.slb.com/, July, 2009.*

Schlumberger. Intelligent Well Overview. *http://www.slb.com/content/services/completion/intelligent/intelligent_completions.asp, July, 2009.*

Schols, R.S. An Empirical Formula for the Critical Oil Production Rate. *Erdoel Erdgas, Z., Vo. 88, No. 1, p. 6-11, January, 1972.*

Seright, R.S. et al. A Strategy for Attacking Excess Water Production. *SPE Production & Facilities Vo. 18, No. 3, p. 158-169, Aug. 2003.*

Settari, A. and Aziz, K. A Computer Model for Two-Phase Coning Simulation. *SPEJ, Vo. 14, No. 3, June, 1974.*

Sheng, J.J. et al. Concept of Geometric Factor and Its Practical Application to Estimate Horizontal and Vertical Permeabilities. *SPEREE, Vo. 9, No. 6, Dec. 2006.*

Shirman, E.L An Analytical Model of 3-D Flow Near a Limited-Entry Wellbore in Multilayered Heterogeneous Strata - Theory and Applications. *Master Thesis, Louisiana State University, Baton Rouge, LA, 8. 1995.*

Shirman, E.I. and Wojtanowicz, A.K. Water Coning Hysteresis and Reversal for Well Completion Using the Moving Spherical Sink Method. *SPE 37467, Proceedings of the SPE Production Operations Symposium, Oklahoma, March 9 –11, 1997a.*

Shirman, E.I., and Wojtanowicz, A.K., Water Coning Reversal Using Downhole Water Sink Theory and Experimental Study. *SPE 38792, Proceedings of the SPE ATCE, San Antonio, TX, Oct. 5– 8, 1997b.*

Shirman, E.I. Experimental and Theoretical Study of Dynamic Water Control in Oil Wells, *Ph.D dissertation, Louisiana State University, Baton Rouge, 1998.*

Shirman, E.I. and Wojtanowicz, A.K. More Oil Using Downhole Water-Sink Technology A Feasibility Study. *SPE Prod. & Facilities, Vo. 15, November, 2000.*

Shook, M., Li, D., Lake, W. L. Scaling Immiscible Flow Through Permeable Media by Inspectional Analysis. *In Situ, Vo. 16, No. 3, p. 311−349, 1992.*

Siddiqi, S.S. A Study of Bottom Water Drive Reservoirs Using a Scaled Physical Model and a Numerical Simulator. *Ms. Thesis, Louisiana State University, December, 2001*.

Siddiqi, S.S. and Wojtanowicz, A.K. A Study of Water Coning Control in Oil Wells by Injected or Natural Flow Barriers Using Scaled Physical Model and Numerical Simulator. *SPE 77415, Proceedings of the SPE ATCE, San Antonio, TX, Sep. 29-Oct. 2, 2002.*

Siemek, J. and Stopa, J. A Simplified Semi-Analytical Model for Water-Coning Control in Oil Wells with Dual Completions System. *Transactions of the ASME. 246 – 252, Vol. 124, DECEMBER 2002.*

Singh, K. Designing a Produced Water Re-Injection Program in Bekapai Field, *SPE 101938, Proceedings of Asia Pacific Oil and Gas Conference, Melbourne, Australia, October, 2002.*

Slider, H. C. Practical Petroleum Reservoir Engineering Methods. *Petroleum Publishing Company, Tulsa, OK, 1976.*

Smith, C.R. and Pirson, S.J. Water Coning Control in Oil Wells by Fluids Injection, *SPE 613, SPEJ, Oct. 1, 1963.*

Snaith, N. et al. Experience with Operation of Smart Wells to Maximize Oil Recovery from Complex Reservoirs. *SPE 84855, Proceedings of the International Improved Oil Recovery Conference, Malaysia, Oct. 20-21, 2003.*

Sobocinski, D. P. and Cornelius, A. J. A Correlation for Predicting Water Coning Time. *JPT. Vo. 17, No. 5, May, 1965.*

Sonin, A. The Physical Basis of Dimensional Analysis. *Department of Mechanical Engineering, MIT, Cambridge, 1997.*

Spivey, J. P. and Lee, W. J. Estimating the Pressure-Transient Response for a Horizontal or a Hydraulically Fractured Well at an Arbitrary Orientation in an Anisotropic Reservoir. *SPE 58119, Proceedings of the SPE ATCE, New Orleans, 27-30 September. 1999.*

Stephens, A.C. et al. Some Model Studies of Bottom Water Driven Reservoirs. *SPE 561, University of Oklahoma-SPE Production Research Symposium, Norman, Oklahoma. Apr. 29-30, 1963.*

Streltsova-Adams, T. D. Pressure Drawdown in a Well with Limited Flow Entry. *JPT. p. 1469, Nov. 1979.*

Swisher, M.D. and Wojtanowicz, A.K. In Situ-Segregated Production of Oil and Water —a Production Method with Environmental Merit Field Application. *SPE 29693, Exploration and Production Environmental Conference, Houston, TX, March 27–29, 1995a.*

Swisher, M.D. and Wojtanowicz, A.K. New Dual Completion Method Eliminates Bottom Water Coning. *SPE 30697, Proceedings of the SPE ATCE, Dallas, TX, Oct. 22– 25, 1995b.*

Tabatabaei, M. et al. Optimization of Completion Interval to Minimize Water Coning. *SPE 113106, Proceedings of Europec/EAGE Conference and Exhibition, Rome, Italy. Jun. 9-12, 2008.*

Takacs, G. and Turzo, Z. Nodal Systems Analysis Using Object-Oriented Programming Techniques. *SPE Computer Applications, Apr. 1994.*

Thambynayagam, R.K.M. Analytical Solutions for Pressure Buildup and Falloff Analysis of Water Injection Tests of Partially Penetrating Wells: Non-Unit Mobility Ratios. *SPE 12951, paper available from SPE, Richardson, TX, 1984.*

Thompson, L.G. and Reynolds, A.C. Well Testing for Radially Heterogeneous Reservoirs under Single-and Multiphase Flow Conditions. *SPEFE Vo. 12, No. 1, 1997.*

Trimble, R.H. McDonald, A.E. Corp.A Strongly Coupled, Fully Implicit, Three-Dimensional, Three-Phase Well Coning Model. *SPEJ, Vo. 21, No. 4, August, 1981.*

USEPA. Underground Injection Control Program --- Classes of Wells. *Available at: http://www.epa.gov/OGWDW/uic/wells.html, Jul. 20, 2009.*

Utama, F.A. An Analytical Model to Predict Segregated Flow in the Downhole Water Sink Completion and Anisotropic Reservoir. *SPE 120196, Proceedings of the SPE ATCE, Denver, CO, Sept. 21–24, 2008.*

Van Daalen, F., Van Domselaar, H. R. Scaled Fluid-Flow Models with Geometry Differing from that of Prototype. *SPEJ, Vo. 12, p. 220−228, 1972.*

Van Der Poel, C. Effect of Lateral Diffusivity on Miscible Displacement in Horizontal Reservoirs. *Trans. AIME 1962, 225, 317−326.*

Van Everdingen, A.F and Hurst, W. The Application of the Laplace Transformation to Flow Problems in Reservoirs. *Trans. AIME, Vo. 186, p. 305, 1949.*

Van Everdingen, A.F. The Skin Effect and Its Influence on the Productive Capacity of a Well. *Trans. AIME, Vo. 198, p. 171, 1953.*

Van Golf-Racht, T.D and Sonier, F. Water-Coning in a Fractured Reservoir. *SPE 28572, Proceedings of the SPE ATCE, New Orleans, LA, Sep. 25-28, 1994.*

Welge, H.J. A Simplified Method for Computing Oil Recovery by Gas or Water Drive. *AIME, Vo. 195, p. 91-98, 1952.*

Welge, H.J. and Weber, A.G. Use of Two-Dimensional Methods for Calculating Well Coning Behavior. *SPEJ, Vo. 4, No. 4, December, 1964.*

WellDynamics. Intelligent Completions. *http://www.halliburton.com/ps/Default.aspx?navid=825&pageid=2018/technology/smartwell_definition.htm, July, 2009.*

Wheatley, M.J. An Approximate Theory of Oil/Water Coning. *SPE 14210, Proceedings of SPE ATCE, Las Vegas, NV September 22-25, 1985.*

Widmyer, R.H. Producing Petroleum from Underground Formations. *U.S. Patent No. 2,855,047. Oct. 3, 1955.*

Wojtanowicz, A.K., Bassiouni, Z.A., Segregated production method for oil wells with active water coning. *JPSE, Vo. 11, p. 21–35 April, 1994.*

Wojtanowicz, A.K. et al. Oil Well Coning Control Using Dual Completion with Tailpipe Water Sink. *SPE 21654, Proceedings of the SPE Production Operation Symposium, OK, April 7 –9, 1991.*

Wojtanowicz, A.K. and Shirman, E.I. An In-Situ Method for Downhole Drainage-Injection of Formation Brine in a Single Oil-Production Well. *Deep Injection Disposal of Hazardous and Industrial Waste, Academic Press, Inc., p. 403-420, San Diego, California, 1996.*

Wojtanowicz, A.K. and Xu, H. A New Method to Minimize Oil well Production Water Cut Using A Downhole Water Loop. *CIM 92-13, Proceedings of the 43rd Annual Technical Meeting of the Petroleum Society of CIM, Calgary, Canada, June, 1992.*

Woodward, D.K. and Thambynayagam, R.K.M. Pressure Build-up and Fall-off Analysis of Water Injection Tests. *SPE 12344, paper available from SPE, Richardson, TX, May, 1983.*

Wu, G. et al. A Field Study of Horizontal Well Design in Reducing Water. *SPE 30016, Proceedings of the SPE International Meeting of Petroleum Engineering, Beijing, China, Nov. 14-17, 1995.*

Wygal, R. J. Construction of Models that Simulate Oil Reservoirs. SPEJ, Vo. 3, p. *281−286, 1963.*

Yang, W. and Wattenbarger, R.A. Water Coning Calculations for Vertical and Horizontal Wells. *SPE 22931, Proceedings of the SPE 66th ATCE, Dallas, TX, Oct. 6 –9, 1991.*

Yang, W. An Analytical Solution to Two-Phase Flow in Porous Media and its Application to Water Coning. *SPE Reservoir Eng. J., 1 – 38, 1992.*

Yildiz, T. Impact of Perforating on Well Performance and Cumulative Production. *J. Energy Resour. Technol. Vo. 124, No. 3, Sep. 2002.*

Ziebel. Intelligent Well. *http://www.ziebel.no/activecompletions/The%20Long%20and%20Winding%20Road%20Towards%20The%20Intelligent%20Completion/Intelligent%20well....html, July, 2009.*

VITA

Lu Jin, son of Weiqin Jin and Huiying Qi, was born in Zhejiang, China, in March, 1982. He attended Daqing Petroleum Institute, receiving a bachelor's degree in 2005. After graduation, he joined China University of Petroleum as a research assistant. In 2007, he enrolled at Louisiana State University to start his studies for master's degree.

He will receive his Master of Science in Petroleum Engineering degree in December, 2009.